



Multi-Target Tracking Using 1st Moment of Random Finite
Sets

by

Kusha Panta

Submitted in total fulfilment of
the requirements for the degree of

Doctor of Philosophy

Department of Electrical and Electronic Engineering
The University of Melbourne
Australia

February, 2007

The University of Melbourne

Australia

Abstract

Multi-Target Tracking Using 1st Moment of Random Finite Sets

by Kusha Panta

The last decade has witnessed exciting developments in multi-target tracking theory and practice. Mahler’s finite set statistics (FISST) provides a general systematic foundation for multi-target tracking based on the theory of random finite set (RFS). The RFS framework has led to the development of novel and efficient multi-target Bayes filters and their tractable approximations, which attracted substantial interests.

The probability hypothesis density (PHD) filter is a tractable approximation to the optimal multi-target Bayes filters based on random set theory. It consists of *prediction* and *update* steps that recursively propagate the first order moment or the intensity function of RFS of targets of interest, from which estimate of the number of time-varying targets as well as their states can be obtained while avoiding any explicit observation-to-track association. While a number of implementations of the PHD recursion have been proposed, in their original forms, they do not provide temporal association amongst individual target estimates over time. Temporal association amongst individual target estimates are needed in order to construct individual target trajectories that are often are required in various multi-target tracking applications.

This thesis primarily focuses on developing practical algorithms based on RFSs that are capable of providing temporal association amongst individual target estimates. In particular, this thesis presents a number of novel “estimate-to-track” association schemes for the sequential Monte Carlo implementation of the PHD (SMC-PHD) filter as well as the Gaussian Mixture PHD (GM-PHD) filter. These techniques are capable of handling track initiation, track maintenance and track

termination. The performance of the proposed algorithms has been benchmarked against that of multiple hypothesis tracker (MHT), in particular *a track-oriented* MHT. Furthermore, this thesis also addresses a shortcoming of the PHD filter, namely its inability to distinguish crossing targets from each other.

This thesis also presents a novel sequential Monte Carlo implementation of the PHD filter, which circumvent some of drawbacks of existing SMC-PHD filters apart from addressing temporal associations. Existing SMC implementations of the PHD filter require the knowledge of the observation likelihood as well as the non-zero observation noise. Moreover, the performances of these filters degrade when the observation noise is very small. The proposed convolution PHD filter overcomes these shortcomings by using convolution kernels that are also known to perform regularization jointly on the observation and the state space to improve the performance of SMC method based filters.

This is to certify that

- (i) the thesis comprises only my original work,
- (ii) due acknowledgement has been made in the text to all other material used,
- (iii) the thesis is less than 100,000 words in length, exclusive of table, maps, bibliographies, appendices and footnotes.

Signature_____

Date_____

Acknowledgments

First, my sincere gratitude to Dr. Ba-Ngu Vo for research supervision, guidance and patience over the entire candidature of my doctorate degree. I have tremendously benefitted from his knowledge and experience. I would also like to thank Co-operative Research Center for Signal, Systems and Information Processing (CSSIP) for their support and the Department of Electrical and Electronic Engineering, The University of Melbourne for providing me with necessary resources to complete this thesis.

I have also had the opportunity to work with Dr. Sumeetpal Singh. Dr. Singh has been a great friend and I would like to thank him for his support and valuable advice. I would also like to thank Daniel E. Clark for taking his time to work with me. Without the help of Dr. Mahindra Mallick, it would have taken a lot longer to implement multiple hypothesis tracking algorithms. I am also grateful to Dr. Musicki and Dr. Morelande here in the CSSIP for their valuable time and advice.

Dr. Roger Hughes, Dr. Thomas Hanselmann and Mr. Michael Feramez have been regular sources of support and encouragement. I also value time and efforts of the supporting staff here in the department of E&E Engineering. In particular, I appreciate the friendship of Ms. Gwenda Pittaway and her help. To Anil, Rahul, Yuping, Ian, Assaf, Tania and Himal, you all have been a great source of friendship and support.

Finally, many thanks to my family. I am eternally grateful to my mother. Many thanks and sincere gratitude to my siblings, Kishor, Minu, Chunu and Laba for being wonderful persons as well as my sources of reasons, humour and lively wits. A great deal of gratitude and indebtedness to Archana and Anika for their love, support and welcoming smile at the end of every day.

Contents

1	Introduction	1
1.1	Motivation	2
1.2	Scope of this Thesis	4
1.2.1	Major Contributions of this Thesis	5
1.2.2	Publications	6
1.3	Organization of this Thesis	7
2	Introduction to Target Tracking	9
2.1	Introduction	9
2.2	Single Target Tracking	9
2.2.1	The Bayes Filter	11
2.2.2	The Kalman Filter	12
2.2.3	The Extended Kalman Filter	13
2.2.4	Particle Filters	15
2.3	Single Target Tracking in Clutter	16
2.4	Overview Multi-target Tracking	17
2.4.1	Problem Statements	17
2.4.2	Traditional Approaches to Multi-target Tracking	18
2.5	Multiple Hypothesis Tracking	19
2.5.1	Overview of a Track-Oriented MHT	21
2.5.2	Measurement-to-Track Association	23
2.5.3	Track Hypothesis Score	25
2.5.4	Evaluation and Management of Tracks and Hypotheses	26
2.6	Summary	29
3	Random Finite Set Framework for Multi-target Tracking	31
3.1	Introduction	31
3.2	Random Finite Set Approach to Multi-target Tracking	32
3.2.1	Definition of Random Finite Set	32
3.2.2	Random Finite Set Model of Multi-target Tracking	32
3.2.3	The Multi-target Bayes Filter	34
3.3	The Probability Hypothesis Density (PHD) Filter	35
3.3.1	The Probability Hypothesis Density (PHD) or Intensity Function	35
3.3.2	The PHD Recursion	36
3.3.3	Implementations of the PHD filter	37
3.3.4	Shortcomings of the PHD Filter	37
3.4	Recent Extensions of the PHD Filter	37
3.5	Summary	39

4	Multi-target Tracking with the SMC-PHD Filter	41
4.1	Introduction	41
4.2	The SMC-PHD Filter	42
4.2.1	Multi-target State Estimation	44
4.2.2	Track Association for the SMC-PHD Filter	45
4.3	Data Association Combined with the SMC-PHD Filter	46
4.3.1	The PHD-with-Association filter	47
4.3.2	The MHT-with-PHD Clutter Filter	49
4.3.3	Simulation Results	50
4.3.4	Discussion	58
4.4	The Improved SMC-PHD Filter for Track Association	60
4.4.1	The Cluster-Indexed SMC-PHD Filter	61
4.4.2	Implementation Issues	63
4.4.3	Simulation Results	64
4.4.4	Discussion	67
4.5	Summary	68
5	Multi-target Tracking with the GM-PHD Filter	75
5.1	Introduction	75
5.2	The PHD Filter: A Closed-Form Solution	76
5.2.1	Linear Multi-Target Models	76
5.2.2	The Gaussian-Mixture Probability Hypothesis Density (GM-PHD) Recursion	77
5.2.3	Multi-target State Estimation	79
5.2.4	Pruning and Merging Step	80
5.3	Track Association for the GM-PHD Filter	82
5.3.1	The GM-PHD tracker	82
5.4	Track Management Scheme for the GM-PHD Tracker	84
5.4.1	Tag Management Scheme	85
5.4.2	Track Initiation, Propagation and Termination	86
5.4.3	Pruning Schemes	87
5.5	Simulation Results	88
5.5.1	The Wasserstein Distance	92
5.5.2	Error in Estimating the Number of Targets	93
5.5.3	Remarks	94
5.6	The GM-PHD Tracker and Crossing Targets	95
5.6.1	Estimate-to-Track Association for the GM-PHD Tracker	96
5.6.2	Example of Crossing Targets	97
5.7	Summary	99
6	The Convolution PHD Filter	101
6.1	Introduction	101
6.2	Convolution Kernels Approach to The Bayes Recursion	102
6.2.1	Kernel Density Estimation	102
6.2.2	The Convolution Filters	103
6.3	The Kernel based SMC-PHD Filter	105

6.3.1	The Convolution PHD Filter	106
6.3.2	Implementation Issues	109
6.4	Simulation Results	109
6.5	Summary	113
7	Conclusion	115
7.1	Concluding Remarks	115
7.2	Future Research	117

List of Figures

2.1	An example of couple of possible hypotheses that can be formed from $Z_1 = \{z_{1,1}, z_{1,2}\}$, $Z_2 = \{z_{2,1}, z_{2,2}, z_{2,3}\}$ and $Z_3 = \{z_{3,1}, z_{3,2}\}$. Scenario (a) hypothesizes two possible tracks; one associated with $z_{1,2}$, $z_{2,3}$ & $z_{3,1}$ and another with $z_{2,1}$ & $z_{3,2}$, and treats $z_{1,1}$ and $z_{2,2}$ as clutter. Scenario (b) considers the possibility of three tracks (two alive and one died at $k = 2$) being in the scene represented by i) $z_{1,2}$, $z_{2,3}$ & $z_{3,2}$, ii) $z_{2,2}$ & $z_{3,1}$ and iii) $z_{1,1}$ & $z_{2,1}$	20
2.2	An example of track hypotheses and global hypotheses generation using measurements of first three time intervals. T_i represents a possible i^{th} targets and ‘o’ denotes a target miss-detection.	22
2.3	Overview of a Track-Oriented MHT algorithm	23
2.4	An Example of Gating. $\hat{z}_{k k-1}$ denotes the predicted measurement that is would have been generated by a target with state \hat{x}_{k-1} at time k . It shows measurements $z_{k,1}$ and $z_{k,3}$ falls within the gate established around the measurement prediction of the track with prior state \hat{x}_{k-1} , other three measurements are not considered for measurement-to-track association with it.	24
2.5	Illustration of N-scan Pruning	28
4.1	Multitarget Tracking with the PHD filter.	47
4.2	‘Example 1’: Plots of true positions of four tracks superimposed over 40 time steps.	52
4.3	Plots of x and y components of true positions of 4 tracks given in figure 4.2 against time.	53
4.4	Target tracks obtained using the track-oriented MHT filter on observation sets modified by the PHD filter (Scheme One) superimposed with the true target tracks (dashed line) of ‘example 1’.	53
4.5	Target tracks obtained using the track-oriented MHT filter on observation sets superimposed with the true target tracks (dashed line) of ‘example 1’.	54
4.6	Target tracks obtained using MHT-with-PHD clutter filter (Scheme Two) superimposed with the true target tracks (dashed line) of ‘example 1’.	55
4.7	The Wasserstein distance between the outputs of the PHD-with-association filter, MHT-with-PHD clutter filter and the MHT, and the ground truth for ‘example 1’ and $\lambda_c = 4.0$	56
4.8	The Wasserstein distance between the outputs of the PHD-with-association filter, MHT-with-PHD clutter filter and MHT, and the ground truth for ‘example 1’ and $\lambda_c = 4.0$	56

4.9	‘Example 2’:Plots of true positions of true tracks superimposed over 50 time steps.	57
4.10	The Wasserstein distance between outputs of the PHD-with-association filter, MHT-with-PHD clutter filter and MHT, and the ground truth for ‘example 2’ and $\lambda_c = 8.0$	58
4.11	The estimation error in the target number between the outputs of the PHD-with-association filter, MHT-with-PHD filter, MHT, and between groundtruths ‘example 2’ and $\lambda_c = 8.0$	58
4.12	Diagrammatic view associating clusters between two time frames. Cluster $c_{k,1}$ at time step k will have its label r_1 and will be associated with the cluster with label r_1 at time step $k - 1$ as most of the particles in cluster $c_{k,1}$ belongs to clusters with label r_1 of the previous time step.	61
4.13	Target trajectories in XY planes.	65
4.14	Target trajectories (target 1 (solid line), target 2 (dashed line) and target 3 (dotted line))in terms of x-coordinate positions and y-coordinate positions separately.	65
4.15	Track-valued estimates given by the cluster-indexed SMC-PHD filter. The SMC-PHD filter uses 1000 particles per target and uses $q_k = f_{k k-1}$ and $p_k = \mathcal{N}(\cdot x_0, Q_b)$ as proposal densities for importance sampling. Different plot symbols are used to represent different tracks.	66
4.16	Track-valued estimates given by the MHT Filter. The MHT filter is a track-oriented MHT that uses two or more target detection to confirm a track and prunes tracks that have more than two consecutive target miss-detections. N -scan pruning uses $N = 3$	67
4.17	The Wasserstein multi-target miss distance for the estimates given by the SMC-PHD filter and the MHT filter.	67
4.18	The Wasserstein multi-target miss distance for the estimates given by the SMC-PHD filter and the MHT filter.	68
5.1	A part of a tree structure for propagating a Gaussian term and its tag from the previous time step $k - 1$ to the time step k given Z_k	84
5.2	An example of track-oriented implementation of the GM-PHD Filter. $Z_1 = \{z_{1,1}, z_{1,2}\}$ and $Z_2 = \{z_{2,1}, z_{2,2}\}$, $v_0 = 0$ and a Gaussian term each is contributed by γ_k at both time steps $k = 1$ and $k = 2$. For simplicity, we denote $w_k^{(i)}$ by w_i	86
5.3	‘Example 1’: True target positions (star) superimposed on the measurements generated (cross).	89
5.4	‘Example 2’: True target positions (star) superimposed on the measurements generated (cross).	89
5.5	Target tracks obtained using GM-PHD tracker (solid lines) superimposed with the true target positions (crosses) for ‘example 1’.	91
5.6	Target tracks obtained using a track-oriented MHT (solid lines) superimposed with the true target positions (crosses) for ‘example 1’.	91

5.7	The multi-target miss distance as given by the Wasserstein metric for the GM-PHD tracker and a track-oriented MHT for ‘example 1’ with $\lambda_c = 10$	92
5.8	The multi-target miss distance as given by the Wasserstein metric for the GM-PHD tracker and a track-oriented MHT for ‘example 2’ with $\lambda_c = 20$	93
5.9	Mean error in the target number estimates for the GM-PHD tracker and a track-oriented MHT for ‘example 1’. $\lambda_c = 10$	93
5.10	Mean error in the target number estimates for the GM-PHD tracker and a track-oriented MHT for ‘example 2’. $\lambda_c = 20$	94
5.11	Crossing target trajectories with target ‘1’ (dashed room) and ‘target 2’ (solid line).	95
5.12	An schematic view of extending the GM-PHD filter to crossing targets. χ_m denotes a distance within which two Gaussian terms becomes unimodal and depends on the variances on the Gaussian terms.	96
5.13	An example of estimate-to-track association for the crossing targets in the GM-PHD filter. w_i denotes the log-likelihood ratio (LLR) of a track hypothesis at the current time step, i.e. $k = 2$ in this case.	97
5.14	Trajectories (identified correctly) given by the GM-PHD tracker for crossing targets.	98
5.15	Trajectories (wrongly identified) given by the GM-PHD tracker for crossing targets.	98
5.16	Trajectories given by the GM-PHD tracker that performs track-to-estimate association between time steps 52 and 55.	99
6.1	Target trajectories (target ‘1’ (solid line), target ‘2’ (dotted line)) in terms of x-coordinate positions and y-coordinate positions separately.	110
6.2	Observations generated by targets immersed in clutter.	111
6.3	State estimates given by the convolution PHD filter for $\sigma_{w_{1,k}} = 0.05$ and $\sigma_{w_{2,k}} = 1.0$	111
6.4	State estimates given by the SMC-PHD filter for $\sigma_{w_{1,k}} = 0.05$ and $\sigma_{w_{2,k}} = 1.0$	112
6.5	State estimates given by the SMC-PHD filter for $\sigma_{w_{1,k}} = 0.05/2$ and $\sigma_{w_{2,k}} = 1.0/25$	112
6.6	State estimates given by the convolution PHD filter with no observation noise.	113

List of Tables

4.1	A SMC-PHD Filter Algorithm	70
4.2	The PHD-with-Association Filter	71
4.3	The MHT-with-PHD Clutter Filter	72
4.4	Error in Target Number Estimate for ‘example 1’	72
4.5	Average of Wasserstein distance for ‘example 1’ for different λ_c	72
4.6	The Cluster-indexed SMC-PHD Filter	73
4.7	Estimate-to-Track Association	74
5.1	Multi-target State Estimation	80
5.2	Pruning for the GM-PHD Filter	81
5.3	Average of Wasserstein distance for ‘example 1’ for different λ_c	93
5.4	Error in Target Number Estimate for ‘example 1’	94
6.1	The Convolution Filter	105
6.2	The Resampled-Convolution Filter	106
6.3	The Convolution PHD Filter	114

Chapter 1

Introduction

The problem of tracking an unknown number of objects (or targets) often arises in various applications such as surveillance, robotics, collision avoidance, econometrics, signal processing and medicine just to name a few [4, 7, 9, 19, 27, 94]. The objective of multi-target tracking is to estimate the number of objects as well as their state trajectories from measurements that are made available by sensors at discrete intervals of time. Measurements are indistinguishable partial observations of objects and some of which are spurious measurements, i.e., not generated by the objects of interest. While this problem is of paramount importance and has generated a large volume of literature since the 1960's, it is only recently that a rigorous mathematical framework has been established. Mahler's finite set statistics (FISST) [27, 56, 58, 65] provided a rigorous mathematical framework for handling multi-target tracking problems using the theory of random finite set (RFS). First the collection of targets and the collection of observations are both treated as separate *set-valued entities*. These set-valued entities are then modelled by separate RFSs so that the problem of multi-target tracking can be formulated in the Bayesian framework. This has led to the development of novel and efficient multi-target filters and their computationally efficient approximations, which have generated substantial interests [57, 58, 60, 62, 91, 90, 100, 107, 116]. This thesis focuses on the probability hypothesis density (PHD) filter for the problem of tracking an unknown and time-varying number of objects.

This chapter provides an overview of research that was undertaken as a part of my doctorate degree. In particular, Section 1.1 presents the motivation for this study. Section 1.2 outlines the scope and also summarizes the major contributions of this thesis. Finally, an outline of this thesis structure is given in Section 1.3.

1.1 Motivation

Multi-target tracking (MTT) has been an intensive research area since the early 1960s, driven primarily by aerospace applications such as radar, sonar, guidance, navigation, and air traffic control. It has also found applications in biological systems, econometrics, robotics and sensor networks. Recent surveys reported a plethora of multi-target tracking techniques and their applications [5, 7, 9, 27, 71, 81]. Most of these approaches to MTT involve modifications of single-target filtering techniques based on estimating correct associations between observations and targets. Over the years, most of the efforts have been focused on finding the correct associations between observations and targets, in what is called ‘measurement-to-track’ association so that target trajectories of individual targets can be accurately estimated. The exhaustive search for correct associations of measurements to targets is computationally infeasible [85, 7]. Suboptimal approaches, employed in practice, often introduce errors and performs poorly in the presence of high clutter density. Furthermore, these techniques use linearized models and Gaussian noise approximation so that the Kalman filters can be applied and hence perform poorly when the non-linearity present in dynamical models are severe or the noise is no longer Gaussian. Particle filtering techniques [54, 23, 29, 86] that are capable of handling nonlinear or non-Gaussian dynamical models may not be suitable to ‘measurement-to-track’ association as a large number of particle filters will be needed to run. Some attempts with limited applications have recently been made to apply particle filters in conjunction with the ‘measurement-to-track’ association [33, 34, 88, 99].

Alternative approaches to multi-target tracking include the association-free formulation that might not be beset by the errors introduced by the explicit association considered before filtering in traditional approaches. The symmetric measurement equation (SME) filter [44, 45] avoids the association problem by applying nonlinear symmetric functions to measurements and using properties of these symmetric functions to obtain individual target state estimates. However, this approach introduces additional non-linearity into observation models. While there exists other association-free formulations [48, 114, 115] of the multi-target tracking problems,

none of these formulations are general and systematic enough to be adopted as the foundation.

The last decade has witnessed exciting developments in multi-target tracking theory and practice. Mahler's finite set statistics (FISST) provided a general systematic foundation for multi-target tracking based on the theory of random finite set (RFS) [27, 30, 56, 57, 58, 60, 61, 62]. The theory of RFS, or point process, is a rigorous mathematical discipline for dealing with random spatial patterns that has long been used by statisticians in many diverse applications including agriculture, geology, seismology, and epidemiology [30, 65]. The RFS framework has led to the development of a number of novel and efficient multi-target filters and their tractable approximations, which attracted substantial interests.

The probability hypothesis density (PHD) filter is a suboptimal but computationally tractable alternative to the optimal multi-target Bayes filter based on theory of the RFS [56, 57, 60, 61]. Though the PHD recursion consists of equations that are considerably simpler than those of the optimal multi-target Bayes filter, it still requires solving multi-dimensional integrals that do not have closed-form solutions in general. A generalized SMC implementation of the PHD filter (SMC-PHD filter or particle-PHD filter) has been proposed in [106, 107]. Similar SMC implementations of the PHD filter have also been proposed independently in [90, 116]. A closed-form solution to the PHD recursion, called the Gaussian-Mixture Probability Hypothesis Density (GM-PHD) filter has been recently derived for linear Gaussian multi-target models [103, 104]. Mahler has also proposed new PHD filters that propagates higher order statistics of the target number [63]. However, these implementations of the PHD filter do not provide identities to individual target state estimates, which are needed to obtain state trajectory estimates of individual targets. Often, the estimation of individual target trajectories is at the core of various multi-target tracking systems.

In particular, this thesis addresses the issue of the track association amongst the individual target state estimates given by the existing implementations of the PHD filter. In this thesis, we show that MTT problems are better addressed by formulating them as multi-object filtering problems first according to the RFS ap-

proach and then attempting to find likely associations of target states estimates to targets rather than the approach employed by traditional approaches that perform “measurement-to-track” association first followed by filtering. In addition, attempts at improving the performance of the PHD filter are also presented.

1.2 Scope of this Thesis

This thesis primarily focuses on developing practical algorithms that are capable of providing track associations amongst the target state estimates produced by the PHD filter based multi-target trackers. In particular, attempts have been made to extend existing implementations of the PHD filter in order to provide the estimates of individual target trajectories.

A number of novel schemes have been developed for the SMC-PHD filter so that the new SMC-PHD filter can provide individual target trajectories and their track labels. In particular, the *PHD-with-association* filter, and *PHD-with-MHT clutter* filter are proposed. The *PHD-with-association* filter uses a PHD filter to obtain individual target state estimates and performs data association on these estimates using MHT. In the *PHD-with-MHT clutter* filter, the PHD filter is essentially used as a clutter filter so that the MHT only has to perform data association on a much reduced measurement sets. Furthermore, we also propose a *cluster-indexed SMC-PHD* filter that assigns additional indices to the posterior intensity particles and uses these indices in conjunction with standard clustering techniques to create track labels and to perform ‘estimate-to-track’ association. The performance of these proposed schemes are benchmarked against that of MHT.

This thesis also addresses the issue of data association for the GM-PHD filter. Unique identifiers are introduced to each of the Gaussian components in the mixtures approximating the posterior intensity function and are used to build association of individual target estimates over time. Possible track management and pruning schemes are also considered in this thesis. We also compare the performance of the proposed tracker, *GM-PHD* tracker against that of the MHT. This thesis also proposes a remedy for the GM-PHD filter for handling identities of crossing targets.

Finally, this thesis presents a more robust SMC implementation of the PHD filter. Existing SMC-PHD filters require the knowledge of the observation likelihood and non-zero observation noise. Moreover these filters performs poorly when the observation noise is too small. This thesis proposes a convolution kernel based SMC implementation of the PHD filter that does not require the analytical knowledge of the observation likelihood and can be used in the presence of very small or no observation noise.

1.2.1 Major Contributions of this Thesis

The major contributions of this study are as follows:

- ✠ Development of novel data-association techniques for the SMC-PHD filter. In particular,
 - development of the *PHD-with-Association filter*
 - development of the *PHD-with-MHT* clutter filter
 - development of the *cluster-indexed SMC-PHD* filter
 - performance study of the SMC-PHD filter based tracking methods benchmarked against that of a track-oriented MHT
- ✠ Development of a novel data association technique for the GM-PHD filter. In particular,
 - development of the *GM-PHD tracker*
 - development of an efficient track management and pruning schemes for the GM-PHD tracker
 - performance study of the GM-PHD tracker based tracking methods benchmarked against that of a track-oriented MHT
 - development of a scheme for the PHD filter for resolving track identities of crossing targets
- ✠ Development of a kernel based SMC approximation of the PHD filter, called the *convolution PHD filter*.

1.2.2 Publications

Publications associated with this thesis are as follows:

- K. Panta, B. Vo and S. Singh, “Novel Data Association Schemes for the Probability Hypothesis Density Filter,” *IEEE Transactions on Aerospace and Electronic Systems (In Press)*. (accepted 2006)
- K. Panta, D. Clark and B. Vo, “Data Association and Track Management for the Gaussian-Mixture Probability Hypothesis Density Filter,” submitted to *IEEE Transactions on Aerospace and Electronic Systems*.
- K. Panta, B. Vo, S. Singh and A. Doucet, “The Probability Hypothesis Density Filter versus Multiple Hypothesis Tracking,” *Proc. SPIE, Signal Processing, Sensor Fusion & Target Recognition XIII*, Vol. 5429, Evan Kadar (Ed.), August 2004, pp. 284-295.
- K. Panta, B. Vo and S. Singh, “Improved Probability Hypothesis Density (PHD) Filter for Multi-target Tracking,” *Proc. IEEE Third International Conference on Intelligent Sensing and Information Processing*, Bangalore, India, 14-17 December, 2005. pp. 213-218.
- D. Clark, K. Panta and B. Vo, “The GM-PHD Filter Multiple Target Tracker,” to appear in *Proc. 8th International Conference on Information Fusion 2006*, 13-16 July 2006, Florence, Italy.
- K. Panta B. Vo and D. Clark, “An Efficient Track Management Scheme for the Gaussian Mixture Probability Hypothesis Density Tracker,” *Proc. IEEE Fourth International Conference on Intelligent Sensing and Information Processing*, Bangalore, India, 15-18 December, 2006
- K. Panta and B. Vo, “Convolution Kernels based Sequential Monte Carlo Approximation of the Probability Hypothesis Density Filter,” *Proc. IEEE Conference on Information, Decision and Control (IDC) 2007*, 12-14 February, 2007, Adelaide, Australia.

1.3 Organization of this Thesis

This thesis is organized as follows:

Chapter 1 provides an overview of this thesis. In particular, it outlines the motivation for the research considered in this thesis and summarizes the major contributions. It also lists the number of publications associated with this thesis.

Chapter 2 provides an overview of target tracking. In particular, summaries of single-target and multiple-target tracking techniques are included. In order to appreciate the problems associated with traditional multi-target tracking approaches, a brief description of a benchmark multi-target tracking (MTT), namely multiple hypothesis tracking (MHT) is provided. In this thesis, MHT is used as a shorthand both for multiple hypothesis tracking algorithm and multiple hypothesis tracker depending on the context. Multiple hypothesis tracker is an implementation of multiple hypothesis tracking algorithm.

Chapter 3 introduces the random finite set approach to multi-target tracking. It presents the probability hypothesis density (PHD) filter that is a tractable sub-optimal approximation to the full multi-target Bayes filter based on RFS. It also contains a brief literature review of the recent developments and applications of the PHD filter. Moreover, it outlines some of the drawbacks of the PHD filter.

Chapter 4 provides a description of the sequential Monte Carlo (SMC) implementation of the PHD (SMC-PHD) filter. It considers the issue of data association for the SMC-PHD filter. It presents a number of novel approaches to combining data association with the SMC-PHD filter; namely *PHD-with-association* filter, *PHD-with-MHT* clutter filter, which were proposed during the course of this thesis study and were also included in [77, 78]. Furthermore, this chapter also presents a computationally efficient extension of the PHD filter, called the *cluster-indexed SMC-PHD filter* that performs ‘estimate-to-track’ association based on the improved implementation of the PHD filter. Preliminary results of the cluster-indexed SMC-PHD filter has also appeared in [76]. Simulation results of these proposed schemes are included in this chapter.

Chapter 5 presents the GM-PHD tracker that is an improved formulation of

the GM-PHD filter and can provide temporal associations of target state estimates over time. The performance of the GM-PHD tracker has been studied via simulation results and is benchmarked against that of the MHT. A description of the tree based hypothesis structure that is developed as a part of this study is also given in this chapter. The proposed tree based structure allows the systematic management of target trajectories and leads to the development of simpler pruning schemes. Finally, a simple and effective ‘track-to-estimate’ association scheme is proposed for the PHD filter in order to enable it to correctly maintain identities of crossing targets. The key contributions of this chapter have also appeared in [17, 73, 75].

Chapter 6 outlines a major shortcoming of existing SMC implementations of the PHD filter. It introduces the concept of the non-parametric density estimation technique using kernel. A kernel based SMC implementation of the standard Bayes filter, called convolution filter is introduced. A similar SMC-PHD filter based on kernels, called convolution PHD filters is also presented. Simulation results have been included to show that the convolution PHD filter can operate without the knowledge of the observation likelihood or in the presence of near-zero or zero observation noise unlike existing SMC-PHD filters. The preliminary results results of the idea presented in this chapter have appeared in [74].

Chapter 7 includes the concluding remarks of this thesis. In particular, it summarizes its main contributions and outlines possible future research directions.

Chapter 2

Introduction to Target Tracking

2.1 Introduction

Multi-target tracking is essentially the estimation of an unknown number of targets and their state trajectories from noisy observations available at discrete intervals of time. A target state includes of kinematic characteristics (like positions and velocities) of the target whereas a state trajectory is a collection of target states of the same target over time. Often the target states are hidden from the observer and are partially observed through the observations made by the sensor. In the rest of this thesis, targets or objects mean the same and so do observations or measurements.

This chapter presents an overview of tracking single and multiple targets. Section 2.2 include a summary of single target tracking that includes the single-target Bayes filter and its Kalman based solutions are outlined. Section 2.3 provides a summary of key techniques for tracking a target. Section 2.4 includes a summary of traditional approaches to multi-target tracking (MTT). Section 2.5 introduces a brief description of a multi-target tracker based on the multiple hypothesis tracking (MHT) algorithm, also named the multiple hypothesis tracker (MHT). Finally, this chapter is summarized in Section 2.6.

2.2 Single Target Tracking

A single target and single sensor scenario consists of a target whose state evolves through time and is only partially observed by a sensor at discrete intervals of time.

The objective here is to estimate the state of a target given a sequence of observations made by the sensor up to the current time step. The target state is modelled as the n_x dimensional random vector x_k (i.e., $x_k \in \mathbb{R}^{n_x}$ denotes the dimension of the state vector) and n_x denotes the dimensions of the state vector.

The target motion is modelled by a target transition density, $f_{k|k-1}(x_k|x_{k-1})$ such that given a realization of the target state x_{k-1} at time interval¹ $k - 1$, the target state x_k at the current time interval follows

$$x_k \sim f_{k|k-1}(\cdot|x_{k-1}) \quad (2.1)$$

where \sim denotes 'distributed as'. The target model given in (2.1) is a Markov process, i.e, the current state of the target x_k only depends on the target state x_{k-1} at the previous time step.

The target of state x_k at time interval k generates an observation at the sensor according to

$$z_k \sim g_k(\cdot|x_k) \quad (2.2)$$

where $z_k \in \mathbb{R}^{n_z}$ is the observation available at time k . n_z gives the dimension of the observation vector and is often smaller than n_x . The observation model given in (2.2) shows that the observation z_k at time k only depends on the current target state x_k .

The objective is to find an estimate \hat{x}_k of target state x_k given a sequence of measurements $z_{1:k}$ generated by the target upto time step k . The problem of tracking a single target modelled by (2.1) and (2.2) is essentially a dynamic state space estimation problem for which the Bayesian approach provides the theoretical optimal filtering solution [54, 27, 46, 68, 86, 94]. In the Bayesian approach one aims to construct the posterior probability density function (pdf) of the target state using all received measurements upto current time interval. The posterior pdf contains all information on the target state and completely characterizes all statistical uncertainty in the target state. Hence it can be used to make any inference on

¹time step and time interval will be used interchangeably in this thesis

the state including its estimate and the statistical uncertainty inherent in the state estimate. Given, the posterior pdf $p_k(\cdot|z_{1:k})$, which is the likelihood that a target has state x_k at time k given all past observations $z_{1:k}$, the target state x_k can be obtained by either taking the maximum a *posteriori* (MAP) estimate as

$$\hat{x}_k^{MAP} = \arg \sup_{x_k} p_k(x_k|z_{1:k}) \quad (2.3)$$

or the expected a *posteriori* (EAP) estimate, as

$$\hat{x}_k^{EAP} = \int x p_k(x|z_{1:k}) dx. \quad (2.4)$$

The EAP estimate minimizes the mean square error (mse) in the estimate where as MAP estimate aim to maximize the conditional posterior pdf.

Given, posterior pdf $p_{k-1}(\cdot|z_{1:k-1})$ at time interval $k-1$, the Bayes filter can now be used to construct the pdf $p_k(\cdot|z_{1:k})$ of target at time interval k , from which the target state estimate \hat{x}_k can be obtained according to (2.3) or (2.4). Often the posterior pdf $p_k(\cdot|z_{1:k})$ is also called the filtered pdf.

2.2.1 The Bayes Filter

The Bayes filter is a recursion that consists of two steps, *prediction* and *update* step. Assuming the posterior pdf $p_{k-1}(\cdot|z_{1:k-1})$ at time $k-1$ is available, the prediction step uses the target dynamics to obtain time predicted pdf of the target in k via the Chapman-Kolmogorov equation

$$p_{k|k-1}(x_k|z_{1:k-1}) = \int f_{k|k-1}(x_k|x) p_{k-1}(x|z_{1:k-1}) dx. \quad (2.5)$$

The update step uses the measurement z_k available at the current time interval k to update the predicted pdf of the state obtained via (2.5) according to Bayes rule [79]

$$p_k(x_k|z_{1:k}) = \frac{g_k(z_k|x_k) p_{k|k-1}(x_k|z_{1:k-1})}{\int g_k(z_k|x) p_{k|k-1}(x|z_{1:k-1}) dx}. \quad (2.6)$$

In (2.6), the denominator $\int g_k(z_k|x)p_{k|k-1}(x|z_{1:k-1})dx$ is essentially the normalizing constant. For simplicity, often we use p_k to $p_k(\cdot|z_{1:k})$.

Theoretically, the Bayes filter allows the construction of the exact posterior pdf $p_k(\cdot|z_{1:k})$ recursively at each time interval. However (2.5) and (2.6) do not admit closed form solution in general. One exception is the Kalman filter that provides analytical solution [54, 86] when dynamical models are linear and Gaussian. When the state space is discrete and has a finite number of states, the solution is available in closed-form. When the analytical solution to the Bayes filter is intractable, which is often the case in real world applications, approximate solutions to the optimal filters are used.

2.2.2 The Kalman Filter

Given the posterior pdf $p_{k-1}(\cdot|z_{1:k-1})$ is a Gaussian, the posterior pdf $p_k(\cdot|z_{1:k})$ is also a Gaussian provided the following assumptions hold [31, 42]:

- the target dynamics $f(\cdot|x_{k-1})$ and measurement process $g_k(\cdot|x_k)$ are linear and Gaussian, i.e,

$$x_k = F_{k-1}x_{k-1} + w_{k-1} \quad (2.7)$$

$$z_k = H_k x_k + v_k, \quad (2.8)$$

where F_{k-1} is a transition matrix, H_k observation matrix, w_k is a zero mean additive Gaussian noise and v_k is a zero mean additive Gaussian noise.

- v_k and w_{k-1} are independent of each other.

A Gaussian density is completely characterized by its mean and the covariance, i.e, $\mathcal{N}(\cdot; x, P)$ denote a Gaussian density of a random variable with mean x and covariance P . The optimal Bayes recursion reduces to

$$p_{k-1}(x_{k-1}|z_{1:k-1}) = \mathcal{N}(x_{k-1}; \hat{x}_{k-1}, \hat{P}_{k-1}) \quad (2.9)$$

$$p_{k|k-1}(x_k|z_{1:k-1}) = \mathcal{N}(x_k; \hat{x}_{k|k-1}, \hat{P}_{k|k-1}) \quad (2.10)$$

$$p_k(x_k|z_{1:k}) = \mathcal{N}(x_k; \hat{x}_k, \hat{P}_k) \quad (2.11)$$

where

$$\hat{x}_{k|k-1} = F_{k-1}x_{k-1} \quad (2.12)$$

$$\hat{P}_{k|k-1} = F_{k-1}\hat{P}_{k-1}(F_{k-1})^T + Q_{k-1} \quad (2.13)$$

$$\hat{x}_k = \hat{x}_{k|k-1} + K_k(z_k - H_k\hat{x}_{k|k-1}) \quad (2.14)$$

$$\hat{P}_k = [I - K_k H_k]\hat{P}_{k|k-1} \quad (2.15)$$

where Q_{k-1} and R_k are the covariances of the noise processes w_{k-1} and v_k respectively, K_k is called the Kalman gain and is given as

$$K_k = P_{k|k-1}(H_k)^T [H_k P_{k|k-1} (H_k)^T + R_k]^{-1}. \quad (2.16)$$

The notation $[\cdot]^T$ denote transpose of a matrix $[\cdot]$. Equations (2.12) and (2.13) constitutes the prediction (or time update) step of the Kalman filter while Equations (2.14) and (2.15) form the update step (or measurement update) of the Kalman filter. Note that the term $(z_k - H_k\hat{x}_{k|k-1})$ is the difference between the measurement z_k available at time step k and the predicted measurement, and is called the innovation.

2.2.3 The Extended Kalman Filter

In practice, the target evolution process or the observation process via which the state are partially observed may no longer be linear. Given the processes modelled by (2.1) and (2.2) are nonlinear

$$x_k = f_{k-1}(x_{k-1}) + w_k \quad (2.17)$$

$$z_k = h_k(x_k) + v_k \quad (2.18)$$

where functions $f_{k-1}(\cdot)$ and $h_k(\cdot)$ are nonlinear, and w_k and v_k are still zero mean Gaussian and statistically independent. The extended Kalman filter (EKF) linearizes the models about the current mean and the variance using Taylor series approximation and apply the Kalman filter directly [2, 39]. The posterior pdf is

approximated by a Gaussian distribution. The approximate solution to the Bayes recursion reduces to

$$p_{k-1}(x_{k-1}|z_{1:k-1}) \approx \mathcal{N}(x_{k-1}; \hat{x}_{k-1}, \hat{P}_{k-1}) \quad (2.19)$$

$$p_{k|k-1}(x_k|z_{1:k-1}) \approx \mathcal{N}(x_k|z_{1:k-1}; \hat{x}_{k|k-1}, \hat{P}_{k|k-1}) \quad (2.20)$$

$$p_k(x_k|z_{1:k}) \approx \mathcal{N}(x_k; \hat{x}_k, \hat{P}_k) \quad (2.21)$$

where

$$\hat{x}_{k|k-1} = \tilde{F}_{k-1} \hat{x}_{k-1} \quad (2.22)$$

$$\hat{P}_{k|k-1} = \tilde{F}_{k-1} \hat{P}_{k-1} (\tilde{F}_{k-1})^T + Q_{k-1} \quad (2.23)$$

$$\hat{x}_k = \hat{x}_{k|k-1} + K_k (z_k - \tilde{H}_k \hat{x}_{k|k-1}) \quad (2.24)$$

$$\hat{P}_k = [I - K_k \tilde{H}_k] \hat{P}_{k|k-1} \quad (2.25)$$

where \tilde{F}_{k-1} and \tilde{H}_k are the local linearization of function $f_{k-1}(\cdot)$ and $h_k(\cdot)$ respectively

$$\tilde{F}_{k-1} = \left. \frac{df_{k-1}(x)}{dx} \right|_{x=\hat{x}_{k-1}} \quad (2.26)$$

$$\tilde{H}_k = \left. \frac{dh_k(x)}{dx} \right|_{x=\hat{x}_{k|k-1}} \quad (2.27)$$

$$K_k = \hat{P}_{k|k-1} (\tilde{H}_k)^T [\tilde{H}_k \hat{P}_{k|k-1} (\tilde{H}_k)^T + R_k]^{-1}. \quad (2.28)$$

The performance of the EKF becomes very poor when $f_{k-1}(\cdot)$ and $h_k(\cdot)$ are highly non-linear. This is due to the fact that the effect of higher order terms of Taylor series expansion becomes significant and is not accounted for by the EKF. Attempts have been made to overcome this problem using *unscented transform* [41, 111, 112]. The resulting filter, called *unscented Kalman filter* (UKF) first approximates the true mean and covariance of the pdf, $p_k(\cdot|z_{1:k})$ by a set points, called *sigma* points that are deterministically selected from the pdf itself. It propagates these points through the true nonlinearity so that the updated mean and covariance at the next time step can be estimated. The UKF provides the posterior mean and the covariance that

are accurate to the second order for any non-linearity. The UKF has been shown to outperform EKF for some problems [112]. However, both the EKF and UKF make the Gaussian assumption on the target state.

The Gaussian sum filter (GSF) has been proposed in [1] as a solution to the Bayes filter when the state distribution is non-Gaussian. It works by first approximating the non-Gaussian distribution with a mixture of Gaussian terms. However it too requires linear approximations to the target and likelihood models. The GSF results in the combinatorial growth in the number of mixture components. Using a fixed grid to numerically approximate the non-Gaussian state [47], an alternative method applies the numerical integration for the prediction step and the Bayes rule for the update (or filtering step). However, the computational cost of such a scheme grows prohibitively large with the dimension of the states.

2.2.4 Particle Filters

Recently, a large number of filters based on sequential Monte Carlo (SMC) approximations to the Bayes filter, called *particle filters* are proposed [22, 23, 24, 28, 29, 53, 54, 86], which require no linear or Gaussian assumptions on the dynamical models. These SMC based numerical approximations of the Bayes filter have been very popular for their efficiency, simplicity, and flexibility. These filters are relatively easier to implement and have allowed successful modelling over a wide range of applications.

The basic idea behind particle filters (or otherwise known as SMC filters) is to approximate the pdf $p_k(\cdot|z_{1:k})$ by a weighted set of particles $\{x_k^{(i)}, w_k^{(i)}\}_{i=1}^n$ and to propagate these particles and their weights through time so that the required pdf at the subsequent time steps can be obtained. It only requires the use of a suitable proposal distribution from which the weighted set of particles (or samples) are generated, and the ability to evaluate the target dynamic and the likelihood models. A detailed discussion of the number of particle filtering schemes and recent developments can be found in [24, 46, 54, 68, 86] and is outside the scope of this thesis.

2.3 Single Target Tracking in Clutter

The recursive Bayesian filtering schemes introduced so far in this chapter applies when a target of interest generates a measurement at each time interval. In many practical applications, spurious measurements, called *clutter*, are received at the sensor in addition to possibly a target generated measurement. These measurements are indistinguishable from each other. The rest of this section summarizes key techniques that are applicable to track single targets in the presence of clutter.

In the presence of clutter, conventional approaches first attempt to find the correct association of measurements to track and then apply approximate Bayesian filtering approaches, in particular KF with linearized models, to recursively obtain the state estimate of the target. A simple and cheap approach to data association is *nearest neighbour standard filter* (NNSF) which uses the measurement that is closest to the track in the measurement space and update the mean and covariance of the track using the EKF. However, the NNSF is prone to error in high clutter density. One alternative to NNSF is the probabilistic data association filter (PDAF). The PDAF considers measurement-to-track association for all measurements that fall within a region, called *gate* in addition for the case of miss-detection. A measurement that falls within the gate is called a validated (or gated) measurement. The posterior mean and covariance of the track at the previous time step are updated to find the mean and covariance for each association. As a result, the posterior pdf of the track at the current time is a mixture of Gaussians that are combined to form a single Gaussian in proportion to likelihoods of the association. However, both NNSF and PDAF assume some prior knowledge on the existence of the track as well as its prior state often approximated by its mean and variance. When there is no prior is available on the existence of the track, the integrated probabilistic data association (IPDA) [69] provides a method for initiating a single target track and recursively provides its state estimate. The integrated track splitter (ITS) considers association of an existing track with each of the validated measurements by performing measurement-to-track association over a number of time steps and picks the most likely association based on their likelihoods. This approach is computationally de-

manding.

When the target motion includes maneuvering (or highly nonlinear), interacting multiple models (IMM) has been proposed in [5, 10] and subsequently used with IPDA with success to give integrated probabilistic data association filter (IMM-PDAF) [6]. The concept of multiple models has also been combined with particle filters in multiple-model particle filters [54, 86]. Another approach to handle maneuvering target is variable dimension filter [4] that uses a higher state model once the target maneuver is detected.

2.4 Overview Multi-target Tracking

This section introduces the multi-target tracking problem. It also provides a summary of the key approaches to multi-target tracking problems.

2.4.1 Problem Statements

In a multi-target tracking scenario, the number of targets changes over time as new targets may appear in the surveillance region due to spontaneous target birth or target spawning. Moreover, existing targets may not survive to the next time interval and disappear from the scene. The duration for which a target exists in the surveillance region is unknown. At the sensor, not all targets present in its field of view generate measurements. Furthermore, the collections of measurements available at each time interval often include spurious measurements not generated by the targets, known as clutter. The number of spurious measurements or false alarms also changes randomly with time. Finally, measurements are indistinguishable from each other and hence there is no way of knowing which measurement is generated by a target or is clutter. As a result, multi-target tracking involves jointly estimating the number as well as the states of a finite but time varying number of targets from a given set of finite and time varying number of measurements of uncertain origins.

To summarize, let Z_k denote the set of measurements at the current time interval k , i.e. $Z_k = \{z_{k,1}, \dots, z_{k,M_k}\} \subseteq \mathbb{R}^{n_z}$. A measurement $z_{k,i}$ is either generated by one of N_k targets or is clutter. M_k and N_k represent the number of measurements

and targets respectively at time k , and are both time dependent. Often, we have $M_k > N_k$. Let $Z_{1:k} = \{Z_1, \dots, Z_k\}$ denote the sequence of measurement sets received at the sensor upto time interval k . Given $Z_{1:k}$, the objective is to find the estimate of the target number, \hat{N}_k , the state estimates of N_k targets and estimates of individual state trajectories. A state trajectory of a target is the path followed by the target and is given by the collection of state estimates of a target for the duration it exists. A target track, a track-valued estimate of a target and a target state trajectory are used interchangeably in this thesis. Often, a set of associated measurements is referred as a track in the literature. This should pose no problem as we can obtain the set of state estimates given the associated measurements.

2.4.2 Traditional Approaches to Multi-target Tracking

In essence, the traditional techniques treat multi-target tracking as two separate functions [4, 5, 7, 49, 85, 93]; association of correct measurement to existing tracks via ‘measurement-to-track’ association, and estimation of target tracks based on these associations via single target tracking techniques. Once the decision has been made on likely measurement to track association, the tracks are updated with associated measurements via Kalman filtering, which uses linearized models and requires Gaussian noise approximation.

A simple approach performs the measurement-to-track association is the nearest neighborhood (NN) method, i.e., associate a measurement that is closest in some statistical sense to a track at hand. Only the measurements that fall within the gate are considered. However, when one or more measurements falls within gates of more than one track, likely associations amongst measurements to tracks depend on which track is considered first. The global nearest neighbour (GNN) method, also known as the 2 – D assignment problem, considers all possible ways of associating measurements to tracks and chooses the one that minimizes the sum of the statistical distances between the tracks and measurements.

Multiple hypothesis tracking (MHT) is a widely used technique that in principle, considers all possible associations amongst measurements and tracks at each time step and allows measurement that will arrive in subsequent time steps to re-

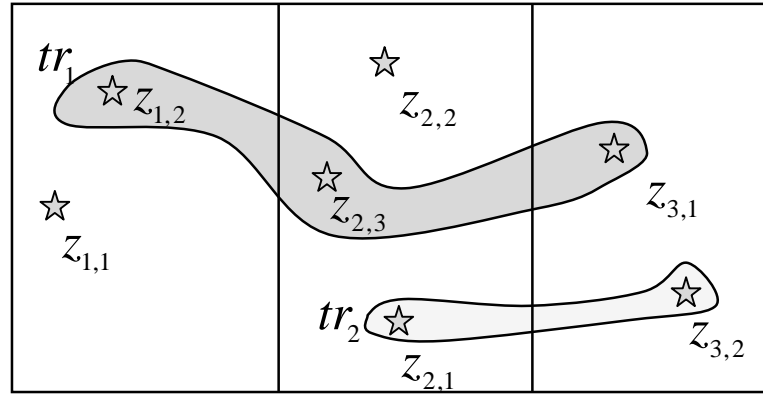
solve the uncertainty in associations at present by maintaining and updating their probabilities. However, the complexity and inherent computational costs of such exhaustive data association are considerable. In practice, MHT uses various ad-hoc techniques to stop the number of hypotheses from growing exponentially with time. Computationally cheaper alternative to MHT is the joint probabilistic data association (JPDA) approach [4, 26]. Instead of allowing all feasible associations to propagate ahead in time, JPDA considers associations that survive gating and combines these associations in proportion to their likelihoods. However, JPDA can only handle a fixed number of targets and its performance suffer when targets are closely spaced [7, 9].

2.5 Multiple Hypothesis Tracking

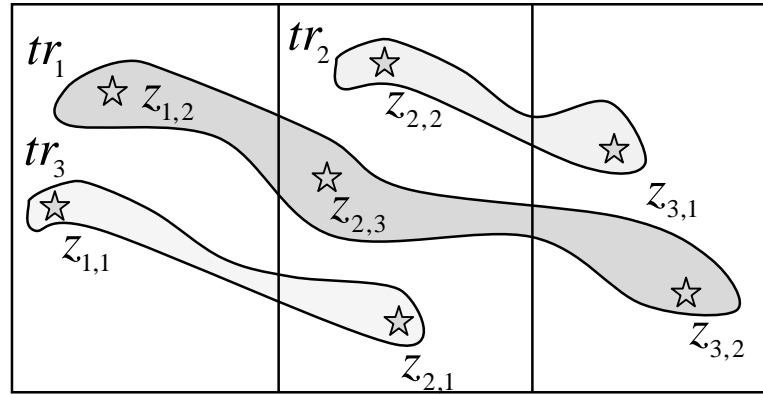
As mentioned in the preceding section, MHT exhaustively searches for all possible measurements to tracks associations over a number of time intervals so that measurements available at subsequent time intervals can be used to resolve uncertainties in associations formed at present. At each time interval, it maintains a number of hypotheses that consider all possible ways of associating past measurements to targets. Since a measurement could be clutter, be generated by an existing target or be generated by a new born target, a hypothesis may discard a measurement as a clutter, associate it with an existing track or use it to initialize a new track while ensuring a measurement is only assigned to one track at maximum. As the new set of measurements is available, a new set of hypotheses is formed for each existing hypothesis. The hypothesis with the highest posterior likelihood is returned. Figure 2.1 shows two possible hypotheses from measurements of the first three time intervals.

Let Ω_k be the collection of all possible partitions (or hypotheses) of $Z_{1:k}$. Each $w_k \in \Omega_k$, called a *joint association event* or a hypothesis satisfies

1. $w_k = \{tr_0, tr_1, \dots, tr_{N_k}\}$
2. $\bigcup_{i=0}^{N_k} tr_i = Z_{1:k}$ and $tr_i \cap tr_j = \emptyset$



(a)



(b)

Figure 2.1: An example of couple of possible hypotheses that can be formed from $Z_1 = \{z_{1,1}, z_{1,2}\}$, $Z_2 = \{z_{2,1}, z_{2,2}, z_{2,3}\}$ and $Z_3 = \{z_{3,1}, z_{3,2}\}$. Scenario (a) hypothesizes two possible tracks; one associated with $z_{1,2}$, $z_{2,3}$ & $z_{3,1}$ and another with $z_{2,1}$ & $z_{3,2}$, and treats $z_{1,1}$ and $z_{2,2}$ as clutter. Scenario (b) considers the possibility of three tracks (two alive and one died at $k = 2$) being in the scene represented by i) $z_{1,2}$, $z_{2,3}$ & $z_{3,2}$, ii) $z_{2,2}$ & $z_{3,1}$ and iii) $z_{1,1}$ & $z_{2,1}$.

3. tr_0 is set of measurements assumed to be spurious

4. $|tr_i| = 2$ for $i = 1, \dots, N_k$.

where N_k denote the number of target for a given w_k . Here tr_i represents the state trajectory of the i^{th} target. Now, the posterior of w_k is given by

$$p(w_k|Z_{1:k}) = K^{-1}p(w_k|Z_{1:k-1})p(Z_k|w_k) \quad (2.29)$$

The aim is to find the likelihood of each partition or hypothesis w_k given $Z_{1:k}$,

which gives the required measurements to tracks associations so that individual target tracks can be obtained. It should be noted that the partitions themselves are functions of measurements.

Though the main idea of MHT was first introduced in [93], a systematic scheme for forming and evaluating measurement-to-track association hypotheses as a solution to multi-target tracking was first outlined in [85]. A number of strategies have been developed over the years to make practical implementations of MHT feasible. A detailed discussion on various implementations of MHT can be found in [7, 9].

This section presents an overview of the *track-oriented* MHT first proposed by Kurien [51, 49, 50]. It will be used to benchmark the performance of new algorithms developed as a part of this study. Track-oriented MHT is preferred over *hypothesis-oriented* MHT (which forms the basis of Reid's algorithm in [85]) for simplicity. While efficient methods for generating hypotheses for hypothesis-oriented MHT has been given in [19], due to the combinatorial nature of hypothesis formation the number of hypotheses generated are much more than that of tracks. It should be noted that the question of which implementation is more efficient to run is still unresolved [8].

2.5.1 Overview of a Track-Oriented MHT

In the track-oriented approach, the collection of measurements that are likely to have originated from the same target is called a track hypothesis². For each target, there may exist multiple track hypotheses representing multiple assignments of measurements over the subsequent time steps and these multiple track hypotheses form a tree structure. The objective now is to choose the most likely track hypothesis from each tree to produce a collection of hypotheses so that each selected track hypothesis represent a true track. A collection of such tracks is known as a global hypothesis. No two track hypotheses in a global hypothesis share the same measurement, i.e., are *consistent*. The sequence of measurements represented by each hypothesis in the

²A track hypothesis is not the same as the hypothesis w_k described above and is only a candidate track for a global hypothesis that captures the notion of the hypothesis w_k . The global hypothesis will be introduced later in this section.

most likely global hypothesis is processed to produce the true track estimates of a target.

Figure 2.2 shows an example of track hypotheses and global hypotheses generation using measurements of the first three time intervals. There are seven track hypotheses at $k = 3$. At $k = 1$, two tracks are initialized for targets T_1 and T_2 with measurements $z_{1,1}$ and $z_{1,2}$ that forms the roots of the trees representing T_1 and T_2 . At $k = 2$, measurements $z_{2,1}$ and $z_{2,2}$ are both gated with track hypotheses $\{z_{1,1}\}$ and $\{z_{1,2}\}$ respectively and hence two track hypotheses for each track are generated giving four hypotheses at $k = 2$. At $k = 3$, while $z_{3,1}$ and $z_{3,3}$ are again gated with the track hypotheses $\{z_{1,1}, z_{2,1}\}$ and $\{z_{1,2}, z_{2,2}\}$, $z_{3,2}$ is not gated with any of the existing track hypotheses. A new track is again initialized for a possible target T_3 . Since no measurement are gated with track hypotheses represented by $\{z_{1,1}, z_{2,2}\}$ and $\{z_{1,2}, z_{2,1}\}$, a target miss-detection is noted.

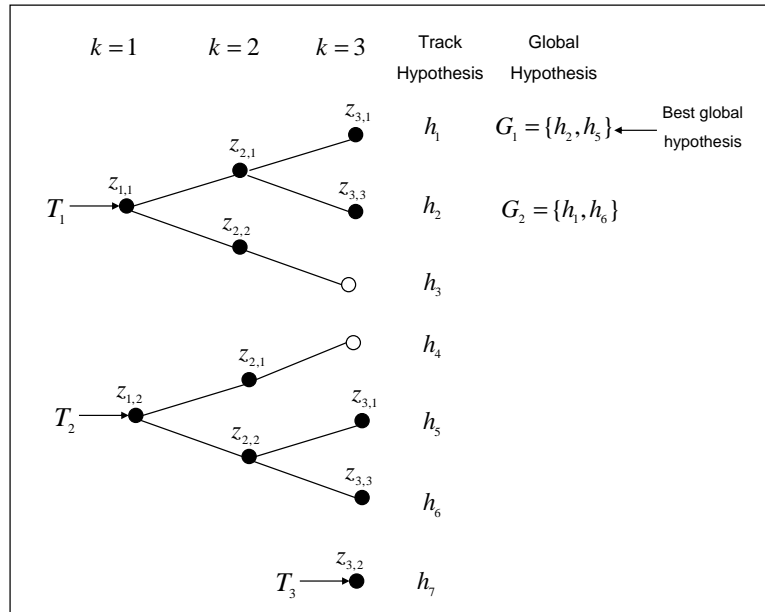


Figure 2.2: An example of track hypotheses and global hypotheses generation using measurements of first three time intervals. T_i represents a possible i^{th} targets and 'o' denotes a target miss-detection.

Figure 2.3 shows the logical overview of the track-oriented MHT algorithm. Given a number of track hypotheses at time interval $k - 1$, MHT allows measurement prediction for each track hypothesis and performs a test to see whether a measurement available at time interval k falls within the gate established around

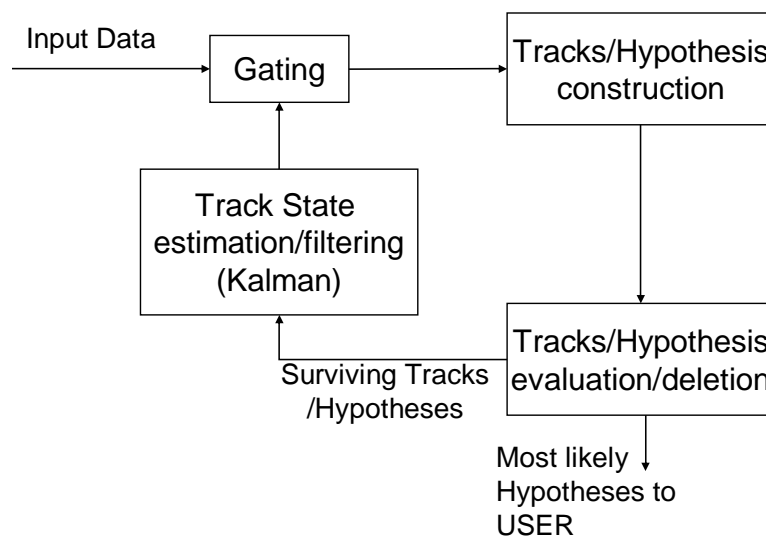


Figure 2.3: Overview of a Track-Oriented MHT algorithm

the measurement prediction. If it does, the track hypothesis from time step $k - 1$ is gated with the noisy measurement of time step k to form a new association hypothesis. Once this association hypothesis survives the pruning and merging, it is then reformed as new track hypothesis for time interval k . The track-oriented MHT makes no assumptions on the origin of the measurements. To begin with tracks are initiated for all measurements and are propagated over subsequent time steps. MHT provides techniques for track-to-measurement association and track hypothesis management so that tracks originating from targets are likely to survive whilst the number of track hypotheses propagated to the next time interval does not explode. Track hypotheses that survive track hypothesis management are updated with its gated measurements and propagated to the next time interval.

The likelihood of each track hypothesis is determined by its likelihood score, often maintained as log-likelihood ratio (LLR). Section 2.5.3 will introduce the calculation of LLRs for track hypotheses.

2.5.2 Measurement-to-Track Association

Gating is often used in MHT in order to eliminate any unlikely measurement-to-track association. A gate is established around the prediction of each track hypothesis in the measurement space via the predicted measurement. Figure 2.4 shows a diagram-

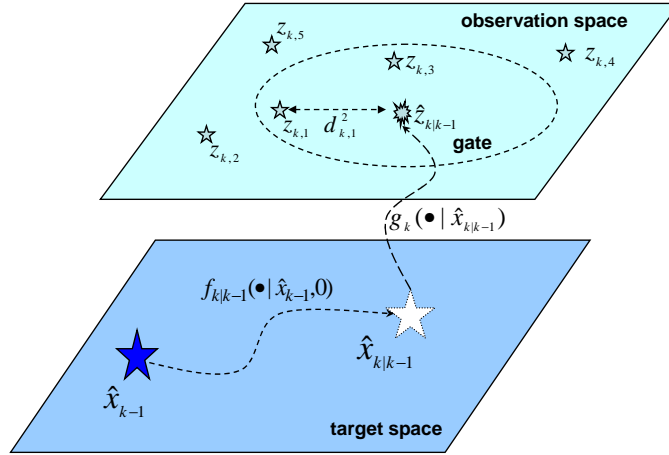


Figure 2.4: An Example of Gating. $\hat{z}_{k|k-1}$ denotes the predicted measurement that is would have been generated by a target with state \hat{x}_{k-1} at time k . It shows measurements $z_{k,1}$ and $z_{k,3}$ falls within the gate established around the measurement prediction of the track with prior state \hat{x}_{k-1} , other three measurements are not considered for measurement-to-track association with it.

matic view of gating. Given that the state and covariance prediction on a track hypothesis is $\hat{x}_{k|k-1}$ and $P_{k|k-1}$, the innovation $\nu_{k,i}$ and the innovation covariance matrix $S_{k,i}$ associated with the measurement $z_{k,i}$ are obtained as

$$\nu_{k,i} = z_{k,i} - \tilde{H}_k \hat{x}_{k|k-1} \quad (2.30)$$

$$S_{k,i} = \tilde{H}_k P_{k|k-1} \tilde{H}_k^T + R_k. \quad (2.31)$$

where \tilde{H}_k is defined in (2.27) and R_k denotes the measurement noise covariance. The quantity $\tilde{H}_k \hat{x}_{k|k-1}$ is the predicted measurement. The innovation is a zero mean Gaussian with the covariance $S_{k,i}$. The random variable $(\nu_{k,i})^T (S_{k,i})^{-1} \nu_{k,i}$ has a chi-square distribution with m degrees of freedom [7], where m denotes the dimension of the measurement. An association of a track hypothesis with a measurement is made if

$$(\nu_{k,i})^T (S_{k,i})^{-1} \nu_{k,i} < \chi_{m,\alpha}^2, \quad (2.32)$$

where $\chi_{m,\alpha}^2$ is the upper $(100\alpha)^{th}$ percentile of a chi-square distribution with m degrees of freedom and if (2.32) is satisfied, the measurement is said to fall within the gate with the probability of $(1 - \alpha)$. A measurement within a gate is also referred to as a validated measurement. For a probability of 0.99, $\chi_{m,\alpha}^2$ has values 6.63, 9.21,

and 11.34 when $m = 1$, $m = 2$, and $m = 3$.

When more than one measurement falls within the gate of a track prediction, multiple association track hypotheses are constructed corresponding to all measurement-to-track associations. When no measurement falls within a gate of an existing track, a target miss-detection is noted in the track and the track is propagated ahead without the measurement update. A new track is started for a measurement that is not associated with any of the existing tracks. Upon the creation of each association track hypothesis, its score or LLR is updated.

2.5.3 Track Hypothesis Score

The likelihood of each track hypothesis is given by its hypothesis score that is often expressed in terms of a log-likelihood ratio (LLR). When a new track hypothesis is created, its log-likelihood ratio, LLR_{new} is calculated as

$$LLR_{new} = \log \left(\frac{\lambda_b(z)}{\lambda_c(z)} \right), \quad (2.33)$$

where $\lambda_b(z)$ and $\lambda_c(z)$ denote the intensity of the birth process of new targets and clutter. Assuming $\lambda_b(z)$ and $\lambda_c(z)$ are constant over the horizon, we have

$$LLR_{new} = \log \left(\frac{\lambda_b}{\lambda_c} \right). \quad (2.34)$$

In the subsequent time steps, the LLR ratio of a track hypothesis is updated by adding an incremental LLR, ΔLLR_k to its LLR from of time interval $k - 1$. When no measurement is associated with a track hypothesis, ΔLLR_k is given by

$$\Delta LLR_k = \log(1 - p_D(x_k)) \quad (2.35)$$

where $p_D(x_k)$ is the probability of target with the state x_k being detected. On the other hand, when a measurement $z_{k,i}$ is gated with an track hypothesis at time

interval k , the incremental LLR is given by

$$\Delta LLR_k = \log \left(\frac{p_D}{\lambda_c} \mathcal{N}(\nu_{k,i}; 0, S_{k,i}) \right). \quad (2.36)$$

If a track hypothesis with LLR, LLR_{k-1} is extended to form an association track hypothesis, the updated LLR, LLR_k is formed by

$$LLR_k = LLR_{k-1} + \Delta LLR_k. \quad (2.37)$$

Hence the uncertainty in an existing association is updated with the measurement available at the current time interval.

2.5.4 Evaluation and Management of Tracks and Hypotheses

Once the measurement-to-track association is completed, the least likely tracks are deleted before the track hypotheses are updated with the validated measurements and are finalized for the next time step. The deletion of the tracks is known as *pruning*. Pruning of the track hypotheses is performed with *track level pruning* and *N-scan pruning* [9, 49].

Clustering of hypotheses into smaller groups known as *clusters* is another technique that reduces the computational cost of MHT. Hypotheses are divided into clusters of track hypotheses so that track hypotheses within each cluster share observations amongst each other and do not share observations with any track hypothesis from other clusters. Clustering of track hypotheses results in breaking up of a large problem into a smaller sets of problems which can be solved in parallel. This results in reduction of the computational complexity of the global hypotheses formation. An efficient algorithm for clustering for the track oriented MHT can be found in [49].

Track level pruning and track confirmation

In track level pruning, track hypotheses that has N (usually 3 or more) consecutive miss-detections are deleted. Track hypotheses that have N (usually 3 or more)

detections are considered to be *confirmed*. There are other methods of confirming tracks in the literature [7, 9]. These include the sequential probability ratio test (SPRT) and Bayesian track confirmation test. Track hypotheses with LLRs less than a *threshold* LLR_{th} are also deleted.

Global hypothesis formation

For each track hypothesis, MHT keeps a record of all other track hypotheses that share at least an observation with it. The record is known as an *inconsistency* or *incompatibility* list. This list is used to form the collection of track hypotheses that may give the estimates of individual target states, their number and their state trajectories. Only confirmed tracks are considered for the global hypothesis formation.

For each cluster, the best global hypothesis is constructed as follows

1. sort the LLR values of all confirmed tracks in a decreasing order
2. include the first track hypothesis in the list for the best global hypothesis
3. include other track hypotheses in the list for the best global hypothesis by taking a track hypothesis from each tree so that all track hypotheses are consistent, i.e., no two track hypotheses share an observation. This also ensures that only a track hypothesis from a tree is included in the list of a global hypothesis.
4. calculate the LLR of the best global hypothesis

A number of other global hypotheses can be formed by choosing the second best confirmed track at the start and following the process given above. As a result, the process of finding the number of global hypotheses is combinatorial and makes up a large part of algorithm processing [9]. In practice, often the best global hypothesis is formed. Looking at the example given in figure 2.2, two possible global hypotheses are G_1 and G_2 . It is assumed that two consecutive target detections are used to confirm a track hypothesis. Track hypothesis h_7 is not considered here as it is not confirmed yet.

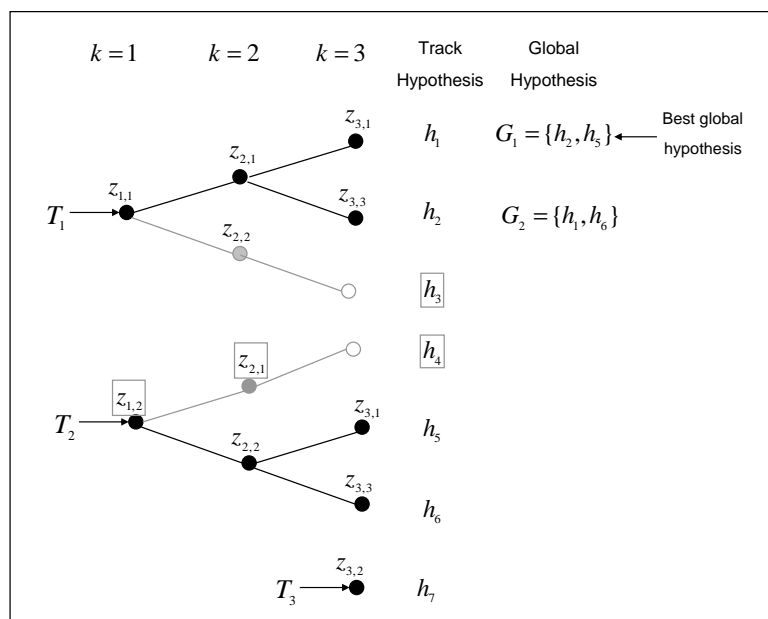


Figure 2.5: Illustration of N-scan Pruning

N-scan pruning

N-scan pruning is used to reduce the number of hypotheses by eliminating the confirmed track hypotheses or branches from every target trees. *N*-scan works as follows:

For each track hypothesis included in the global hypothesis list

1. Go back *N* scans (or time steps) from the node at the current time step,
2. Delete all other branches except the branch represented by the current global hypothesis.

The value of *N*-scan depends on the multi-target tracking scenario. However a reasonable value could be 3 or more [49]. For example, consider the scenario presented in figure 2.5. Assume hypotheses h_1, \dots, h_6 confirmed and the best global hypothesis G_1 include h_2 and h_5 . Using $N = 2$, branches represented by track hypotheses h_2 and h_4 are deleted from the tree T_1 and T_2 respectively.

2.6 Summary

This chapter presented an introduction to target tracking. In particular, the theoretical optimal filter has been outlined for single sensor single target tracking. A number of approximations of the optimal filter has been summarized. This chapter also provided an overview of multi-target tracking problems and outlined a number of traditional multi-target tracking techniques. Finally, an overview of a track-oriented MHT has been included.

Chapter 3

Random Finite Set Framework for Multi-target Tracking

3.1 Introduction

The random finite set (RFS) approach to multi-target tracking provides a Bayesian framework for recursive update of the multi-target posterior density with the noisy measurement set received at the sensor. The probability hypothesis density (PHD) filter is a computationally efficient filter based on the RFS framework and can be used to jointly estimate the number of targets and their states from the noisy measurement sets available upto the current time interval.

This chapter describes the multi-target tracking based on the RFSs. Section 3.2 presents an overview of the random finite set framework for modelling of multi-target systems. The multi-target Bayes filter is also introduced. Section 3.3 describes a computationally efficient approximation of the multi-target Bayes filter, called the probability hypothesis density (PHD) filter. A summary of recent developments of the PHD filter and its applications is given in Section 3.4. Significant challenges associated with the application of the PHD filter are also posed in the context of this thesis. Finally, a summary of this chapter is included in Section 3.5.

3.2 Random Finite Set Approach to Multi-target Tracking

The main idea behind the RFS approach to multi-target tracking is to first treat the collection of targets as a set-valued state called *multi-target state* and the collection of measurements as a set-valued observation, called *multi-observation* and then to characterize uncertainties present in a multi-target tracking problem by modelling these set-valued entities as random finite sets. Rest of this section presents an overview of the RFS approach to multi-target tracking.

3.2.1 Definition of Random Finite Set

In essence, a RFS X is simply a finite set-valued random variable whose cardinality $|X|$ as well as the values of the individual elements in X are also random [20, 27, 95]. The randomness of $|X|$ is described by a discrete probability distribution and an appropriate density characterizes the joint distribution of the elements of X for each $|X|$. In the context of multi-target tracking, the cardinality of $|X|$ could represent the number of targets or the number of measurements, and the values of the elements of X could represent the individual target states or the individual measurements received at the sensor. Hence, the random finite set theory provides a natural framework for handling the problem of multi-target tracking. Finite set statistics (FISST) enables the use of RFSs in order to formulate the multi-target tracking in Bayesian framework [27, 65, 56, 58].

3.2.2 Random Finite Set Model of Multi-target Tracking

The RFS multi-target state model that incorporates individual target dynamics, target birth and target death is described as follows. The collection of the targets at time interval k is modelled by the RFS X_k . Given a realization X_{k-1} of the multi-target RFS at time interval $k - 1$, the behaviour of each target with state

$x_{k-1} \in X_{k-1}$ is modelled by the RFS

$$S_{k|k-1}(x_{k-1}) \quad (3.1)$$

that can either take on state $\{x_k\}$ with probability $p_{S,k}(x_{k-1})$ or \emptyset with probability $1 - p_{S,k}(x_{k-1})$. The evolution of x_k from x_{k-1} is modelled by $f_{k|k-1}(\cdot|x_{k-1})$. A new target may appear in the horizon either due to spontaneous target birth independently of existing targets or by spawning from a target at time interval $k-1$. Hence at time interval k , the multi-target state modelled by the RFS X_k is given by

$$X_k = \left(\bigcup_{x \in X_{k-1}} S_{k|k-1}(x) \right) \cup \left(\bigcup_{x \in X_{k-1}} B_{k|k-1}(x) \right) \cup \Gamma_k, \quad (3.2)$$

where $B_{k|k-1}(x)$ denotes the RFS of targets spawned at time interval k from the target with state x at time interval $k-1$ and Γ_k denotes the RFS of spontaneous birth at time interval k . It is assumed that RFSs $S_{k|k-1}(\cdot)$, $B_{k|k-1}(\cdot)$ and Γ_k are independent of each other.

Similarly the RFS observation model incorporates the measurement likelihood, target detection uncertainty at the sensor and clutter. Assuming the set-valued observation at time interval k is modelled by the RFS Z_k , it is obtained as

$$Z_k = \left(\bigcup_{x \in X_k} \Theta_k(x) \right) \cup K_k \quad (3.3)$$

where $\Theta_k(x)$ denotes the RFS generated by target with state x at time interval k and K_k denotes the RFS of clutter. For each $x_k \in X_k$, $\Theta_k(x_k)$ either contributes measurement $\{z_k\}$ with a probability of detection $p_{D,k}(x_k)$ or \emptyset with a probability of $1 - p_{D,k}(x_k)$. The generation of z_k from x_k is modelled by $g_k(\cdot|x_k)$. It is assumed that the RFSs $\Theta_k(X_k)$ and K_k are independent of each other.

The uncertainties in the evolution of X_k over time and the generation of Z_k can be respectively characterized by the multi-target transition density, $f_{k|k-1}(X_k|X_{k-1})$ and the multi-target measurement likelihood, $g_k(Z_k|X_k)$. The multi-target transition density incorporates all aspects of the multi-target motion such as the random

number of targets, individual target dynamics, target birth, target spawning, target death and target interactions. Similarly, the multi-target measurement likelihood incorporates all sensor characteristics such as the measurement likelihood, the target detection probability and clutter models. Given that the multi-target posterior density of the multi-target state X_{k-1} given $Z_{1:k-1}$, $p_{k-1}(\cdot|Z_{1:k-1})$ is known at time interval $k-1$, the multi-target posterior density $p_k(\cdot|Z_{1:k})$ at time interval k is given by multi-target Bayes filter.

Traditionally, it is difficult to compute the multi-target transition density and measurement likelihood as a Radon-Nikodym derivatives (see [107] for details) of the appropriate probability measures. Finite set statistics (FISST) [27, 65, 58, 62] provides a set of mathematical tools that can be used to construct the multi-target transition density and measurement likelihood from the underlying physical models of sensors, individual target dynamics, target birth and target death.

3.2.3 The Multi-target Bayes Filter

Given the multi-target posterior density $p_{k-1}(\cdot|Z_{1:k-1})$ at time interval $k-1$, the multi-target density predicted to time interval k is given as

$$p_{k-1}(X_k|Z_{1:k-1}) = \int f_{k|k-1}(X_k|X_{k-1})p_{k-1}(X_{k-1}|Z_{1:k-1})\mu_s(dX_{k-1}), \quad (3.4)$$

where μ_s denotes an appropriate measure as described in [107].

The updated multi-target posterior density (or the multi-target filtered density) $p_k(\cdot|Z_{1:k})$ is obtained from the predicted multi-target density using the measurement Z_k set available at time interval k as

$$p_k(X_k|Z_{1:k}) = \frac{g_k(Z_k|X_k)p_{k|k-1}(X_k|Z_{1:k-1})}{\int g_k(Z_k|X)p_{k|k-1}(X|Z_{1:k-1})\mu_s(dX)}. \quad (3.5)$$

While the full Bayes filter have been used in practice [91, 55] with success for a small number of targets, it is computationally intractable as the number of targets increases. Analogous to the Kalman filter that provides a computationally efficient approximation to the theoretically optimal single-target Bayes filter, an approxima-

tion to the multi-target Bayes filter, called the probability hypothesis density (PHD) filter has been proposed by Mahler in a series of papers [56, 57, 58, 59, 60, 64, 61]. The basic idea is to approximate the multi-target posterior density by its first order statistical moments and propagate it with the PHD filter.

3.3 The Probability Hypothesis Density (PHD) Filter

The PHD filter is a suboptimal but computationally tractable alternative to the multi-target Bayes filter. It is a recursion that only propagates the first order moments of the RFS of the targets, which is known as the PHD function or the intensity function. Rest of this section introduces the intensity function and its recursion via the PHD filter. This section also presents the major drawbacks of the PHD filter.

3.3.1 The Probability Hypothesis Density (PHD) or Intensity Function

For a RFS X on $\mathcal{X} \subseteq \mathbb{R}^{n_x}$ with a probability distribution \mathcal{P} , its first order moment, is a non-negative function v on \mathcal{X} , called the intensity or the PHD function, with the property that for any closed subset $S \subseteq \mathcal{X}$ [20, 95]

$$\int_S v(x)dx = \int |X \cap S| \mathcal{P}(dX) \quad (3.6)$$

where $|X|$ denotes the cardinality of X . Given the intensity function v , its integral over any region S gives an estimate for the number of elements in X that are present in S . The local maxima of the intensity function v are points in \mathcal{X} with the highest local concentration of expected number of elements, and hence can be used to generate estimates for the elements of X .

3.3.2 The PHD Recursion

The PHD filter is a computationally cheaper alternative to propagating the multi-target posterior density recursively in time and propagates the posterior intensity function of the multi-target RFS as follows [60]: given the posterior intensity v_{k-1} at time interval $k-1$, the intensity function $v_{k|k-1}$ to time interval k is predicted as

$$v_{k|k-1}(x) = \int [p_{S,k}(\xi) f_{k|k-1}(x|\xi) + \beta_{k|k-1}(x|\xi)] v_{k-1}(\xi) d\xi + \gamma_k(x), \quad (3.7)$$

and the posterior intensity v_k at time interval k is updated as

$$v_k(x) = [1 - p_{D,k}(x)] v_{k|k-1}(x) + \sum_{z \in Z_k} \frac{p_{D,k}(x) g_k(z|x) v_{k|k-1}(x)}{\kappa_k(z) + \int p_{D,k}(\xi) g_k(z|\xi) v_{k|k-1}(\xi) d\xi}, \quad (3.8)$$

where $\kappa_k(\cdot)$ is the intensity of the clutter RFS and equals $\lambda_c c_k(z)$; Z_k is the multi-target measurement available at time interval k ; $\gamma_k(\cdot)$ denotes the intensity of spontaneous target birth; $\beta_{k|k-1}(\cdot|\xi)$ denotes the intensity of the target RFS spawned by a target of previous state ξ at time interval k ; and $c_k(\cdot)$, denotes the clutter density that is often assumed to be uniform density in the literature.

For the recursion given in (3.7)–(3.8), the following assumptions hold:

1. Each target evolves and generates observations independently of one another.
2. The clutter RFS is Poisson (or distribution on the number of clutter is Poisson) and independent of the target-generated observations.
3. The predicted multi-target RFS is Poisson.

First two assumptions are common in most multi-target applications [4, 9]. The third assumption is a simplification needed to derive the PHD update. A RFS X is a *Poisson* with the mean $N = \int v(x) dx$ and given a cardinality, elements of X are i.i.d. according to v/N . Thus a Poisson RFS is completely characterized by its intensity.

Further details on the derivation of the PHD filter and the underlying assumptions can be found in [60, 105]. An tutorial introduction to the proof can also be found in [13, 96].

3.3.3 Implementations of the PHD filter

Though the PHD recursion consists of equations that are considerably simpler than those of the multi-target Bayes filter, it still requires solving multi-dimensional integrals that do not have closed-form solutions in general. When the closed form solution does exist, the Gaussian-mixture PHD (GM-PHD) filter provides it [103, 104]. A generalized SMC implementation of the PHD filter, called the SMC-PHD filter has been proposed in [106, 107]. Similar SMC implementations of the PHD filter have also been proposed in [90, 116, 89].

While the PHD filter provides a posterior intensity function conditional on $Z_{1:k}$, additional techniques should be employed to determine the location of its peaks so that the state estimates of individual targets can be obtained. Further details on the peak extraction techniques will be included in the subsequent chapters which discuss the implementation of both the SMC-PHD filter and the GM-PHD filter.

3.3.4 Shortcomings of the PHD Filter

One of the main shortcomings of the PHD filter is that it is association free. The state estimates of the individual targets given by the PHD filter have no labels associated with them. Given two sets of target state estimates of two consecutive time intervals, there is no way of knowing which two state estimates from these two time intervals belong to the same target. The lack of temporal association renders the PHD filter unable to provide estimates of the state trajectories of individual targets, i.e., individual target tracks. Another shortcomings of the PHD filter is its inability to maintain identities of targets as they cross each other or come closer each other within a certain distance of one another [27, 60]. This thesis is aimed at providing solutions to both of these shortcomings.

3.4 Recent Extensions of the PHD Filter

The development of the PHD filter as a computationally efficient approximation to the multi-target Bayes filter have attracted substantial interests. This it was

initially proposed as a tool primarily for group target tracking and detection [59], a number of implementations of the PHD filter have been developed and applied in various applications. A number of sequential Monte Carlo (SMC) methods have been developed to approximate the PHD filter in order to obtain its tractable solution [90, 89, 106, 107, 116, 74]. Zajic *et. al.* and Sidenbladh have independently proposed particle filtering methods for the PHD filter respectively in [116] and [90], which can be considered special cases of the generalized SMC implementation of the PHD filter proposed by Vo *et. al.* in [106, 107]. Convergence properties of the particle PHD filter has been established by Vo *et. al.* [107], Clark [15] and Johansen *et. al.* [40]. A kernel based sequential Monte Carlo (SMC) approximation of the PHD filter, called *convolution PHD filter* has been proposed in [74]. The convolution PHD filter does not require the knowledge of the observation likelihood and can operate in the presence of zero or near-zero observation noise. A closed-form solution to the PHD filter has been derived in [103, 104] and is provided by the GM-PHD filter.

Practical applications of the PHD filter have also been the subjects of a number of papers [16, 18, 36, 37, 43, 82, 89, 98, 101]. The SMC-PHD filter has been applied to sonar problems in [16, 43]. The SMC-PHD filter has been applied to bearing-only tracking in [101] and, to target detection and tracking using bistatics radio-frequency observations in [98]. Ikoma *et. al.* have applied the SMC-PHD filter in computer vision to track feature points in dynamic images. The SMC-PHD filter has also been considered for track-before-detect approach to multi-target tracking [82]. The PHD filter has been considered to tracking an unknown number of sources using an array of sensors. Recently, the GM-PHD filter has also been applied to sonar problems jointly for multi-target detection and estimation [18].

The PHD filter has been shown to handle the maneuvering targets [80, 83, 102]. Punithakumar *et. al.* have proposed a multiple model version of the PHD filter in [83]. In [102], it is shown that the SMC-PHD filter is capable of accurately estimating the motions of multiple maneuvering targets that appear and disappear at unknown time instants. A closed form solution to the PHD filter for linear jump Markov systems has been proposed in [80]. Furthermore, the SMC-PHD filter has also been considered for sensor networks [3, 84].

A main shortcoming of the PHD filter is its inability to provide track labelling of the state estimates so that individual target state trajectories can be obtained. The issue of track labelling and continuity has been considered for the PHD filter in [14, 52, 78, 76, 77, 17, 75]. The early attempts for the data association of the PHD filter has been considered independently in [78] and [52]. Schemes presented in [78, 77] propose to use the PHD filter to reduce the size of the data input to a multiple hypothesis tracker. Lin *et. al.* proposed to associate peaks of the PHD function between two subsequent time intervals via gating in order to construct tracks. Recently, an ‘estimate-to-track’ association has been considered by associating target state estimates between the subsequent time steps [14]. However, such a technique is a special case of the PHD-with-association filter and assumes that the estimates given by the PHD filter are almost free of clutter. A more efficient ‘estimate-to-track’ association technique for the SMC-PHD filter has been presented in [76], which performs ‘estimate-to-track’ association without using traditional data association techniques. Recently, based on the GM-PHD filter, the GM-PHD tracker has been proposed in [17], which provides the track labels of individual target estimates by tagging individual Gaussian terms of the mixtures. An efficient track management scheme for the GM-PHD tracker has been proposed for the GM-PHD tracker in [75].

3.5 Summary

This chapter included an overview of the Bayesian framework for handling multi-target tracking problems based on the random finite set theory. The multi-target Bayes filter based on FISST has been introduced. This chapter also described the PHD filter, which is the subject of this thesis. Finally, a summary of the recent developments and applications of the PHD filter has been included.

Recently, the poor performance of the PHD filter when the probability of detection is low has been noted in [25]. This is a consequence of the fact that the PHD filter propagates only the mean of the target number estimate. This has led to the development of the PHD filters that propagate higher order statistics of the target

number estimate [63]. In particular, the performance of the cardinalized PHD filter have been promising [108, 109, 110].

Chapter 4

Multi-target Tracking with the SMC-PHD Filter

4.1 Introduction

The PHD filter is a computationally efficient approximation of the RFS Bayes multi-target filter, which propagates the first moment or the intensity function of the multi-target RFS. Nevertheless, the PHD recursion requires solving multi-dimensional integrals that do not have closed-form solutions in general. Sequential Monte Carlo (SMC) methods provide a way of solving such integrals and a generalized SMC implementation of PHD filter, called the *SMC-PHD filter* has been proposed in [106, 107]. The convergence property of the SMC-PHD filter has been established in [15, 105]. However, the existing SMC implementations of the PHD filter only provide the state estimates of individual targets. It keeps no record of the target identities and avoids the problem of associating the state estimates obtained at each time interval to individual targets. Recently, some attempts have been made to address the task of associating individual state estimates to their respective targets for the SMC-PHD filter [14, 52, 76, 77, 78].

Section 4.2 of this chapter provides a description of the SMC-PHD filter that was presented by Vo *et. al.* in [106, 107]. A summary of recent extensions of the PHD filter for the track association is also given in this section. Two extensions of the PHD filter that employ existing data association methods for the purpose of track association are presented in Section 4.3. For illustration purposes, simulation results of the proposed schemes for a number of tracking scenarios are included in Section 4.3 and their performances are benchmarked against that of a track-oriented

MHT. Section 4.4 presents a computationally efficient extension of the PHD filter, which does not employ existing data association methods. Finally, this chapter is summarized in Section 4.5

4.2 The SMC-PHD Filter

For general multi-target models that include nonlinear and non-Gaussian target dynamical models, the sequential Monte Carlo approximation of the PHD filter has been proposed as a general multi-target tracking algorithm [106, 107]. As each time step the posterior intensity function is approximated by a weighted set of particles, from which the state estimates of individual targets are generated via standard clustering techniques. The expected number of the targets is given by the sum of the particle weights.

Given an initial intensity function v_0 at time step $k = 0$ and the sequence of measurement sets $Z_{1:k}$ upto time step k , the posterior intensity function at time step $k > 0$ is given as follows.

Initialization Step: At time step $k = 0$, the SMC-PHD filter is initialized with the particle representation of the initial intensity function v_0 , i.e., $\{x_0^{(i)}, w_0^{(i)}\}_{i=1}^{L_0}$, such that

$$\hat{v}_0(x) = \sum_{i=1}^{L_0} w_0^{(i)} \delta(x - x_0^{(i)}) \quad (4.1)$$

where $\delta(x)$ is the Dirac delta function, L_0 is the number of particles at $k = 0$, $w_0^{(i)} = N_0/L_0$ and N_0 denotes the number of targets at $k = 0$ (i.e. $\int v_0 dx = N_0$).

Prediction Step: For time step $k > 0$, given that the intensity function v_{k-1} at time step $k-1$ is approximated by the set of particles and their weights, $\{x_{k-1}^{(i)}, w_{k-1}^{(i)}\}_{i=1}^{L_{k-1}}$ as

$$\hat{v}_{k-1}(x) = \sum_{i=1}^{L_{k-1}} w_{k-1}^{(i)} \delta(x - x_{k-1}^{(i)}) \quad (4.2)$$

the predicted intensity function $\hat{v}_{k|k-1}$ at time step k is given by

$$\hat{v}_{k|k-1}(x) = \sum_{i=1}^{L_{k-1}+J_k} \tilde{w}_{k|k-1}^{(i)} \delta(x - \tilde{x}_k^{(i)}) \quad (4.3)$$

where

$$\tilde{x}_k^{(i)} \sim \begin{cases} q_k(\cdot | x_{k-1}^{(i)}, Z_k), & i = 1, \dots, L_{k-1} \\ p_k(\cdot | Z_k), & i = L_{k-1} + 1, \dots, L_{k-1} + J_k \end{cases} \quad (4.4)$$

and

$$\tilde{w}_{k|k-1}^{(i)} = \begin{cases} \frac{\phi_{k|k-1}(\tilde{x}_k^{(i)}, x_{k-1}^{(i)})}{q_k(\tilde{x}_k^{(i)} | x_{k-1}^{(i)}, Z_k)} w_{k-1}^{(i)}, & i = 1, \dots, L_{k-1} \\ \frac{1}{J_k} \frac{\gamma_k(\tilde{x}_k^{(i)})}{p_k(\tilde{x}_k^{(i)} | Z_k)}, & i = L_{k-1} + 1, \dots, L_{k-1} + J_k \end{cases} \quad (4.5)$$

In the particle representation of $\hat{v}_{k|k-1}$, the L_{k-1} particles are predicted forward from time step $k-1$ by the kernel $\phi_{k|k-1}$ and the additional J_k particles are drawn to detect the new born targets. The number of particles drawn at each time step can be function of time step k to accommodate the time-varying number of the new born targets so long as the average number of the new born particles per target is maintained, i.e., $J_k = \rho \int \gamma_k(x) dx$ and ρ denotes the number of particles per target.

Update Step: Given that the particle representation of the predicted intensity function is available at time step k , i.e., $\{\tilde{x}_k^{(i)}, \tilde{w}_{k|k-1}^{(i)}\}_{i=1}^{L_{k-1}+J_k}$, the updated intensity function \hat{v}_k is given by

$$\hat{v}_k(x) = \sum_{i=1}^{L_{k-1}+J_k} \tilde{w}_k^{(i)} \delta(x - \tilde{x}_k^{(i)}) \quad (4.6)$$

For $i = 1, \dots, L_{k-1} + J_k$, the particle weight $\tilde{w}_k^{(i)}$ is updated as

$$\tilde{w}_k^{(i)} = \left[1 - p_{D,k}(\tilde{x}_k^{(i)}) + \sum_{z \in Z_k} \frac{p_{D,k}(\tilde{x}_k^{(i)}) g_k(z | \tilde{x}_k^{(i)})}{\kappa_k(z) + C_k(z)} \right] \tilde{w}_{k|k-1}^{(i)} \quad (4.7)$$

where $C_k(z) = \sum_{j=1}^{L_{k-1}+J_k} p_{D,k}(\tilde{x}_k^{(j)}) g_k(z | \tilde{x}_k^{(j)}) \tilde{w}_{k|k-1}^{(j)}$. The update step of the SMC-PHD filter uses the measurement set Z_k to update the particle weights at each time step.

Resampling Step: Given a particle representation of the updated intensity function \hat{v}_k , i.e., $\{\tilde{x}_k^{(i)}, \tilde{w}_k^{(i)}\}_{i=1}^{L_{k-1}+J_k}$, the new set of particles and their weights, i.e., $\{x_k^{(i)}, w_k^{(i)} / \tilde{N}_k\}_{i=1}^{L_k}$ are obtained by resampling from $\{\tilde{x}_k^{(i)}, \tilde{w}_k^{(i)} / \tilde{N}_k\}_{i=1}^{L_{k-1}+J_k}$, where $\tilde{N}_k = \sum_{i=1}^{L_{k-1}+J_k} \tilde{w}_k^{(i)}$ denotes the estimate of the target number at time step k . The particle

weights are scaled by \tilde{N}_k so that the sum of the particle weights in the resampled particle set is the same as before.

The resampling step is needed in the filter to avoid the problem of degeneracy as a number of the particle weights would otherwise become negligible after a few iterations. It should be noted that the resampling step given above maintains the number of particles per target constant so that the number of particles does not increase with time, i.e., $L_k = \rho\tilde{N}_k$. Otherwise, we have $L_k = L_{k-1} + J_k$ as the J_k number of particles are added at each time step.

Once the SMC-PHD filter is initialized at time step $k = 0$, the *prediction*, *update* and *resampling* steps are repeated at the subsequent time steps as the measurement set Z_k becomes available. A generalized SMC-PHD filter is summarized in Table 4.1.

4.2.1 Multi-target State Estimation

From the particle representation of the posterior intensity $\{x_k^{(i)}, w_{k|k-1}^{(i)}\}_{i=1}^{L_k}$ at each time step, the state estimates of the individual targets are generated by extracting peaks of \hat{v}_k via clustering. This has been achieved via the expectation-maximization (EM) method in [16, 90, 97]. Similarly, the k -means algorithm has been used in [106, 107]. While the EM method iteratively attempts to find the Gaussian mixture that best fits the particle representation of the posterior intensity \hat{v}_k , the k -means clustering technique partitions the given particle representation into the number of clusters given by the integer approximation of the expected number of targets, \hat{N}_k , i.e., $\hat{N}_k = \lfloor \tilde{N}_k \rfloor$ and $\lfloor \cdot \rfloor$ denote the integer approximation. The center of each cluster represents a local maximum of the intensity function and hence gives the state estimate of a target. The performance of both techniques have been studied by Clark in [13]. It has been shown that the EM algorithm is computationally expensive and performs poorly in comparison to the k -means clustering. In the SMC-PHD filter based tracking algorithms presented in this chapter, the k -means clustering has been employed for multi-target state estimation.

4.2.2 Track Association for the SMC-PHD Filter

One attractive feature of the PHD filter is that it avoids the issue of explicit data association which besets most traditional approaches to multi-target tracking. Existing implementations of the PHD filter recursively provides set-valued estimates of the multi-target RFS, which is a collection of the state estimates of individual targets and makes no attempts to identify the state estimate of one target from another. In other words, given the state estimates from targets from two different time steps, there is no way of knowing which two state estimates from these time steps represent the same target. Hence the SMC-PHD filter cannot provide the state trajectory estimates of individual targets.

Recently, attempts have been made at adding data association capability to the SMC-PHD filter so that the track-valued estimates of individual targets can be obtained [14, 52, 76, 77, 78]. Two schemes developed as a part of this study combine the SMC-PHD filter with existing data association techniques albeit in a different way and are included in Section 4.3. The techniques, called the *PHD-with-association filter* and the *MHT-with-PHD clutter filter* both use the PHD filter to reduce the size of the measurement sets on which the data association techniques are applied. Furthermore, a computationally efficient estimate-to-track association scheme based on the improved implementation of the SMC-PHD filter has been developed as part of this study. In the proposed filter, called the *cluster-indexed SMC-PHD filter*, the particle representation of the posterior intensity function is updated to include particle labels. These particle labels are used to create and to store the track identity of the posterior intensity particles, and to perform the 'estimate-to-track' association. The techniques developed as a part of this study have appeared in [76, 77, 78].

Data association for the PHD filter has also been addressed in [52] and more recently, in [14]. The works presented in [78] and [52] though independent of each other, are amongst the first attempts at obtaining the state trajectory estimates of individual targets with the PHD filter. In [52], the peak-to-track association is considered as a two-dimensional assignment problem. However, it does not use the

state estimates that arrive subsequently to reduce the uncertainty in the association. Clark *et. al.* present two methods for the data association with the SMC-PHD filter in [14]; the first method uses partitions created during peak extraction via clustering techniques and is not general enough to handle spontaneous target birth. The second method proposed in [14] finds the best association of target state estimates over consecutive time steps and is a special case of the PHD-with-association filter in which the uncertainty in the association are not improved by using the estimates that will be given by the PHD filter later in time.

4.3 Data Association Combined with the SMC-PHD Filter

This section presents two novel methods that attempts to combine existing data association techniques with the SMC-PHD filter in order to generate the track-valued estimates of the individual targets.

In particular, the ‘PHD-with-association’ filter treats the state estimates of individual targets given by the SMC-PHD filter as the new measurements and performs partition on batches of estimates over time by performing ‘estimate-to-track’ association in order to produce the state trajectory estimates of individual targets. The size of the target estimate set generated by the SMC-PHD filter is much smaller than that of the actual measurement set as the SMC-PHD filter outputs are almost free of clutter. This results in a substantial reduction on the computation and memory, which would have been required if data association were to be performed directly on the measurement sets. Furthermore, individual data partitions produced by the estimate-to-track association already consist of target state estimates and hence require no further filtering on them. We show in Section 4.3.3 that the scheme performs comparatively well against the benchmark algorithm, MHT. The SMC implementation of the PHD filter means this technique will be applicable to multi-target tracking problems with non-linear and/or non-Gaussian target and measurement models.

This section also presents the ‘MHT-with-PHD clutter’ filter, in which the PHD filter is used as a clutter filter to eliminate the measurements that are unlikely to have originated from targets before the measurements are tracked with the existing data-association algorithms like MHT. This can be seen as a gating operation on the measurements on a global level and eliminates most of the spurious measurements provided the estimates given by the SMC-PHD filter are good.

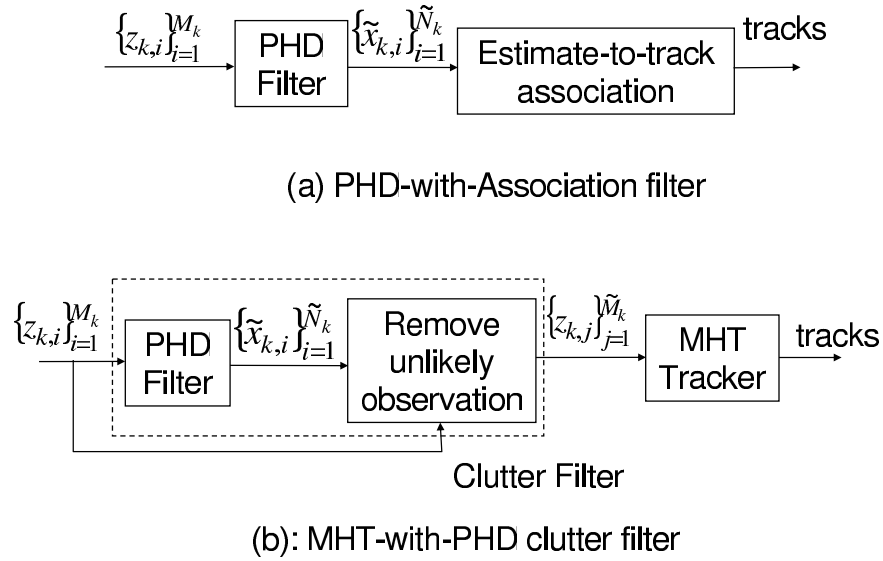


Figure 4.1: Multitarget Tracking with the PHD filter.

4.3.1 The PHD-with-Association filter

This approach takes the set-valued estimates of individual targets given by the SMC-PHD filter and performs data association on them to produce correct association of target estimates to targets (see Figure 4.1(a)). At time step k , the SMC-PHD filter provides an estimate of the number of the targets present in the surveillance region, \hat{N}_k and their set-valued state estimates, i.e. \tilde{X}_k . Assuming these estimates are sufficiently accurate, we may regard the output of the PHD filter as defining a new observation model given by

$$\tilde{z}_{k,i} = \tilde{x}_{k,i} = x_{k,i} + n_{k,i}, \quad i = 1, \dots, \hat{N}_k \quad (4.8)$$

and

$$\tilde{Z}_k = \{\tilde{z}_{k,i}\}_{i=1}^{\hat{N}_k} \quad (4.9)$$

where \hat{N}_k is the estimate of the target number at time step k and \tilde{Z}_k is the new observation set given by the SMC-PHD filter. The error in the state estimate, $n_{k,i} = \tilde{x}_{k,i} - x_{k,i}$ can be regarded as the additive noise. Thus, regardless of the fact that the observation process at the sensor is nonlinear/non-Gaussian, the data-association functionality is given a linear observation process. Implicit in this scheme is the assumption that $\hat{N}_k \approx N_k$. There are a number of ways to estimate the statistics of the noise $n_{k,i}$ [66, 67]. For the sake of simplicity, we assume $n_{k,i}$ is a zero-mean Gaussian process with variance $\tilde{Q}_{k,i}$ that can be estimated from the particle approximation of the PHD recursion. In simulations, we find that this approach works well even though the true distribution of $n_{k,i}$ may not be Gaussian.

This scheme uses the SMC-PHD filter first to recursively produce estimates of target states, \tilde{X}_k from the noisy observations Z_k and then applies data association techniques on \tilde{X}_k , $k \geq 0$ to produce individual target tracks treating \tilde{X}_k as the new observation set at time step k . The implementation of the ‘estimate-to-track’ association is very similar to the track-oriented MHT introduced in Section 2.5. However other versions of MHT should be applicable provided the effect of the PHD filter on the measurements is reasonable accounted. Table 4.2 presents a summary of the PHD-with-association filter. The motivation behind the PHD-with-association filter scheme is that the size of the modified observation set \tilde{Z}_k given by Eq. (4.8) is smaller than that of the original observation set Z_k . This is because almost every observation in \tilde{Z}_k is associated with a target where as Z_k has additional clutter. As a result, a much smaller number of track hypotheses are created at each time step and the computational cost of the ‘estimate-to-track’ association becomes smaller. Moreover, pruning of the track hypotheses can be simpler than in the MHT due to the smaller number of hypotheses thus reducing the overall complexity of the MHT. Since a track hypothesis consists of the state estimates that are associated with a target over time, there is no need for further filtering on them. This scheme is readily available to tracking scenarios that have nonlinear/non-Gaussian state models.

4.3.2 The MHT-with-PHD Clutter Filter

In the above method, the PHD filter was effectively used as a clutter pre-filter that feeds a modified observation set to the data-association functionality, namely MHT. We now describe how to use the PHD filter as a clutter filter but without modifying the observation process seen by the data association functionality. The aim would be to eliminate the most of the measurements that are likely to be clutter so that the computational cost of the data association would be reduced. In addition, the number of false tracks picked by the MHT should decrease.

The proposed scheme is represented by the block diagram in Figure 4.1(b). The SMC-PHD filter outputs \tilde{X}_k are used to define validation gates in the observation space. The observations that fall outside the gates are discarded as clutter and the reduced observation set is feed to the MHT to produce track-valued estimates of the targets. In summary, given an observation set $Z_k = \{z_{k,i}\}_{i=1}^{M_k}$ at time step k , the new observation set is given by

$$\tilde{Z}_k = \{z_{k,i} : g_k(z_{k,i}|\tilde{x}_{k,j}) > g_d \text{ for some } j\},$$

where $\tilde{X}_k = \{\tilde{x}_{k,j}\}_{j=1}^{\tilde{N}_k}$ is the PHD output at time step k and g_d is the observation gate threshold. Provided the measurement noise is additive and Gaussian, the test for gating becomes very similar to the method of gating used in the ‘measurement-to-track’ association described in [9]. Approximating each $\tilde{x}_{k,j} \in \tilde{X}_k$, with its mean position $\tilde{x}_{k,j}$ and covariance $\tilde{Q}_{k,j}$, a measurement $z_{k,i}$ is included in $\tilde{Z}_{k,i}$ if

$$(z_{k,i} - g_k(\tilde{x}_{k,j})) S_k^{-1} (z_{k,i} - g_k(\tilde{x}_{k,j}))^T < G_{th} \quad (4.10)$$

where $S_k = H_{k,j} \tilde{Q}_{k,j} (H_{k,j})^T + R_k$, R_k is the covariance of the measurement noise, G_{th} is the size of the observation gate and

$$H_{k,j} = \left. \frac{\partial g_k(x)}{\partial x} \right|_{x=\tilde{x}_{k,j}}.$$

In cases when noise is only additive, the unscented transform [41, 111] can be used

instead.

The choice of the gate size g_d or G_{th} depends on the tracking scenarios as well as the accuracy of the target state estimates given by the SMC-PHD filter. As the approximation of the full posterior with its PHD requires high SNR [60], the size of g_d could be small. In effect, the SMC-PHD filter is used to eliminate most of the observations that are unlikely to have originated from the targets. Hence, this clutter filter approach can be viewed as a way of performing gating on a global level. The implementation of the MHT-with-PHD clutter filter is summarized in Table 4.3.

The main motivation behind the MHT-with-PHD clutter filter is to remove out most of the clutter by exploiting the fact that the state estimates of the targets given the PHD filter are fairly accurate. These estimates have been shown to outperform MHT in terms of their multi-target miss distances later in this section. This type of global gating should perform well in nonlinear/non-Gaussian case as this does not approximate the nonlinearity present in the target dynamics and/or measurement process. Further investigation is required to determine the merit of tradeoff between the added computational cost of the global gating and the reduction in that of the data association as a result of smaller observation set.

4.3.3 Simulation Results

For illustration purposes, we consider a two-dimensional scenario, in which each target can appear or disappear in the horizon at any time. The number of targets at any time is unknown and time-varying. The target states consist of positions and velocities. Each target moves according to the following linear and Gaussian target dynamics,

$$x_k = \begin{bmatrix} 1 & T & 0 & 0 \\ 0 & 1 & 0 & 0 \\ 0 & 0 & 1 & T \\ 0 & 0 & 0 & 1 \end{bmatrix} x_{k-1} + \begin{bmatrix} T^2/2 & 0 \\ T & 0 \\ 0 & T^2/2 \\ 0 & T \end{bmatrix} \begin{bmatrix} v_{1,k} \\ v_{2,k} \end{bmatrix} \quad (4.11)$$

where $x_k = [p_k^x, \dot{p}_k^x, p_k^y, \dot{p}_k^y]^T$, and $[p_k^x, p_k^y]^T$ and $[\dot{p}_k^x, \dot{p}_k^y]^T$ represent position and velocity of the target at time step k . $T = 1$ unit in time is the sampling period. The

process noise $v_{1,k}$ and $v_{2,k}$ are independent zero mean Gaussian noise.

The bearing θ_k and range r_k measurement of a target are generated by a sensor located at $[0, -100]^T$ and are given by

$$\theta_k = \arctan\left(\frac{p_k^x}{p_k^y + 100}\right) + w_{1,k} \quad (4.12)$$

$$r_k = \sqrt{((p_k^x)^2 + (p_k^y + 100)^2)} + w_{2,k} \quad (4.13)$$

The measurement noise $w_{1,k}$ and $w_{2,k}$ are independent zero mean Gaussian noise with standard deviations. Moreover, the measurement noise is also independent of the process noise. Without the loss of generality, probability of detection is assumed almost unity.

The particle implementation of the PHD filter uses 1000 particles per target. The proposal densities used for importance sampling are $q_k = f_{k|k-1}$ and $p_k = \mathcal{N}(\cdot|x_0, Q_b)$. At each time step, the target state estimates are extracted from the set of particles representing the updated intensity function by applying the k -means clustering technique. This particular implementation of the track-oriented MHT uses an ellipsoid gate of size 9.21. Track hypotheses are confirmed once they have at least two target detections. A hypothesis track is deleted if it has either three or more consecutive target miss-detections. Confirmed tracks are also subject to N -scan pruning with N equals three. Tracks are not deleted on the basis of their likelihoods as this implementation of the MHT can handle the number of track hypotheses without. For data output, the best global hypothesis is considered. G_{th} takes a value of 9.21 in the implementation of the MHT-with-PHD clutter filter. Rest of this section present simulation results for a number of tracking scenarios.

Example 1

Figure 4.2 shows an example in which target moves within the surveillance region $[-100, 100] \times [-100, 100]$ and $\sigma_{v_{1,k}} = 1.0$ and $\sigma_{v_{2,k}} = 0.1$. Figure 4.2 shows the ground truth positions of four tracks that appear around the origin and move radially outwards. The start and finish time of each track is displayed in Figure 4.3 that

plots the x and y components of the tracks separately against time. An existing target has a survival probability of $p_{S,k} = 0.95$ and this probability is state independent. We assume that the target birth follows a Poisson model with the intensity $0.2\mathcal{N}(\cdot|x_0, Q_b)$, where $\mathcal{N}(\cdot|x_0, Q_b)$ represents a normal distribution with a mean x_0 , covariance Q_b and

$$x_0 = \begin{bmatrix} 0 \\ 3 \\ 0 \\ -3 \end{bmatrix}, \quad Q_b = \begin{bmatrix} 10 & 0 & 0 & 0 \\ 0 & 1 & 0 & 0 \\ 0 & 0 & 10 & 0 \\ 0 & 0 & 0 & 1 \end{bmatrix}. \quad (4.14)$$

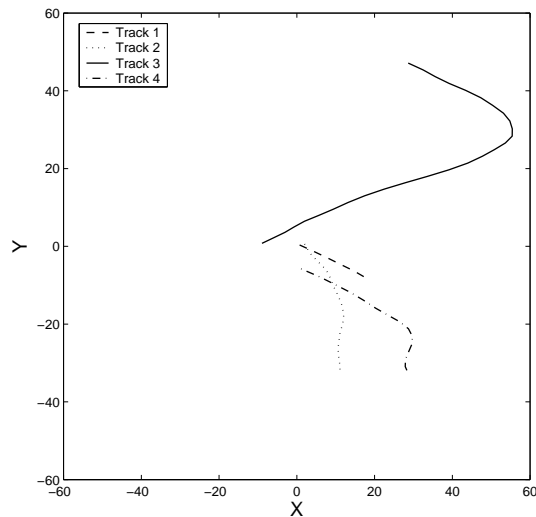


Figure 4.2: ‘Example 1’: Plots of true positions of four tracks superimposed over 40 time steps.

At the sensor, we take standard deviations of $w_{1,k}$ and $w_{2,k}$ as of 0.05 and 1.0 respectively. Clutter is taken to be uniform in the observation with average clutter points, λ_c .

Next, we present simulation results for the track-valued estimates of targets given by the PHD-with-association filter for $\lambda_c = 4.0$ points per scan, i.e., $40 \times 10^{-5} m^{-2}$ per hyper volume. The noisy measurement set at each time step is filtered with the SMC-PHD filter and the outputs are then subject to estimate-to-track association to form the track-valued estimates of individual targets. This is achieved by applying a track-oriented MHT on the outputs of the SMC-PHD filter. The MHT algorithm treats

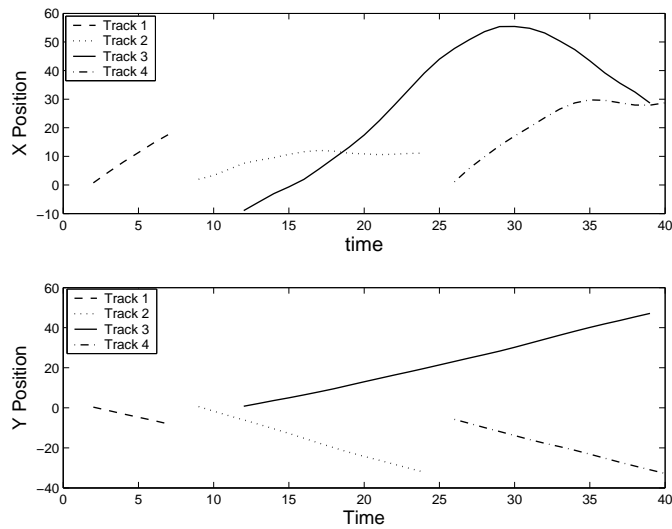


Figure 4.3: Plots of x and y components of true positions of 4 tracks given in figure 4.2 against time.

the outputs of the SMC-PHD filter as the measurements generated according to the linear process given in equation (4.8). Figure 4.4 presents the track-valued estimates

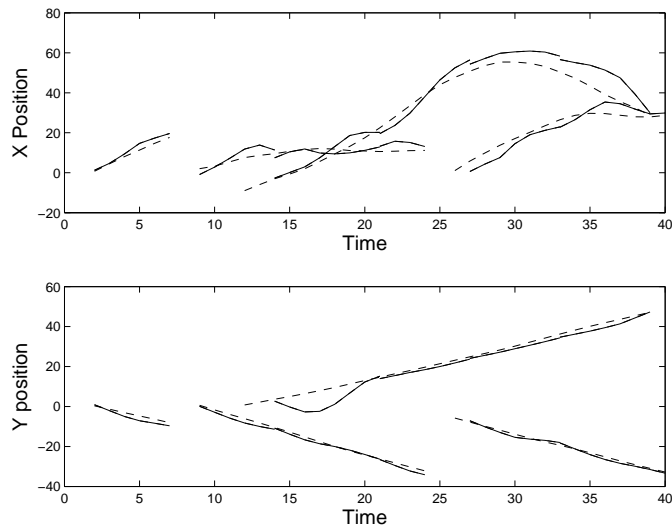


Figure 4.4: Target tracks obtained using the track-oriented MHT filter on observation sets modified by the PHD filter (Scheme One) superimposed with the true target tracks (dashed line) of ‘example 1’.

that are given by the PHD-with-association filter. The target tracks produced by the PHD-with-association filter matches closely with the true target tracks. There are no false tracks. It misses the start of the third and fourth track for two time steps. However, estimates of the target positions at these two time steps are available from

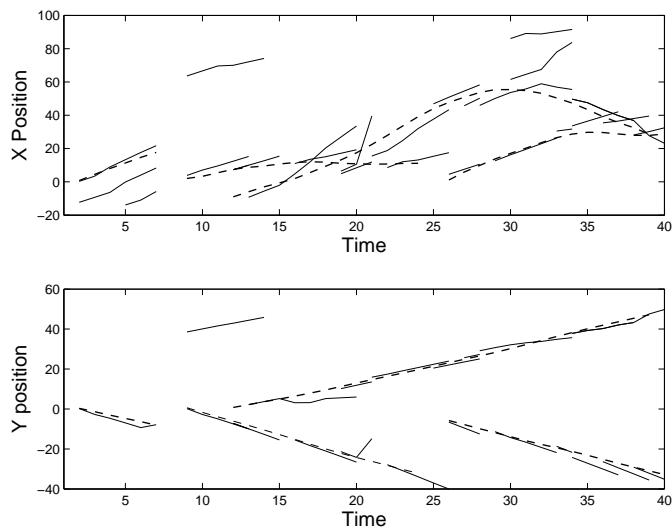


Figure 4.5: Target tracks obtained using the track-oriented MHT filter on observation sets superimposed with the true target tracks (dashed line) of ‘example 1’.

the SMC-PHD filter and the end user should benefit from the state estimates as well as the individual target tracks obtained from these estimates.

Figure 4.5 shows the track-valued estimates given by the MHT from the noisy observation set obtained according to the target and measurement models given earlier in this section. In addition to picking up the majority parts of true tracks, it picks a number of false tracks. False tracks are created when some of the randomly created clutter at successive time steps gate with one another. One way of reducing the number of false alarms picked by the MHT is to increase the number of target detections needed in each association hypothesis to be classified as a confirmed hypothesis. However this will result in the true targets being missed more often. The quality of tracks here also suffers from the drawbacks of the EKF that the MHT uses for predictions and updates on the track hypotheses during gating and measurement updates. It should also be noted that for the MHT to pick up a target track, the target must be present in the surveillance region for at least a number of time steps equal to the number of target-detections (equals two in this simulation) needed for a track hypothesis to be confirmed.

Figure 4.6 shows the track estimates of the targets given by the MHT-with-PHD clutter filter. It shows that the number of false tracks picked by the MHT-with-PHD clutter filter is smaller than the ones given by the stand alone MHT. However, it still

picks up a few more false tracks than the PHD-with-association filter. Figure 4.6 shows that the MHT-with-PHD clutter filter gives good track estimates of targets provided by the individual target estimates given by the PHD filter are good.

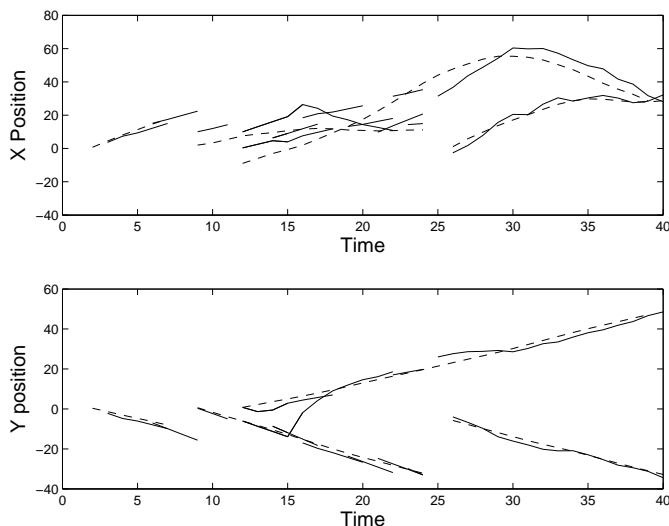


Figure 4.6: Target tracks obtained using MHT-with-PHD clutter filter (Scheme Two) superimposed with the true target tracks (dashed line) of ‘example 1’.

Quantitatively, the goodness of the set-valued estimates are better measured in terms of the multi-target miss-distance between two finite sets representing the true target positions and their respective estimates.

Hoffman and Mahler [32] have shown the Wasserstein distance to be a good measure of the multi-target miss distance. Given the multi-target ground truth $X = \{x_1, \dots, x_{|X|}\}$ and its point state estimate $\tilde{X} = \{\tilde{x}_1, \dots, \tilde{x}_{|\tilde{X}|}\}$, the Wasserstein distance d_p^W is defined as

$$d_p^W(\tilde{X}, X) = \min_C \sqrt[p]{\sum_{i=1}^{|\tilde{X}|} \sum_{j=1}^{|X|} C_{i,j} \|\tilde{x}_i - x_j\|^p}, \quad (4.15)$$

where the minimum is taken over the set of all transportation matrices $C = \{C_{i,j}\}$; and each entry of the matrix C satisfies the followings: $C_{i,j} \geq 0$, $\sum_{i=1}^{|\tilde{X}|} C_{i,j} = 1/|\tilde{X}|$ and $\sum_{j=1}^{|X|} C_{i,j} = 1/|X|$. In this work, p takes a value of two.

Figure 4.7 shows that the Wasserstein distance averaged over 500 Monte Carlo runs. It shows that the mean Wasserstein distance is small for the PHD filter

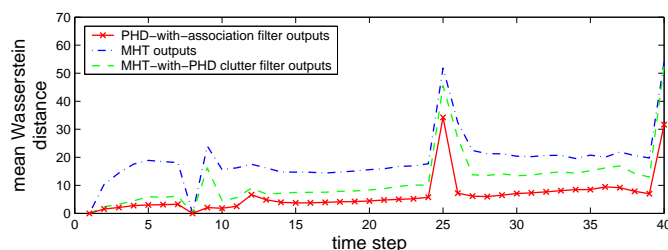


Figure 4.7: The Wasserstein distance between the outputs of the PHD-with-association filter, MHT-with-PHD clutter filter and the MHT, and the ground truth for ‘example 1’ and $\lambda_c = 4.0$

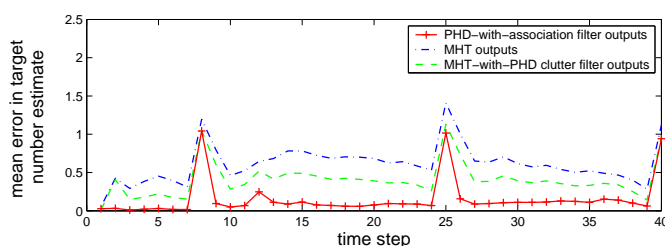


Figure 4.8: The Wasserstein distance between the outputs of the PHD-with-association filter, MHT-with-PHD clutter filter and MHT, and the ground truth for ‘example 1’ and $\lambda_c = 4.0$

generated state estimates except at a few time steps. Peaks in the plot at time step 8 and 25 is due to the fact that the track-oriented MHT does not immediately picks up the target death. The Wasserstein distance is considerably larger for the state estimates given by the MHT at majority of time steps. This is because the MHT picks additional false tracks and the Wasserstein distance penalizes the different cardinalities of two finite sets. The Wasserstein distance of the MHT can be reduced by using the PHD filter as a clutter filter. Figure 4.7 shows that the Wasserstein distance of the estimates given by the MHT-with-PHD clutter filter is smaller than ones obtained with the MHT only. During time steps (between time step 25 and 40) when the target estimates given the PHD filter are good, the MHT-with-PHD clutter filter works very well. In this work, when both sets are empty, we assigned a zero distance to the multi-target miss distance. However, when one of the set is empty, the Wasserstein distance becomes infinite and might not be very meaningful in tracking. In practice, the penalty one wants to impose on the tracker when one of the set is empty, depends on the user and the applications. Similarly, the ability of the PHD-with-association filter to track the targets with a smaller error in the

target number estimate is shown in figure 4.8 that shows the error in the target number estimate averaged over 500 Monte Carlo runs.

Next, we show the mean of the estimation error in the target number and the mean Wasserstein distance obtained over 500 Monte Carlo runs over 40 time steps for a number of clutter level in Table 4.4 and 4.5 respectively. Both tables show that PHD based schemes provide better estimate of the target number than the MHT. As the average clutter points per scan is increased, the performance loss in the PHD-based schemes are smaller than than of the MHT. However, it should be noted that the PHD filter has the advantage of using prior information on target birth whereas the track-oriented MHT initiates a track on each measurement. Further discussion on the comparison on the performance of the PHD based schemes and the MHT will be included in the following section.

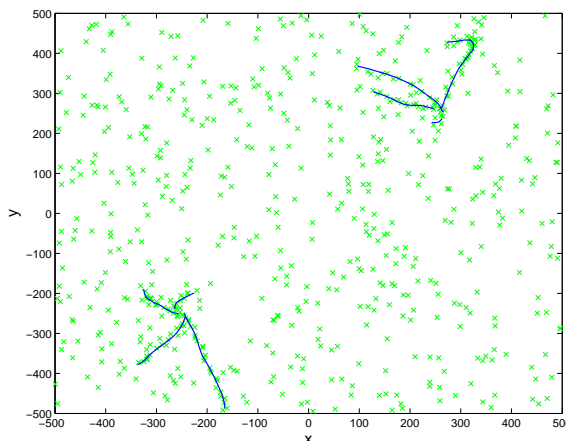


Figure 4.9: ‘Example 2’: Plots of true positions of true tracks superimposed over 50 time steps.

Example 2

Figure 4.9 shows another tracking example in which targets move in $[-500, 500] \times [-500, 500]$. There are maximum of five targets at the surveillance region at any time. Targets appear around two points in the surveillance region. We take $\sigma_{v_{1,k}} = \sigma_{v_{1,k}} = 1.0$. Observation noise values are the same as the ones used in example given above. We collect measurements in the presence of clutter with $\lambda_c = 8$. 500 sets of measurements over 50 timestep have been collected to find the average Wasserstein

distance and the estimation error in the target number. Figure 4.10 and 4.11 shows that the PHD-based filter outperforms the particular implementation of the MHT considered in this work. While the error in the MHT is due to number of additional false tracks, the PHD-with-association filter misses some of the targets between time steps 15 and 35 as the targets are close to each other. The clustering algorithm also introduces errors as the number of targets increases in a given area. This will also translates to higher Wasserstein distance and the higher estimation error in the target in case of the MHT-with-PHD clutter filter.

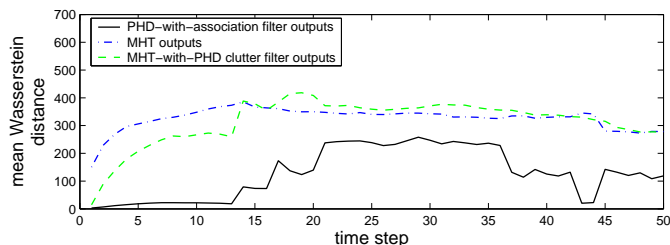


Figure 4.10: The Wasserstein distance between outputs of the PHD-with-association filter, MHT-with-PHD clutter filter and MHT, and the ground truth for ‘example 2’ and $\lambda_c = 10.0$

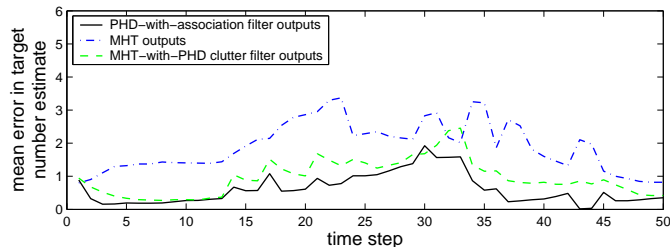


Figure 4.11: The estimation error in the target number between the outputs of the PHD-with-association filter, MHT-with-PHD filter, MHT, and between groundtruths ‘example 2’ and $\lambda_c = 10.0$

4.3.4 Discussion

Simulation results presented above in Section 4.3.3 show that the SMC-PHD filter provides good track-valued estimates of the targets in addition to recursively providing good state estimates of targets. The results also show that the PHD filter can also be used as a clutter filter to improve the performance of the MHT.

The PHD-with-association filter finds the most likely associations of the state estimates over time using primarily the individual target dynamics. In this scheme, some of the clutter that are picked up by the PHD filter can be eliminated during the estimate-to-track association by discarding the estimates that do not get associated with any of the estimates at the following time step. The main effect of the PHD filter in the PHD-with-association filtering is to provide fairly accurate state estimates of the target states. For the purpose of the ‘estimate-to-track’ association, these state estimates can be seen as the new measurements produced according to the linear measurement process given by Equation (4.8). Thus it enables the ‘estimate-to-track’ association functionality to do away with the need to use EKFs that, in general, does not work well in the presence of severe nonlinearity in the target dynamics and/or the measurement process.

Moreover, the SMC-PHD filter provides almost clutter free state estimates of the individual targets. As a result, substantially smaller number of hypothesis tracks will be created during the ‘estimate-to-track’ association, requiring a simpler hypotheses pruning scheme in the PHD-with-association filter. Similarly, the MHT-with-PHD filter also benefits from the almost clutter free estimates of targets that are used to eliminate unlikely measurements before applying the MHT. The performance of both of these schemes mainly depends on the accuracy of the PHD filter generated state estimates of the targets and hence on the implementation details of the SMC-PHD filter; i.e. the number of particles per target, the choice of the proposal density function and the choice of resampling method. It also depends on the accuracy of the peak extracting methods employed for the multi-target state estimation.

The peak-to-track association presented in [52] considers the formation of tracks based on association of peaks over two consecutive time steps by keeping validation gates on each of the tracks. It does not use the state estimates that becomes available later in time to resolve the uncertainty in the association. The algorithm presented in [52] is primarily intended for tracking scenarios with linear/Gaussian state models. Moreover, the paper proposes to sample particles around each measurement as well as proposes to modify the update step of the SMC-PHD filter so that the contribution of the measurements that fall within the validation gates of

existing tracks are weighted more than the ones that fall outside the validation gates. Drawing samples around every measurement means that the computational cost of the algorithm now depends on the number of measurements. This results in the increased number of false tracks being picked up. Moreover, the effect this proposed modification may have on the convergence properties of the SMC-PHD filter have not been looked into.

It has been claimed in [52] that the proposed PHD filter based scheme outperforms a data association algorithm like MHT. It is misleading to claim the SMC-PHD filter outperforms the MHT or vice versa, as the performances of both schemes depend on their particular implementations and how much computational load they are prepared to tolerate. The performance of the MHT can be improved upon by allowing it to consider more exhaustive associations amongst measurements. Similarly, the performance of the SMC-PHD filter can be improved by using larger number of particles per target, and by employing better proposal density functions and better peak extraction methods. Another claim in [52] is that the proposed SMC-PHD based scheme is computationally worse off than the MHT. This might be true for tracking scenarios that consist of linear/Gaussian state models. However, for general tracking purposes with nonlinear/non-Gaussian state models, multiple particle filters (working in parallel) would be required to operate on each track hypothesis and would make the MHT computationally more expensive than the PHD filter. The comparison of the computational cost between a SMC-PHD filter based multi-target tracker and the MHT requires careful considerations of implementation details of both schemes and their particular applications.

The PHD-with-association filter developed as a part of this study is applicable to tracking scenarios with the nonlinear/non-Gaussian state models. The subsequent state estimates given by the PHD filter have been used to reduce the uncertainty in the ‘estimate-to-track’ association. The computational cost of the SMC-PHD filter does not depend on the number of measurements.

4.4 The Improved SMC-PHD Filter for Track Association

First two schemes given earlier in Section 4.3 propose to combine existing data association methods with the PHD filter to find the association of state estimates of individual targets over time. This section presents an improved implementation of the SMC-PHD filter, called the cluster-indexed SMC-PHD filter and a novel ‘estimate-to-track’ association scheme for the proposed filter. The proposed estimate-to-track association scheme exploits the particle representation of the posterior intensity function to provide target identities to the individual state estimates given by the PHD filter.

The multi-target state estimation in the SMC-PHD filter involves the clustering of posterior intensity particles at each time step. Given a number of clusters at the previous time step, we can track individual particles as they are propagated ahead in time and find which cluster they belong to at the next time step in order to build association between clusters from one time step to the next. Figure 4.12 shows a diagram that illustrates the key concept of this scheme. At time step $k - 1$ there are two clusters with identities r_1 and r_2 . All the particles that form the clusters r_i also have labels that is the same as r_i . There are two clusters formed at time step k , and their identities are determined by the labels of majority of particles that belong to them.

4.4.1 The Cluster-Indexed SMC-PHD Filter

In this method, the clustering of particles during peak extraction is used to assign labels to the posterior intensity particles so that the particles within the same cluster get assigned the same label. The clusters between time steps are associated if there exists a large intersection of particles of the same label. These labels are stored in $\{J_k^{(i)}\}_{i=1}^{L_k}$ that are called cluster indices. First, we propose to update the SMC-PHD recursion so that it can recursively handle the propagation of the cluster indices of the posterior intensity particles. The proposed filter is termed the *cluster-indexed*

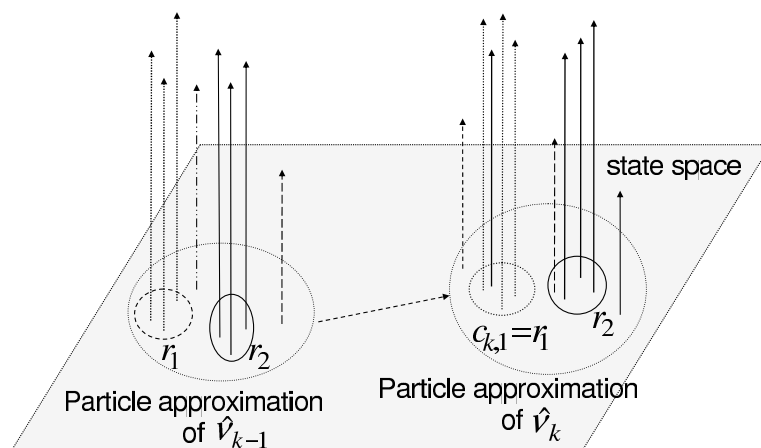


Figure 4.12: Diagrammatic view associating clusters between two time frames. Cluster $c_{k,1}$ at time step k will have its label r_1 and will be associated with the cluster with label r_1 at time step $k - 1$ as most of the particles in cluster $c_{k,1}$ belongs to clusters with label r_1 of the previous time step.

SMC-PHD filter is given in Table 4.6.

The cluster-indexed SMC-PHD recursion gives the posterior intensity particles with their weights and cluster indices at each time step. The new born particles are given zeroes as their cluster indices. The cluster indices of the particles after the prediction step are the same as the one they have at the previous time step. The resampled particles will preserve the cluster indices of the original particles that they are resampled from. The cluster indices are later set to the track identities of the clusters they belong to during the ‘estimate-to-track’ association.

Given the posterior intensity particles and their cluster indices at time step k , we determine the identity of a cluster as follows: we group the particles in the cluster at hand according to their cluster indices so that particles in a group share the same cluster index, we then find the total weights for each group by summing the weights of all particles in it. The cluster identity is given by the cluster index of the group with the largest total weight. The rest of this section will show how this cluster identity is used to initiate track and to perform the ‘estimate-to-track’ association.

Assume, the set of live tracks at time step k is represented by \mathfrak{S}_k and a track in \mathfrak{S}_k is given by $\tau_{k_s:k}^r = (\{\hat{x}_{k_s}, \dots, \hat{x}_k\}, r)$ that represent a track started at an earlier time step k_s and has a track identity (or track label) r . Given the posterior intensity particles $\{w_k^{(i)}, x_k^{(i)}\}_{i=1}^{L_k}$ and their associated cluster indices $\{j_k^{(i)}\}_{i=1}^{L_k}$ at time step k ,

the process of obtaining the set of tracks \mathfrak{S}_k at time k from the set of tracks \mathfrak{S}_{k-1} at time step $(k - 1)$ is as follows.

First the $\{w_k^{(i)}, x_k^{(i)}\}_{i=1}^{L_k}$ are clustered to produce \widehat{N}_k clusters. For each cluster we find its cluster identifier as described earlier in the third paragraph of this section. If the cluster identifier is zero, a new track is initiated with the target state estimate given by its centroid location as its starting point and is included in \mathfrak{S}_k . The track identity r for the new track is given by $r = r_{max} + 1$ and $k_s = k$. Every time a new track is initiated, r_{max} is incremented by one. Finally the cluster indices of all particles in the cluster at hand with zero as entries are assigned the track identity r . When the cluster identifier is a number other than zero, we associate this cluster with the track of label r from \mathfrak{S}_{k-1} . The track is then copied into \mathfrak{S}_k . Tracks in \mathfrak{S}_{k-1} , which do not get associated with any estimates from time step k , are not copied into \mathfrak{S}_k and are stored for data output purposes. The ‘estimate-to-track’ association to construct the track-valued estimates of targets with the cluster-indexed SMC-PHD filter is summarized in Table 4.7.

An ‘estimate-to-track’ association method that also uses labels of posterior intensity particles to find association of clusters between two subsequent time steps has been proposed by Clark *et. al.* in [14] independent of this work. However, the proposed implementation is limited in its ability to handle new born targets. Moreover, the implementation of the cluster-indexed SMC-PHD filter enables us to reduce the computational cost of the SMC-PHD filter by avoiding the need to perform clustering at every time step. Provided that no more than one target is born at a time step and the targets in the surveillance region are separated, posterior particles can be clustered according to their particle indices.

4.4.2 Implementation Issues

The implementation of any SMC-PHD recursion based algorithm requires some careful consideration. First, it involves extracting the peaks of the posterior intensity and the number of these peaks may not equal to the total target number estimate \widehat{N}_k . In such cases, it may be an option to pick the highest \widehat{N}_k peaks as higher the peak more likely is the chance of a target being there. Locating all the peaks in

the posterior intensity is computationally expensive. This can be approximated by using standard clustering techniques to cluster the posterior intensity particles into \widehat{N}_k clusters and use the cluster centers as peaks. Previous works in the SMC-PHD filter [106, 107] use this approach to extract target state estimates from the posterior intensity particles. In practice, the number \widehat{N}_k given by the SMC-PHD recursion may not be an exact integer. So standard clustering techniques end up taking integer approximation to \widehat{N}_k , i.e., \widetilde{N}_k and form \widehat{N}_k clusters. This will introduce errors in the target state estimates. Moreover, there might be two or more targets are in close proximity. These situations require that we closely look at the weight of the particles belonging to the clusters before we extract estimates from them and perform estimate-to-track association.

Given \widehat{N}_k clusters, we first sum of the weights associated with the particles in each of the clusters. If the total weights of particles in a cluster is smaller than a chosen threshold, the cluster will be either pruned or merged with another cluster that is in its proximity. We also merge two or more clusters to form a new one if their centers are within a carefully chosen threshold distance. In cases where the total weight of a cluster is closer to an integer higher than one, we assume that two or more targets being in close proximity to each other and represent them with a common state.

4.4.3 Simulation Results

For illustration purposes, we consider a two-dimensional scenario, in which each target moves in the region $[-200, 200] \times [-200, 200]$ and can appear or disappear in the horizon at any time. The number of targets at any time is unknown and time-varying. The target states consist of positions and velocities in x - and y - directions. Each target moves according to the following linear and Gaussian target dynamics, given in 4.11. The process noise $v_{1,k}$ and $v_{2,k}$ are independent zero mean Gaussian noise with standard deviations of 1.0 and 0.1 respectively. An existing target has a survival probability of $p_{S,k} = 0.95$ and this probability is state independent. We assume that target birth follows a Poisson model with the intensity $0.2\mathcal{N}(\cdot|x_0, Q_b)$, where $\mathcal{N}(\cdot|x_0, Q_b)$ represent a normal distribution with a mean x_0 and covariance

Q_b , and

$$x_0 = \begin{bmatrix} 0 & 2 & 0 & -2 \end{bmatrix}^T \text{ \& } Q_b = \text{diag} \left(\begin{bmatrix} 10 & 5 & 10 & 5 \end{bmatrix} \right).$$

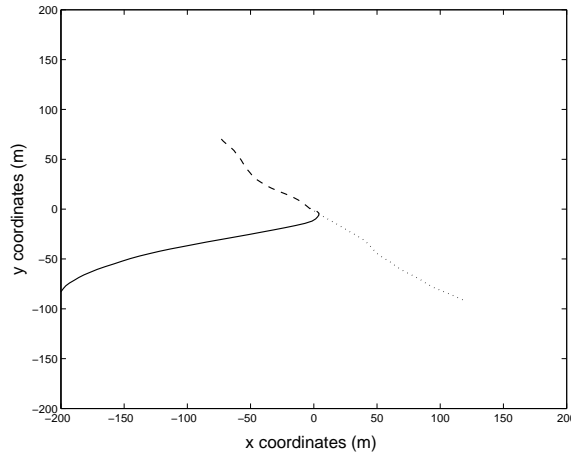


Figure 4.13: Target trajectories in XY planes.

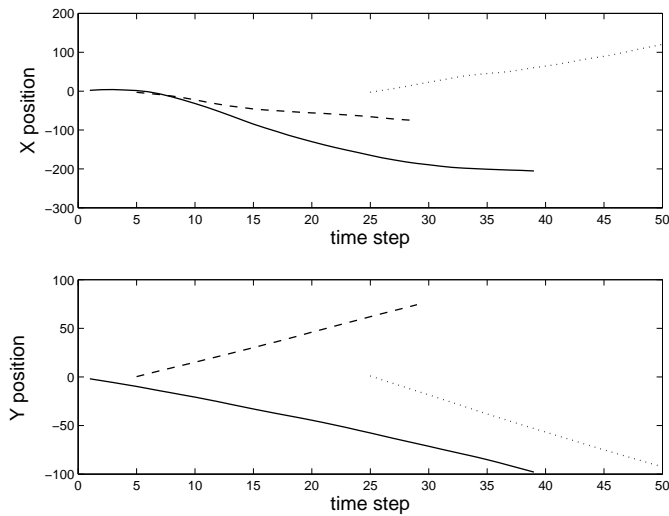


Figure 4.14: Target trajectories (target 1 (solid line), target 2 (dashed line) and target 3 (dotted line)) in terms of x-coordinate positions and y-coordinate positions separately.

The bearing θ_k and range r_k measurement of a target are generated by a sensor located at $[0, -100]^T$ according to (4.12) and (4.13). The measurement noise $w_{1,k}$ and $w_{2,k}$ are independent zero mean Gaussian noise with standard deviations of 0.05 and 2.0 respectively. The measurement noise is also independent of the process noise. Without the loss of generality, probability of detection is assumed almost unity. Clutter is uniformly distributed with an average rate of 4 points per scan, i.e,

$25 \times 10^{-6} m^{-2}$ is the average number of clutter return per hyper volume. At each time step, the target state estimates are extracted from the set of posterior intensity particles by applying the k -mean clustering technique.

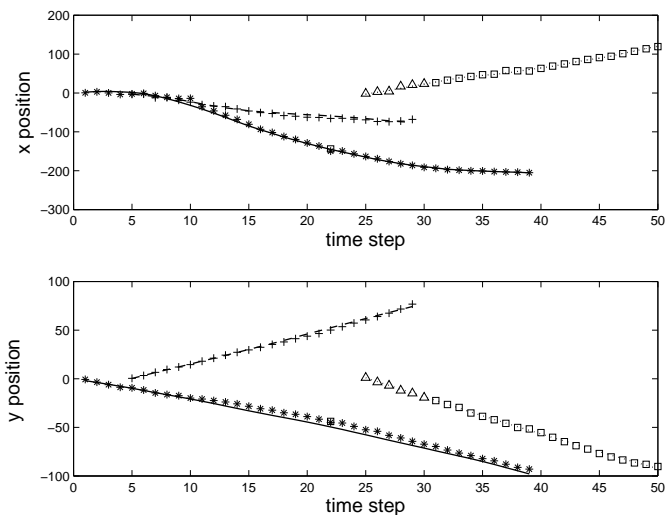


Figure 4.15: Track-valued estimates given by the cluster-indexed SMC-PHD filter. The SMC-PHD filter uses 1000 particles per target and uses $q_k = f_{k|k-1}$ and $p_k = \mathcal{N}(\cdot|x_0, Q_b)$ as proposal densities for importance sampling. Different plot symbols are used to represent different tracks.

Figure 4.15 shows the track-valued estimates given by the cluster-indexed SMC-PHD filter. It shows that the cluster-indexed SMC-PHD filter gives the reasonably accurate estimates of the target tracks that are almost free of false tracks. A track-valued estimate of a target is represented by the same plot symbol. The state trajectory of the target '3' is regarded by the filter as belonging to two targets. This is because of the particular implementation of the SMC-PHD filter used in this work. As most of the particles representing target '3' from the previous step were killed in update step, the proposed filter treats the estimate as coming from a new target and assigns a new target identity. A few clutter that are occasionally picked by the SMC-PHD filter are mostly eliminated as they do not get updated during the 'estimate-to-track' association here. Figure 4.16 shows the estimates of the target tracks that are given by the MHT. In comparison, the MHT generates a larger number of false tracks.

Figures 4.18 and 4.17 shows the mean Wasserstein distance and the mean error in the target number estimate of the target state estimates generated by the

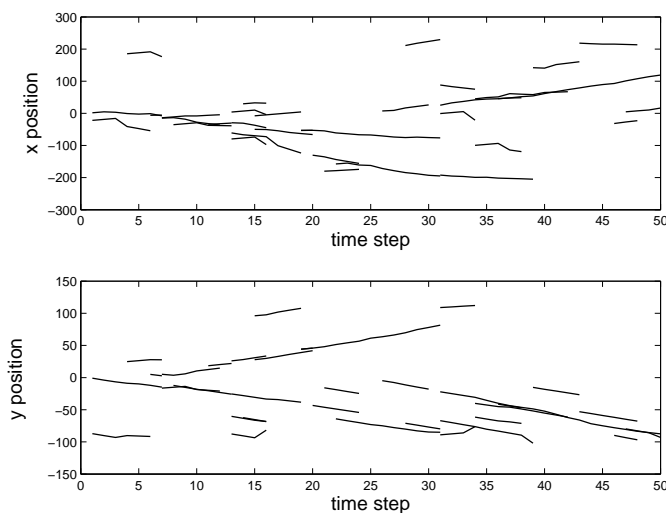


Figure 4.16: Track-valued estimates given by the MHT Filter. The MHT filter is a track-oriented MHT that uses two or more target detection to confirm a track and prunes tracks that have more than two consecutive target miss-detections. N -scan pruning uses $N = 3$.

cluster-indexed SMC-PHD filter and the MHT from the ground truth. 500 sets of measurements over 50 timesteps were taken with $\lambda_c = 4.0$. Figure 4.17 shows that the mean error in the target number estimate is smaller for the cluster-indexed SMC-PHD filter than the MHT. The MHT picks up a few tracks. The average of the mean error in the target number estimate over 50 time steps is 0.2330 and 1.0403 for the cluster-indexed PHD filter and the MHT respectively. It also takes couple of time steps to detect the death of a track and hence a high error in target number estimate in the neighbourhood of timesteps 25 and 40. Due to the Monte Carlo variation of particle implementation of the PHD filter, it occasionally misses out target ‘2’ and hence cause a higher error in the target number estimate between timesteps 5 and 30. Similarly, Figure 4.18 shows that the multi-target miss distance for the state estimates given by the SMC-PHD filter is smaller than the ones given by the MHT. This is because SMC-PHD filter gives a better estimate of the target number and the Wasserstein distance penalizes for picking the wrong target number.

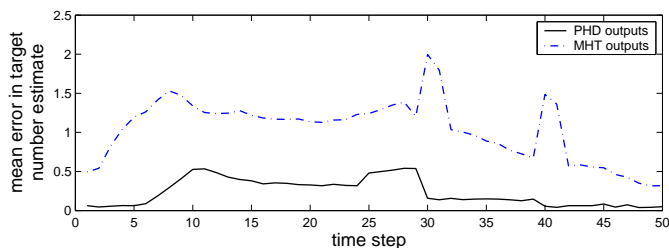


Figure 4.17: The Wasserstein multi-target miss distance for the estimates given by the SMC-PHD filter and the MHT filter.

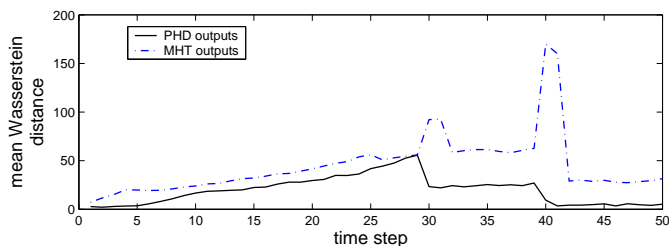


Figure 4.18: The Wasserstein multi-target miss distance for the estimates given by the SMC-PHD filter and the MHT filter.

4.4.4 Discussion

The introduction of the cluster indices in the particle representation of the posterior intensity function does not affect the SMC-PHD recursion. The ‘estimate-to-track’ association scheme based on the cluster indices is computationally cheaper compared to the cost of employing data association methods as described in Section 4.3. However, this technique is less general in the sense that it requires the targets to be well apart so that there are no large overlaps amongst individual clusters. Provided the targets are separately enough and no more than one target appears in the surveillance region during a time interval, cluster indices can be used to extract peaks instead of clustering techniques. It should also be noted that, the ability of this method to correctly propagate track identity from one time steps to the next decreases in the presence of higher clutter density.

It should be noted that the success of the proposed scheme depends primarily on the performance of the peak extraction techniques that are employed for multi-target state estimation. It also depends on the goodness of the proposal densities used to generate particles and the ability of the particle implementation to propagate the intensity particles from one time step to the next. We also need SMC recursions

that are reasonably insensitive to the outliers.

4.5 Summary

This chapter provided a description of the SMC-PHD filter and presented the novel schemes developed as a part of this study for extending the use of the SMC-PHD filter to obtain the state trajectory estimates of individual targets. It included the description of the PHD-with-association filter, the MHT-with-PHD clutter filter and the cluster-indexed SMC-PHD filter. Simulation results are included for these schemes and their performances are benchmarked against that of the MHT. While traditional approaches to multi-target tracking perform the ‘measurement-to-track’ association first followed by filtering on the associated measurements, the PHD-with-association filter and the cluster-indexed SMC-PHD filter first performs filtering on the measurements to sequentially produce the set-valued estimates of the multi-target state and then performs novel ‘estimate-to-track’ association schemes on the state estimates. In the MHT-with-PHD clutter filter, the PHD filter has been used to improve the performance of the MHT.

Amongst the three schemes presented in this chapter, the PHD-with-association filter provides a more general solution to multi-target tracking problems. The PHD-with-association filter has the ability to track multiple number of targets with a fewer number of false tracks. It should be noted that the performance of MHT is subject to the particular implementation and can be improved upon at the expense of added computation cost and complexity. However, when the non-linearity and/or non-Gaussianity in the target dynamics and/or measurement process are considerable, the PHD-with-association filter should be preferred over MHT as the EKF used would not perform satisfactorily and would require running a large number of particle filters on each track hypothesis.

Table 4.1: A SMC-PHD Filter Algorithm

Given a particle representation $\{w_0^{(i)}, x_0^{(i)}\}_{i=1}^{L_0}$ of the intensity function ν_0 at $k = 0$ and $Z_{1:k}$, the particle representation of ν_k at time step $k > 0$ is obtained by:

Step 1: Prediction

- Draw samples according to the proposal densities $q_k(\cdot|x_{k-1}^{(i)}, Z_k)$ and $p_k(\cdot|Z_k)$ as

$$\tilde{x}_k^{(i)} \sim \begin{cases} q_k(\cdot|x_{k-1}^{(i)}, Z_k), & i = 1, \dots, L_{k-1} \\ p_k(\cdot|Z_k), & i = L_{k-1} + 1, \dots, L_{k-1} + J_k \end{cases}$$

- Compute associated weights as

$$\tilde{w}_{k|k-1}^{(i)} = \begin{cases} \frac{\phi_{k|k-1}(\tilde{x}_k^{(i)}, x_{k-1}^{(i)})}{q_k(\tilde{x}_k^{(i)}|x_{k-1}^{(i)}, Z_k)} w_{k-1}^{(i)}, & i = 1, \dots, L_{k-1} \\ \frac{1}{J_k} \frac{\gamma_k(\tilde{x}_k^{(i)})}{p_k(\tilde{x}_k^{(i)}|Z_k)}, & i = L_{k-1} + 1, \dots, L_{k-1} + J_k \end{cases}$$

Step 2: Update

- Update each weight as

$$\tilde{w}_k^{(i)} = \left[1 - p_{D,k}(\tilde{x}_k^{(i)}) + \sum_{z \in Z_k} \frac{p_{D,k}(\tilde{x}_k^{(i)}) g_k(z|\tilde{x}_k^{(i)})}{\kappa_k(z) + C_k(z)} \right] \tilde{w}_{k|k-1}^{(i)}$$

where $C_k(z) = \sum_{j=1}^{L_{k-1}+J_k} p_{D,k}(\tilde{x}_k^{(j)}) g_k(z|\tilde{x}_k^{(j)}) \tilde{w}_{k|k-1}^{(j)}$.

Step 3: Resampling

- Compute the total mass $\tilde{N}_k = \sum_{j=1}^{L_{k-1}+J_k} \tilde{w}_k^{(j)}$,
 - Resample $\{\tilde{w}_k^{(i)}/\tilde{N}_k, \tilde{x}_k^{(i)}\}_{i=1}^{L_{k-1}+J_k}$ to get $\{w_k^{(i)}/\tilde{N}_k, x_k^{(i)}\}_{i=1}^{L_k}$,
 - Rescale the weights by \tilde{N}_k to $\{w_k^{(i)}, x_k^{(i)}\}_{i=1}^{L_k}$.
-

Table 4.2: The PHD-with-Association Filter

Step 1 – Step 3: Follow Step 1–3 of the SMC-PHD Filter Algorithm given in Table 4.1

Step 4: Perform clustering to obtain target state estimates $\{\hat{x}_k^{(i_1)}\}_{i_1=1}^{\hat{N}_k}$ and respective covariances $\{\hat{P}_k^{(i_1)}\}_{i_1=1}^{\hat{N}_k}$.

Step 5: Given $\{\tilde{x}_{k,i}\}_{i=1}^{\hat{N}_k}$, the estimate-to-track association follows:

- *initialization:*
 1. Initialize a new track hypothesis with initial state $\tilde{x}_{k,i}$ and initial covariance
 2. Create a new cluster of the target represented by each track
 - *prediction:* For $k > 1$, propagate the state and the covariance of each track hypothesis according to equation (2.1)
 - *gating:* For each measurement $\tilde{z}_{k,i}$ (given by $\tilde{x}_{k,i}$)
 1. Create association hypothesis for every tracks it is associated with
 2. Initialize a track if it is not associated with any tracks
 3. Note a target *miss-detection* on every tracks that have no measurement associated to it
 - Update existing clusters
 - Update of LLRs of each association hypothesis
 - Perform tracks confirmation and track-level pruning
 - form global hypothesis formation from confirmed tracks
 - Perform N-scan pruning
 - Perform measurement update on tracks that survived pruning according to equation (4.8)
 - Tracks represented by the best global hypotheses is used for data output
-

Table 4.3: The MHT-with-PHD Clutter Filter

-
- *PHD filtering*: Apply Step 1-3 of the SMC-PHD filter filter (Table 4.1)
 - *Multi-target state estimation*: Perform clustering techniques on the posterior PHD particles to obtain state estimates $\tilde{X}_k = \{\tilde{x}_{k,j}\}_{j=1}^{\hat{N}_k}$
 - *Global gating*: Obtain \tilde{Z}_k from $Z_k = \{z_{k,i}\}_{i=1}^{M_k}$ as follows:
 - for $i : 1, \dots, M_k$
 - for $j : 1, \dots, \hat{N}_k$
 - if $g_k(z_{k,i}|\tilde{x}_{k,j}) > g_d$
 - $z_{k,i}$ in \tilde{Z}_k
 - end
 - end
 - end
 - *Data association & tracking*: Apply MHT on \tilde{Z}_k
-

Table 4.4: Error in Target Number Estimate for ‘example 1’

	$\lambda_c = 4$	$\lambda_c = 8$	$\lambda_c = 12$	$\lambda_c = 16$
PHD-with-association	0.1557	0.1980	0.2514	0.3029
MHT-with-PHD Clutter Filter	0.4052	0.4880	0.6999	0.8177
MHT	0.6143	1.3341	2.5534	4.0151

Table 4.5: Average of Wasserstein distance for ‘example 1’ for different λ_c

	$\lambda_c = 4$	$\lambda_c = 8$	$\lambda_c = 12$	$\lambda_c = 16$
PHD-with-association	6.3733	7.2072	8.0579	8.6544
MHT-with-PHD Clutter Filter	11.8861	13.4809	16.2527	18.8005
MHT	19.1619	35.5014	50.2462	60.6544

Table 4.6: The Cluster-indexed SMC-PHD Filter

Given a set of L_k particles $\{w_k^{(i)}, x_k^{(i)}\}_{i=1}^{L_k}$ representing the posterior intensity ν_0 at $k = 0$ and their associated with the cluster indices $\{j_k^{(i)}\}_{i=1}^{L_k}$, the posterior intensity at time step $k > 0$ is obtained by:

- *Prediction step*: Step 1 of the SMC-PHD filter (Table 4.1), and its associated target indices as

$$\tilde{j}_k^{(i)} = \begin{cases} j_{k-1}^{(i)}, & i = 1, \dots, L_{k-1} \\ 0, & i = L_{k-1} + 1, \dots, L_{k-1} + J_k \end{cases}$$

- *Update step*: Step 2 of the SMC-PHD filter (Table 4.1)
 - *Resampling step*:
 - Compute the total weight $\tilde{N}_k = \sum_{i=1}^{L_{k-1}+J_k} \tilde{w}_k^{(i)}$.
 - Obtain $\{w_k^{(i)}/\tilde{N}_k, x_k^{(i)}, j_k^{(i)}\}_{i=1}^{L_k}$ by resampling $\{\tilde{w}_k^{(i)}/\tilde{N}_k, \tilde{x}_k^{(i)}, \tilde{j}_k^{(i)}\}_{i=1}^{L_{k-1}+J_k}$ where $\tilde{N}_k = \sum_{i=1}^{L_{k-1}+J_k} \tilde{w}_k^{(i)}$.
 - Rescale the weight by \tilde{N}_k to get $\{w_k^{(i)}, x_k^{(i)}, j_k^{(i)}\}_{i=1}^{L_k}$
-

Table 4.7: Estimate-to-Track Association

Given a set of L_k particles $\{w_k^{(i)}, x_k^{(i)}\}_{i=1}^{L_k}$ and their associated cluster indices at $\{j_k^{(i)}\}_{i=1}^{L_k}$ at k , the set of target tracks \mathfrak{S}_{k-1} at time step $k-1$,

- *Clustering*: Perform clustering to obtain target estimates $\{\hat{x}_k^{(i_1)}\}_{i_1=1}^{\hat{N}_k}$ as

$$\left[\{\hat{x}_k^{(i_1)}\}_{i_1=1}^{\hat{N}_k}, \{c_k^{(i)}\}_{i=1}^{L_k} \right] = \text{Clustering}(\{x_k^{(i)}\}_{i=1}^{L_k}, \hat{N}_k)$$

- *Cluster identification*: Find the cluster identity of cluster i_1 for $i_1 = 1, \dots, \hat{N}_k$ as

$$Id = \max_{i_2} \{SumWgt(i_2)\}; \quad i_2 = 1, \dots, r_{max}$$

where $SumWgt(i_2) = \sum_{l_1} (w_k^{l_1})$ for all l_1 that belongs to cluster i_1 .

- *Estimate-to-track Association*: For cluster i_1 with its identity Id , perform estimate-to-track association as

if $Id = 0$

Start a new track

$$r = r_{max} + 1$$

$$r_{max} = r_{max} + 1$$

$$k_s = k$$

Change the cluster indices from zero to r

else

Associate $\hat{x}_k^{i_1}$ with the track of identity Id from \mathfrak{S}_{k-1} and copy into \mathfrak{S}_k

end

- *Track Termination*: A track in \mathfrak{S}_{k-1} that is not associated with an estimate from time step k is not copied into \mathfrak{S}_k
-

Chapter 5

Multi-target Tracking with the GM-PHD Filter

5.1 Introduction

As pointed out in the previous chapter, the probability hypothesis density (PHD) recursion does not admit closed-form solutions in general. However, for a limited cases of multi-target tracking problems, a closed-form solution exists and is given by the Gaussian mixture probability hypothesis density (GM-PHD) filter [103, 104]. Under linear/Gaussian assumptions on the target motion and the observation model, and Gaussian assumption on the target birth, the posterior intensity function is approximated by a sum of Gaussians whose means, covariances and weights are analytically propagated in time. The GM-PHD filter in its original form only provides the state estimate of individual targets as a set-valued estimate of the multi-target state and the estimate of the target number. However, the target state estimates have no identities and are indistinguishable from each other. This chapter presents an extension of the GM-PHD filter that provides identities to state estimates of individual targets so that state trajectories of the individual targets can be obtained. The key contributions of this chapter have appeared in [17, 73, 75].

Section 5.2 of this chapter summarizes the class of multi-target models for which the PHD filter admits a closed-form solution. The description of the *GM-PHD filter* is also included. Section 5.3 presents the GM-PHD filter based multi-target tracker, the *GM-PHD tracker* that was developed as a part of this study. A general track management scheme capable of track initiation, propagation and termination is given in Section 5.4.1. Section 5.5 presents simulation results of the GM-PHD

tracker for a tracking example. In Section 5.6, the GM-PHD filter has been extended to resolve the identities of closely spaced targets. A summary of this chapter is given in Section 5.7.

5.2 The PHD Filter: A Closed-Form Solution

This section includes an overview of the linear/Gaussian multi-target model for which the PHD recursion admits a closed-form solution. A description of the closed-form solution, called the GM-PHD recursion is given. The GM-PHD recursion forms the basis of a general multi-target tracking algorithm, the GM-PHD filter, which has been shown to track an unknown and time-varying number of targets [104, 106].

5.2.1 Linear Multi-Target Models

The linear/Gaussian multiple target model includes a number of assumptions on the birth, death and detection of targets as well as the linear/Gaussian assumptions on the target dynamical model. The assumptions are summarized below.

- Each target follows a linear Gaussian dynamical model, i.e.,

$$f_{k|k-1}(x|\zeta) = \mathcal{N}(x; F_{k-1}\zeta, Q_{k-1}) \quad (5.1)$$

$$g_k(z|x) = \mathcal{N}(z; H_k x, R_k) \quad (5.2)$$

where $\mathcal{N}(\cdot; m, P)$ denotes the Gaussian density with mean m and covariance P , F_{k-1} is the state transition matrix and Q_{k-1} is the process noise covariance, H_k is the observation matrix, and R_k is the observation noise covariance.

- The survival and detection probabilities are both state independent, i.e.,

$$p_{S,k}(x) = p_{S,k}, \quad (5.3)$$

$$p_{D,k}(x) = p_{D,k}. \quad (5.4)$$

The GM-PHD recursion has also been derived the state dependent target sur-

vival and detection probabilities in [104].

- The intensities of the birth and spawn RFSs are both Gaussian mixtures of the form

$$\gamma_k(x) = \sum_{i=1}^{J_{\gamma,k}} w_{\gamma,k}^{(i)} \mathcal{N}(x; m_{\gamma,k}^{(i)}, P_{\gamma,k}^{(i)}), \quad (5.5)$$

$$\beta_{k|k-1}(x|\zeta) = \sum_{j=1}^{J_{\beta,k}} w_{\beta,k}^{(j)} \mathcal{N}(x; F_{\beta,k-1}^{(j)}\zeta + d_{\beta,k-1}^{(j)}, Q_{\beta,k-1}^{(j)}) \quad (5.6)$$

where $J_{\gamma,k}$, $w_{\gamma,k}^{(i)}$, $P_{\gamma,k}^{(i)}$, $m_{\gamma,k}^{(i)}$, $i = 1, \dots, J_{\gamma,k}$ are given model parameters that determine shape of the birth intensity; similarly $J_{\beta,k}$, $w_{\beta,k}^{(j)}$, $F_{\beta,k-1}^{(j)}$, $d_{\beta,k-1}^{(j)}$, $Q_{\beta,k-1}^{(j)}$, $j = 1, \dots, J_{\beta,k}$ determine the shape of the spawning intensity of a target with the previous state ζ . Further remarks on these assumptions can be found in [104].

5.2.2 The Gaussian-Mixture Probability Hypothesis Density (GM-PHD) Recursion

For the multi-target models described above, the GM-PHD recursion propagates the intensity function that is approximated with a Gaussian mixture by analytically propagating the weights, means and covariances of the Gaussian mixture terms. The updated intensity function is also a Gaussian mixture.

The GM-PHD recursion consists of the following prediction and update steps.

Prediction Step: Given that the posterior intensity v_{k-1} at time step $k-1$ is a Gaussian mixture of the form

$$v_{k-1}(x) = \sum_{i=1}^{J_{k-1}} w_{k-1}^{(i)} \mathcal{N}(x; m_{k-1}^{(i)}, P_{k-1}^{(i)}), \quad (5.7)$$

the predicted intensity to time step k is also a Gaussian mixture and is given by

$$v_{k|k-1}(x) = v_{S,k|k-1}(x) + v_{\beta,k|k-1}(x) + \gamma_k(x), \quad (5.8)$$

where $\gamma_k(x)$ is given in (5.5),

$$v_{S,k|k-1} = p_{S,k} \sum_{j=1}^{J_{k-1}} w_{k-1}^{(j)} \mathcal{N}\left(x; m_{S,k|k-1}^{(j)}, P_{S,k|k-1}^{(j)}\right), \quad (5.9)$$

$$m_{S,k|k-1}^{(j)} = F_{k-1} m_{k-1}^{(j)}, \quad (5.10)$$

$$P_{S,k|k-1}^{(j)} = Q_{k-1} + F_{k-1} P_{k-1}^{(j)} (F_{k-1})^T, \quad (5.11)$$

$$v_{\beta,k|k-1}(x) = \sum_{j=1}^{J_{k-1}} \sum_{l=1}^{J_{\beta,k}} w_{k-1}^{(j)} w_{\beta,k}^{(l)} \mathcal{N}\left(x; m_{\beta,k|k-1}^{(j,l)}, P_{\beta,k|k-1}^{(j,l)}\right), \quad (5.12)$$

$$m_{\beta,k|k-1}^{(j,l)} = F_{k-1}^{(l)} m_{k-1}^{(j)} + d_{\beta,k-1}^{(l)}, \quad (5.13)$$

$$P_{\beta,k|k-1}^{(j,l)} = Q_{\beta,k-1}^{(l)} + F_{\beta,k-1}^{(l)} P_{\beta,k-1}^{(j)} (F_{\beta,k-1}^{(l)})^T. \quad (5.14)$$

Update Step: Assuming that the predicted intensity $v_{k|k-1}$ to time step k is a Gaussian mixture of the form

$$v_{k|k-1}(x) = \sum_{i=1}^{J_{k|k-1}} w_{k|k-1}^{(i)} \mathcal{N}\left(x; m_{k|k-1}^{(i)}, P_{k|k-1}^{(i)}\right), \quad (5.15)$$

the posterior intensity v_k at time step k is also a Gaussian mixture, and is given by

$$v_k(x) = (1 - p_{D,k}) v_{k|k-1}(x) + \sum_{z \in Z_k} v_{D,k}(x; z), \quad (5.16)$$

where

$$v_{D,k}(x; z) = \sum_{j=1}^{J_{k|k-1}} w_k^{(j)}(z) \mathcal{N}\left(x; m_{k|k}^{(j)}(z), P_{k|k}^{(j)}\right), \quad (5.17)$$

$$w_k^{(j)}(z) = \frac{p_{D,k} w_{k|k-1}^{(j)} q_k^{(j)}(z)}{\kappa_k(z) + p_{D,k} \sum_{l=1}^{J_{k|k-1}} w_{k|k-1}^{(l)} q_k^{(l)}(z)}, \quad (5.18)$$

$$q_k^{(j)} = \mathcal{N}(z; H_k m_{k|k-1}^{(j)}, R_k + H_k P_{k|k-1}^{(j)} (H_k)^T), \quad (5.19)$$

$$m_{k|k}^{(j)}(z) = m_{k|k-1}^{(j)} + K_k^{(j)}(z - H_k m_{k|k-1}^{(j)}), \quad (5.20)$$

$$P_{k|k}^{(j)} = \left[I - K_k^{(j)} H_k \right] P_{k|k-1}^{(j)}, \quad (5.21)$$

$$K_k^{(j)} = P_{k|k-1}^{(j)} (H_k)^T (H_k P_{k|k-1}^{(j)} (H_k)^T + R_k)^{-1}. \quad (5.22)$$

The *prediction step* and *update step* of the GM-PHD recursion forms the basis of a general multi-target tracking algorithm, called the GM-PHD filter. Given that an initial intensity function ν_0 at time step $k = 0$ is a known Gaussian mixture, the posterior intensity function at time step $k > 0$ is also a Gaussian mixture from which the estimates of individual target states needs to be extracted via peak extractions. The expected number of targets $\hat{N}_{k|k-1}$ and \hat{N}_k associated with $\nu_{k|k-1}$ and ν_k are obtained by summing the appropriate mixture weights. The closed-form recursions for $\hat{N}_{k|k-1}$ and \hat{N}_k are as follows:

$$\hat{N}_{k|k-1} = \hat{N}_{k-1} \left(p_{S,k} + \sum_{j=1}^{J_{\beta,k}} w_{\beta,k}^{(j)} \right) + \sum_{j=1}^{J_{\gamma,k}} w_{\gamma,k}^{(j)}, \quad (5.23)$$

$$\hat{N}_k = \hat{N}_{k|k-1} (1 - p_{D,k}) + \sum_{z \in Z_k} \sum_{j=1}^{J_{k|k-1}} w_k^{(j)}(z). \quad (5.24)$$

The estimate of the target number given above in (5.24) suffers from the instability in low probability of target detection [25]. Rest of this section provides a multi-target state estimation technique specific to the GM-PHD recursion, which provides a better estimate of the target number.

It should be noted that the GM-PHD filter has also been extended to handle nonlinear target dynamical and nonlinear measurement models by replacing the Kalman filter with its extended or the unscented counterparts to propagate the means and covariances of individual Gaussian terms [104].

5.2.3 Multi-target State Estimation

Given that the posterior intensity function at each time step is a mixture of weighted Gaussian terms, the means of all Gaussian terms give the local maxima of the intensity function. However, it has been pointed out in [104] that it is better to select the means of Gaussians of weights greater than an appropriately chosen threshold as the state estimates of individual targets rather than selecting the \hat{N}_k highest peaks

(i.e., local maxima). This is because selecting the \widehat{N}_k highest peaks may result in the state estimates whose weights are very small. Given that a weight threshold is w_{Th} , the state estimates of individual targets are obtained by selecting means of the Gaussian terms with weights greater than w_{Th} ,

$$\widehat{X}_k = \{m_k^{(i)} : w_k^{(i)} > w_{Th}\}. \quad (5.25)$$

As a result, the GM-PHD filter avoids the need for standard clustering techniques that are needed for the SMC-PHD filter. Standard clustering techniques are computationally demanding and their performances suffer when \widehat{N}_k differs from the natural number of clusters present in the particle approximation of v_k . A summary of the multi-target estimation for the GM-PHD filter is given in Table 5.1.

Table 5.1: Multi-target State Estimation

```

given  $\{w_k^{(i)}, m_k^{(i)}, P_k^{(i)}\}_{i=1}^{J_k}$ ,
Set  $\widehat{X}_k = \emptyset$ .
for  $i = 1, \dots, J_k$ 
    if  $w_k^{(i)} > w_{Th}$ ,
         $\widehat{X}_k := [\widehat{X}_k, m_k^{(i)}]$ 
    end
end
output  $\widehat{X}_k$  as the multi-target state estimate.

```

5.2.4 Pruning and Merging Step

A closer inspection of the update step of the GM-PHD recursion shows that the number of Gaussian terms J_k in v_k at time step k equals $(J_{k-1}(1 + J_{\beta,k}) + J_{\gamma,k})(1 + |Z_k|)$. The value of J_k increases over time without any bound and hence increases the computational cost of the GM-PHD recursion. The pruning and merging techniques proposed in [103, 104] in order to stop J_k from increasing with time. Pruning of the

Gaussian terms is performed by either removing the Gaussian terms of low weights or keeping a certain number of terms of the strongest weights. Gaussian terms that are within a certain distance of each other are also merged into one.

Given a truncation threshold T_{Th} , a merging threshold U and a maximum allowable number number of Gaussian terms J_{max} , the number of Gaussian terms at each time step is pruned as follow.

Table 5.2: Pruning for the GM-PHD Filter

given $\{w_k^{(i)}, m_k^{(i)}, P_k^{(i)}\}_{i=1}^{J_k}$, a truncation threshold T , a merging threshold U , and a maximum allowable number of Gaussian terms J_{max} .
Set $\ell = 0$, and $I = \{i = 1, \dots, J_k | w_k^{(i)} > T_{Th}\}$.

repeat

$$\ell := \ell + 1.$$

$$j := \arg \max_{i \in I} w_k^{(i)}.$$

$$L := \{i \in I | (m_k^{(i)} - m_k^{(j)})^T (P_k^{(i)})^{-1} (m_k^{(i)} - m_k^{(j)}) \leq U\}.$$

$$\tilde{w}_k^{(\ell)} = \sum_{i \in L} w_k^{(i)}.$$

$$\tilde{m}_k^{(\ell)} = \frac{1}{\tilde{w}_k^{(\ell)}} \sum_{i \in L} w_k^{(i)} x_k^{(i)}.$$

$$\tilde{P}_k^{(\ell)} = \frac{1}{\tilde{w}_k^{(\ell)}} \sum_{i \in L} w_k^{(i)} (P_k^{(i)} + (\tilde{m}_k^{(\ell)} - m_k^{(i)}) (\tilde{m}_k^{(\ell)} - m_k^{(i)})^T).$$

$$I := I \setminus L.$$

until $I = \emptyset$. if $\ell > J_{max}$ then replace $\{\tilde{w}_k^{(i)}, \tilde{m}_k^{(i)}, \tilde{P}_k^{(i)}\}_{i=1}^{\ell}$ by those of the J_{max} Gaussians with largest weights.

output $\{\tilde{w}_k^{(i)}, \tilde{m}_k^{(i)}, \tilde{P}_k^{(i)}\}_{i=1}^{\tilde{J}_{max}}$ as pruned Gaussian components where $\tilde{J}_{max} = \min(L, J_{max})$.

where $\{\tilde{w}_k^{(i)}, \tilde{m}_k^{(i)}, \tilde{P}_k^{(i)}\}_{i=1}^{\tilde{J}_k}$ denote the remaining Gaussian components after merging.

The intensity function after pruning is given by

$$\tilde{v}_k(x) = \sum_{i=1}^{\tilde{J}_k} \tilde{w}_k^{(i)} \mathcal{N}(x; \tilde{m}_k^{(i)}, \tilde{P}_k^{(i)}). \quad (5.26)$$

5.3 Track Association for the GM-PHD Filter

At each time step, the GM-PHD filter provides the state estimates of individual targets that may be in the surveillance region, i.e., the set-valued estimate of the multi-target state. However, it does not provide identities of the targets detected, i.e. we have no way of knowing which two state estimates between any two time steps belong to the same target. In another words, it does not provide the track continuity of the estimates, which are needed if state trajectory estimates of individual targets are required. As a part of this study, it has been shown that the GM-PHD filter can be extended into a robust and computationally efficient multi-target tracker that provides not only the state estimates of individual targets but also their identities [17, 73, 75]. These identities are used to obtain the estimates of target state trajectories. The GM-PHD filter based multi-target tracker first appeared in [17] and has been successfully applied to sonar problems in [18]. An efficient track management scheme have also appeared in [75].

This section presents a multi-target tracker based on the GM-PHD filter, referred to as the *GM-PHD tracker* from here onwards. The idea behind the GM-PHD tracker is to assign identities to individual Gaussian terms of the mixture representing the posterior intensity function and to allow these identities to evolve through time without affecting the GM-PHD recursion. This formulation of the GM-PHD tracker was motivated by the formulation of the improved particle PHD filter proposed in [76], which uses additional indices associated with samples to obtain target identities during the clustering of particles.

5.3.1 The GM-PHD tracker

The algorithm for the GM-PHD tracker consists of the following steps:

Step 0: Initialization

At time step $k = 0$, the intensity function, v_0 is the mixture of J_0 Gaussians as

$$v_0(x) = \sum_{i=1}^{J_0} w_0^{(i)} \mathcal{N}(x; m_0^{(i)}, P_0^{(i)}), \quad (5.27)$$

where these Gaussians are distributed across the state space. A unique identifier (or tag) is assigned to each Gaussian to form the set

$$\mathcal{T}_0 = \{\tau_0^{(1)}, \dots, \tau_0^{(J_0)}\} \quad (5.28)$$

where $\tau_0^{(j)}$ denotes the tag of the j^{th} Gaussian term whose mean is given by $m_0^{(j)}$.

Step 1: Prediction

Predict the intensity forward in time according to (5.8) and construct the set of new tags as follows:

$$\mathcal{T}_{k|k-1} = \mathcal{T}_{k-1} \cup \{\tau_{\gamma,k}^{(1)}, \dots, \tau_{\gamma,k}^{(J_{\gamma,k})}\} \cup \{\tau_{\beta,k}^{(1,1)}, \dots, \tau_{\beta,k}^{(J_{k-1}, J_{\beta,k})}\} \quad (5.29)$$

where $m_{k|k-1}^{(i)}$ retains the tag of its prior $m_{k-1}^{(i)}$, $\tau_{\gamma,k}^{(i)}$ is the new tag associated with the i^{th} Gaussian term introduced by birth process and $\tau_{\beta,k}^{(i,j)}$ is the tag of the j^{th} Gaussian term spawned by the i^{th} Gaussian term of the mixture. Here, a new tag is given to each new spawned Gaussian term.

Step 2: Update

Update the predicted intensity according to (5.16).

Each term in the predicted Gaussian mixture gives rise to $(1 + |Z_k|)$ terms in the updated mixture and we assign the same tag to each of the updated Gaussian terms as its associated predicted term, i.e., $m_k^{(j)}(z)$ gets the same tag as that of $m_{k|k-1}^{(j)}$ for each z or no observation. As a result, we have a multiple number of updated Gaussian terms for every predicted Gaussian term and their weights.

Step 3: Pruning and Merging

Pruning of Gaussian terms is performed according to Table 5.2. The intensity func-

tion after pruning is given by

$$\tilde{v}_k(x) = \sum_{i=1}^{\tilde{J}_k} \tilde{w}_k^{(i)} \mathcal{N}(x; \tilde{m}_k^{(i)}, \tilde{P}_k^{(i)}). \quad (5.30)$$

Step 4: Target State Estimation

At time step k , state estimates of individual targets are given by (5.25). The set of tags associated with target states is given by

$$\hat{T}_k = \{\tau_k^{(i)} : w_k^{(i)} > w_{Th}\}. \quad (5.31)$$

A complete and systematic method for the construction and the management of tracks using these tagged Gaussians is given in the following section.

5.4 Track Management Scheme for the GM-PHD Tracker

This section presents a scheme for initiating, propagating and terminating track for the GM-PHD tracker. A tree based structure is used to propagate target identities and build track association amongst state estimates of individual targets over time. A number of pruning schemes based on the tree structure are also proposed in this section.

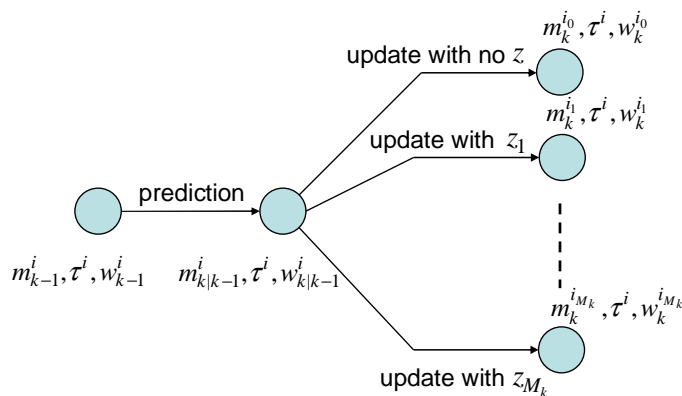


Figure 5.1: A part of a tree structure for propagating a Gaussian term and its tag from the previous time step $k - 1$ to the time step k given Z_k .

5.4.1 Tag Management Scheme

As mentioned in Section 5.3.1, new tags are assigned either for Gaussian terms during initialization or for new Gaussian terms contributed by the birth term γ_k . The propagation of tags associated with individual terms in the Gaussian mixture approximating $v_{k|k-1}$ is summarized in Figure 5.1. $(m_k^{(i)})$ denotes the mean of the Gaussian that results when $m_{k|k-1}^{(i)}$ is updated with measurement z_l , where $l = 0$ represents the case of no measurement update to account for the case of miss-detection). All of the $(1 + |Z_k|)$ updated Gaussians are assigned the same tag as that of its prior, $\tau^{(i)}$. Over time, each Gaussian initialized at time step $k = 0$ and contributed by γ_k form the root of a tree that grows linearly with the number of measurements available at the subsequent time steps (see Figure 5.2). Each tree is identified by its unique label that is the same as the tag of the Gaussian term at its root. Each branch of a tree is a possible state trajectory of a target. At the end of the GM-PHD recursion at each time step, we have a number of tree structures where each tree provides a collection of possible tracks of a target. The likelihood of each track is given by its weight. One solution is to pick a branch with the largest weight $w_k^{(i)} > w_{Th}$ from every tree to form collection individual target tracks and their respective track labels. For each selected track, its label is the same as that of the tree it belongs to.

For the purpose of devising an efficient scheme for track initiation, propagation and termination, we first classify tree structures as *confirmed* and *tentative* ones. A confirmed tree structure is one that has at least one branch with its weight $w_k^{(j)} > w_{Th}$. Otherwise the tree is classified as tentative. All confirmed trees contribute a track and its label towards a collection of output tracks called the *track set*, \mathfrak{S}_k . Each member of \mathfrak{S}_k is an estimate of a target state trajectory with its unique label, i.e., $(\{m_{k_i}^{(i)}, \dots, m_k^{(i)}\}, \tau^{(i)})$ where k_i denotes the time step at which i^{th} target is first detected in the surveillance region and $\{m_{k_i}^{(i)}, \dots, m_k^{(i)}\}$ represents the estimate of its state trajectory. For illustration purposes, Figure 5.2 represents a tracking example where there are no Gaussian terms at initialization. The birth process contributes a Gaussian term each with the mean $m_{\gamma,1}^1$ at time step $k = 1$ and $m_{\gamma,2}^2$ at time

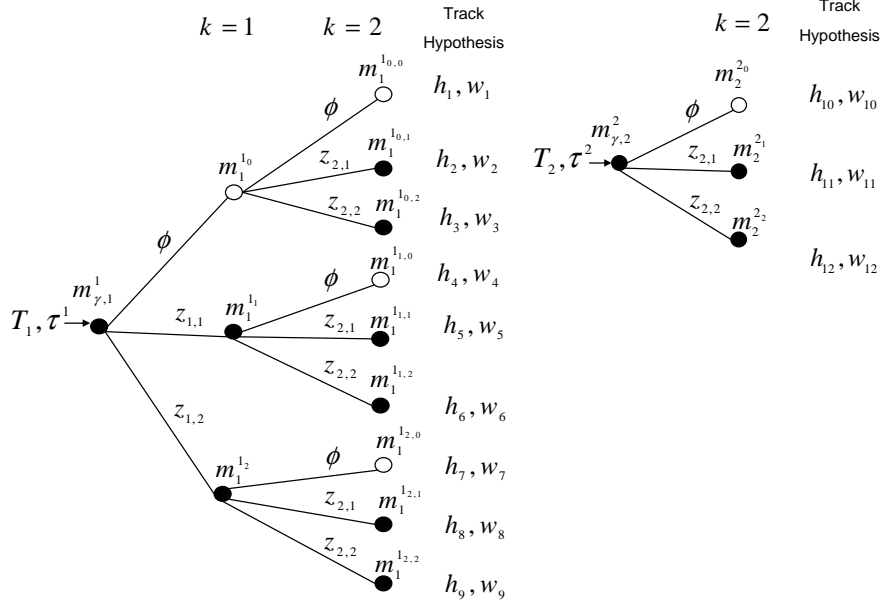


Figure 5.2: An example of track-oriented implementation of the GM-PHD Filter. $Z_1 = \{z_{1,1}, z_{1,2}\}$ and $Z_2 = \{z_{2,1}, z_{2,2}\}$, $v_0 = 0$ and a Gaussian term each is contributed by γ_k at both time steps $k = 1$ and $k = 2$. For simplicity, we denote $w_k^{(i)}$ by w_i .

step $k = 2$. A tree with the label τ^1 is initialized for $m_{\gamma,1}^1$ at time step $k = 1$ and similarly another tree with the label τ^2 for $m_{\gamma,2}^2$ at time step $k = 2$. At both time steps $k = 1$ and $k = 2$, there are two measurements each. The branch with ϕ denotes the case of miss-detection. At time step $k = 2$, tree T_2 is a tentative track and tree T_1 is a confirmed track assuming only the branch represented by h_6 has its weight $w_6 > w_{Th}$.

5.4.2 Track Initiation, Propagation and Termination

Track Initiation

At time step $k = 0$, we initialize a tree with $m_0^{(i)}$ as its root and $\tau_0^{(i)}$ as its label for $i = 1, \dots, J_0$. We also initialize a tree for every Gaussian term $m_{\gamma,k}^{(i)}$ contributed by γ_k at time step $k > 0$, with its mean $m_{\gamma,k}^{(j)}$ as its root and is given a label $\tau_{\gamma,k}^{(j)}$. All trees are classified as tentative trees.

Track Confirmation, Propagation and Termination

At each time step, we classify a tree as confirmed if at least a Gaussian at one of its leaves has weight $w_k^i > w_{Th}$. From every confirmed tree, a branch with the highest weight gives the trajectory estimate of a target and is selected into the track set \mathfrak{S}_k . The label of the selected track is the same as that of the tree it belongs to. We may also pick a branch of the strongest weight at time step k from a tree that was previously confirmed at time step $k - 1$ even though the tree has no branch with $w_k^{(i)} > w_{Th}$ at the current time step. This will enable the GM-PHD filter to track target accurately for target detection uncertainty. A track that was in \mathfrak{S}_{k-1} and not in the current time step k , can be regarded as being no longer live in the surveillance region.

5.4.3 Pruning Schemes

Tree based structures for managing tags and tracks leads to a number of pruning schemes that are effective and easier to use. Pruning schemes reduce the computational load of the recursion by eliminating the Gaussian components and tracks (represented by the tree branches) that are least likely to represent targets. The likelihoods of Gaussian terms and tracks are determined by their associated weights.

In addition to pruning Gaussian terms of smaller weights according to the pruning step outlined in Section 5.3.1), we also propose to prune least likely Gaussian terms on the basis of missed detections. We keep a counter n_{missed} on each branch of a tree to denote the number of consecutive missed detections on that branch. For example, n_{missed} for the branch represented by branch h_1 in Figure 5.2 is two. All branches with an appropriately chosen value of n_{missed} (three or more) are removed.

We also propose a pruning scheme similar to the N -scan pruning used in MHT [49]. Once a track associated with a Gaussian with $w_k^{(j)} > w_{Th}$ from a tree is chosen as output track, we eliminate all other branches that shares the same node as the chosen branch (or track) at N time steps back.

For all tentative trees, if weights of none of the Gaussians at its leaves reaches w_{Th} in a carefully chosen number of time frames (for example five or more), we

delete them.

5.5 Simulation Results

For illustration purposes, we consider a two-dimensional scenario with an unknown and time varying number of targets observed in clutter over the surveillance region $[-500, 500] \times [-500, 500]$ (in m). The state $x_k = [p_{x,k}, p_{y,k}, \dot{p}_{x,k}, \dot{p}_{y,k}]^T$ of each target consists of its position $(p_{x,k}, p_{y,k})$ and velocity $(\dot{p}_{x,k}, \dot{p}_{y,k})$, while the measurement is a noisy version of its position. $[\cdot]^T$ denotes a transpose of a matrix $[\cdot]$.

Each target follows the linear Gaussian dynamics

$$x_k = \begin{bmatrix} 1 & T & 0 & 0 \\ 0 & 1 & 0 & 0 \\ 0 & 0 & 1 & T \\ 0 & 0 & 0 & 1 \end{bmatrix} x_{k-1} + \begin{bmatrix} T^2/2 & 0 \\ T & 0 \\ 0 & T^2/2 \\ 0 & T \end{bmatrix} \sigma_v^2 \quad (5.32)$$

with $p_{S,k} = 0.90$ and $\sigma_v = 1$. Each target, if detected, generates an observation according to

$$z_k = \begin{bmatrix} 1 & 0 & 0 & 0 \\ 0 & 0 & 1 & 0 \end{bmatrix} x_k + \sigma_\epsilon^2, \quad (5.33)$$

with the detection probability $p_{D,k} = 0.98$. The sampling period $T = 1$ unit in time and $\sigma_\epsilon = \text{diag}([5, 5])$.

We assume no spawning, and the spontaneous birth intensity is Poisson with four Gaussian terms distributed across the surveillance region,

$$\gamma_k(x) = \sum_{i=1}^4 0.05 \mathcal{N}(x; m_{\gamma,i}, P_\gamma)$$

giving the mean number of spontaneously appearing targets at any time, λ_b is 0.2.

The detected measurements of targets are immersed in clutter that is typically

modelled with as a Poisson RFS with intensity function

$$\kappa_k(z) = \lambda_c V u(z), \quad (5.34)$$

where $u(\cdot)$ represents the uniform density over the surveillance region, and λ_c is the average number of clutter returns per unit hyper volume.

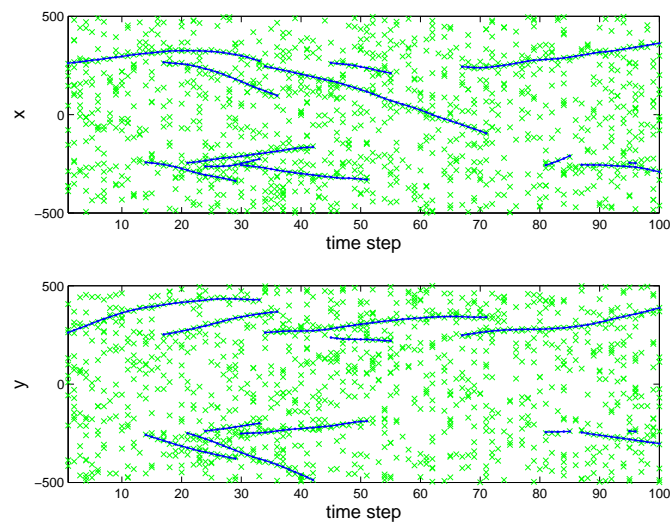


Figure 5.3: ‘Example 1’: True target positions (star) superimposed on the measurements generated (cross).

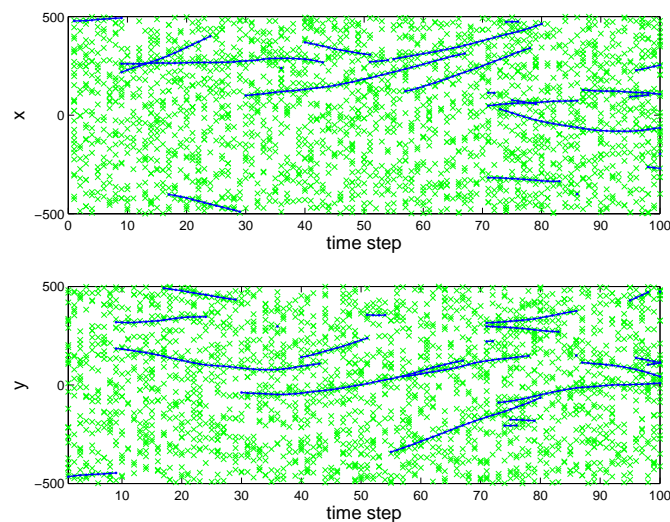


Figure 5.4: ‘Example 2’: True target positions (star) superimposed on the measurements generated (cross).

In the GM-PHD filter, pruning parameter threshold $T_{Th} = 10^{-5}$, merging thresh-

old $U = 4$, weight threshold $w_{Th} = 0.5$ and maximum number of Gaussian terms $J_{max} = 200$. We implemented a track-oriented MHT [49] with a batch of 10 frames, in which the log-likelihood ratio was used to rank tracks and the best global hypothesis was considered for data outputs.

Figures 5.3 and 5.4 respectively show a simulated scenario of with true target trajectories together with measurements generated at the sensor for duration of 100 time steps for two different examples respectively in the presence of clutter. In ‘example 1’ given in Figure 5.3, targets appear in the neighbourhood of either $[-250, -250]$ or $[250, 250]$ and move outwards. The maximum of number of targets in the surveillance region at any time is five. In ‘example 2’ given in Figure 5.4, targets are more distributed across and the maximum number of targets in the surveillance region is eight.

Figure 5.5 gives the results of the GM-PHD tracker for a typical scenario for ‘example 1’ and shows that the GM-PHD tracker gives good estimates of true target trajectories. Here we used $\lambda_c = 4 \times 10^{-5} m^{-2}$ and this translates to 10 clutter measurements per scan. The estimates given by the GM-PHD tracker is almost free of false tracks. Figure 5.6 shows estimates of target trajectories given by a track-oriented MHT that has been used here to benchmark the performance of the GM-PHD tracker. In comparison, the MHT picks up more false tracks as well as occasionally failing to pick up some true tracks. The ability to minimize the number of false tracks picked up by MHT depends on its particular implementation. By choosing a larger number of target detection-hits required for a track to be confirmed during track confirmation will reduce the number of false tracks albeit causing true tracks to be lost more often. Since only the confirmed tracks are considered for output in the MHT, any track that does not exist in the surveillance region for long enough will not be picked up by MHT.

The performance of the GM-PHD tracker can also be quantified in terms the multi-target miss distance and the estimation error in the target number. Five hundred sets of measurements for these target trajectories have been generated and average of these simulation runs are presented in the rest of this section. Simulations are carried out for $\lambda_c = 5, 10, 15,$ and 20 per scan in the surveillance region. We also

obtain average error in the target number estimate and the wasserstein distance for the ‘example 2’ given in Figure 5.4 in the presence of $\lambda_c = 20$. (Note that standard performance measures such as the mean square distance error is not applicable to multi-target filters that jointly estimate number of targets and their states.)

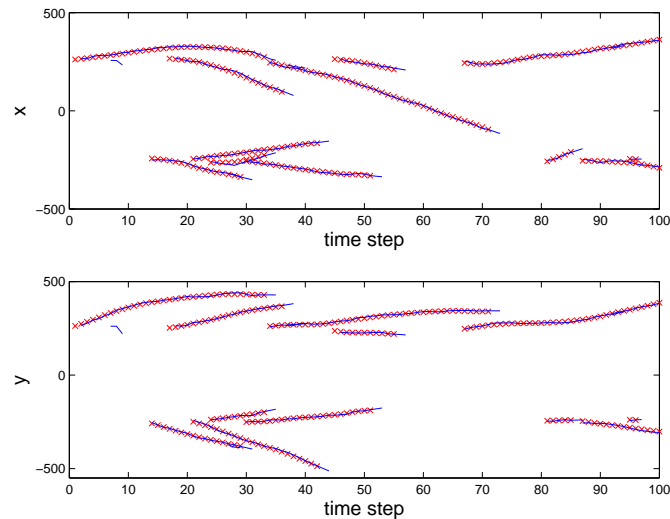


Figure 5.5: Target tracks obtained using GM-PHD tracker (solid lines) superimposed with the true target positions (crosses) for ‘example 1’.

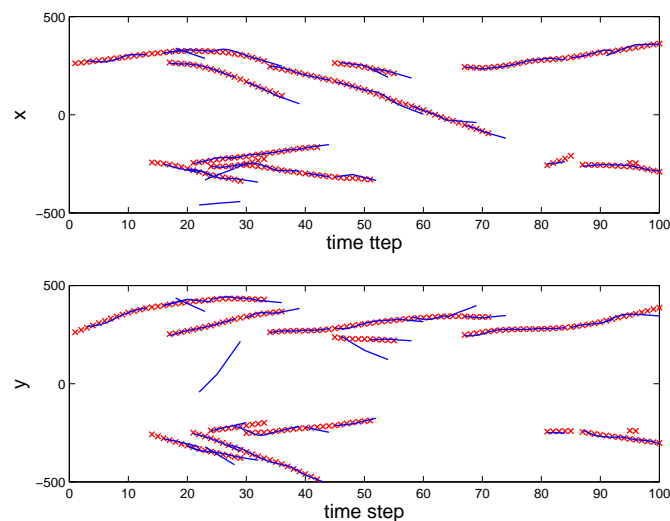


Figure 5.6: Target tracks obtained using a track-oriented MHT (solid lines) superimposed with the true target positions (crosses) for ‘example 1’.

5.5.1 The Wasserstein Distance

The Wasserstein distance from theoretical statistics was adopted as a means of defining a metric for multi-target distances as it penalizes when the estimate of the number of targets is incorrect [32]. When number of targets is estimated correctly, the Wasserstein distance is the same as the Hausdorff distance but the Hausdorff distance do not penalize for incorrectly estimating the target number. This metric has been used for assessing the performance of the PHD filter [107, 78].

Figure 5.7 shows results of the Wasserstein distance averaged over for 500 measurement sets for 100 time steps for ‘example 1’ when $\lambda_c = 10$. The occasional spikes in the plot of the Wasserstein distance for the GM-PHD tracker is usually due to the fact that either a new target has entered the surveillance region and has not yet been detected, or a target has just died and has not yet been eliminated. In comparison, the plot of Wasserstein distance for the MHT has larger peaks more frequently. Moreover, the Wasserstein distance for the GM-PHD tracker is consistently smaller than that for the MHT as GM-PHD tracker is more accurate in estimating the number of targets. Similar observations can be made in the presence of different number of average clutter points per scan. Table 5.3 shows mean value of the average wasserstein distance over the 100 time steps for $\lambda_c = 5, 10, 15$ for, 20. In each case, the average wasserstein distance for the GM-PHD tracker is smaller than that of the MHT and it decreases more slowly with the increase in the λ_c .

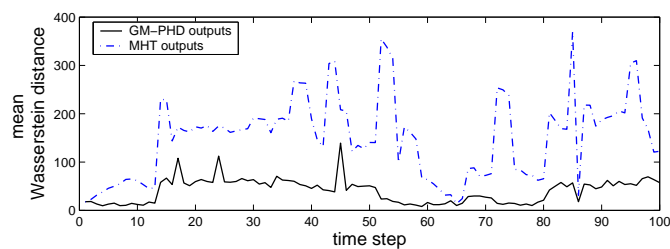


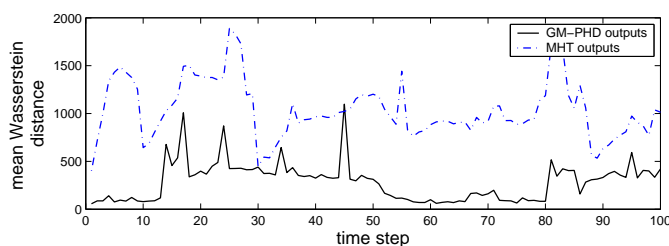
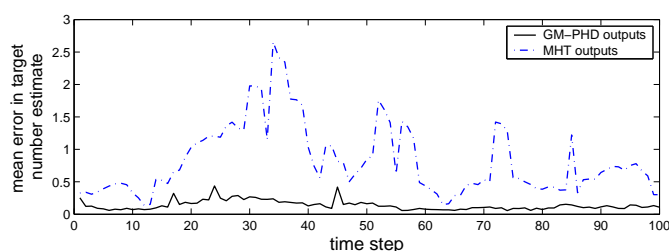
Figure 5.7: The multi-target miss distance as given by the Wasserstein metric for the GM-PHD tracker and a track-oriented MHT for ‘example 1’ with $\lambda_c = 10$.

Similarly, Figure 5.8 show the Wasserstein distance averaged over 500 measurements ‘example 2’ when $\lambda_c = 20$. Figure 5.8 also demonstrates the ability of the GM-PHD tracker to provide a better estimate of individual target trajectories. In

Table 5.3: Average of Wasserstein distance for ‘example 1’ for different λ_c

	$\lambda_c = 5$	$\lambda_c = 10$	$\lambda_c = 15$	$\lambda_c = 20$
GM-PHD Tracker	6.2530	40.1625	50.9499	56.8149
MHT	130.5379	150.7159	193.9543	224.0479

all of these cases, the higher Wasserstein distance for the MHT is mainly due to the fact that the GM-PHD tracker gives more accurate estimate of the target number (as is pointed out in the next section).

Figure 5.8: The multi-target miss distance as given by the Wasserstein metric for the GM-PHD tracker and a track-oriented MHT for ‘example 2’ with $\lambda_c = 20$.Figure 5.9: Mean error in the target number estimates for the GM-PHD tracker and a track-oriented MHT for ‘example 1’. $\lambda_c = 10$.

5.5.2 Error in Estimating the Number of Targets

Figure 5.9 also shows the absolute error in estimating the number of targets (i.e., $E\{||X_k| - |\hat{X}_k||\}$), averaged over results obtained from 500 measurement sets for ‘example 1’ when $\lambda_c = 10$. It shows that the plot of error in estimating target number for the MHT has a peaks higher and more often than that for the GM-PHD tracker. The absolute error in total target number estimates is consistently smaller for the GM-PHD tracker than for the MHT. The absolute error in estimating target numbers averaged over 100 time steps is 0.1378 for the GM-PHD tracker and 0.8261

Table 5.4: Error in Target Number Estimate for ‘example 1’

	$\lambda_c = 5$	$\lambda_c = 10$	$\lambda_c = 15$	$\lambda_c = 20$
GM-PHD Tracker	0.0967	0.1378	0.1769	0.2013
MHT	0.6351	0.8261	1.1786	1.7486

for the MHT. Similar observations can be made when the GM-PHD tracker is applied to data with different λ_c . Table 5.4 shows the mean of average error in the target number estimate over 100 time steps.

Similarly, Figure 5.10 shows the mean error in the target number estimate when the simulations are carried out for ‘example 2’ and $\lambda_c = 20$. Again, the average of the error in the target number over 100 time steps is 0.65487 for the GM-PHD tracker and 1.6681. This shows that the GM-PHD tracker provides target number estimates more accurately than the MHT.

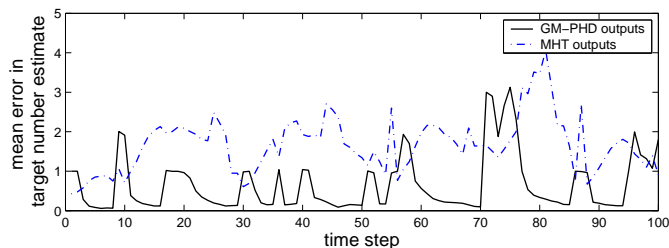


Figure 5.10: Mean error in the target number estimates for the GM-PHD tracker and a track-oriented MHT for ‘example 2’. $\lambda_c = 20$.

5.5.3 Remarks

For the linear Gaussian multi-target models, the proposed tracker is an alternative method to the *PHD-with-association filter* that is proposed to provide data association for the SMC-PHD filter [77, 78]. Data association techniques that are proposed for the SMC-PHD filter [14, 77, 78] can also be applied to the GM-PHD tracker. However, such schemes would require additional steps like prediction and gating, and the required computational cost would be considerably more than the cost of using tags. However, such techniques could be employed in conjunction with the GM-PHD tracker in some situations and will be presented in the following section.

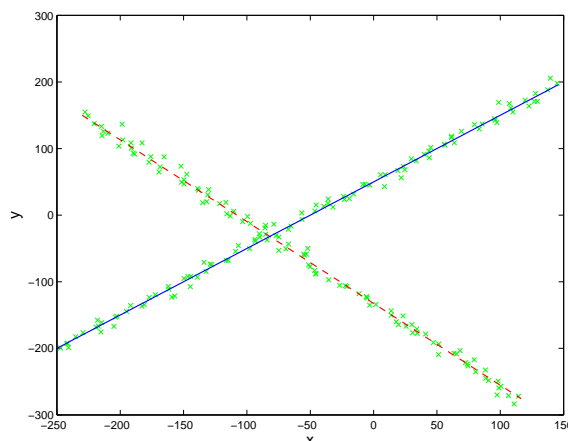


Figure 5.11: Crossing target trajectories with target ‘1’ (dashed room) and ‘target 2’ (solid line).

5.6 The GM-PHD Tracker and Crossing Targets

The algorithm presented in Section 5.3.1 has a theoretical limitation that it is unable to distinguish between any two target tracks when they are within a certain distance of each other [60]. Consider a situation where two targets are in the surveillance region. Ideally the intensity function would be represented by two Gaussians as

$$v_k(x) = w_k^1 \mathcal{N}(x; m_k^1, P_k) + w_k^2 \mathcal{N}(x; m_k^2, P_k) \quad (5.35)$$

(For simplicity, we take the covariance matrix for both Gaussians to be the same.)

Suppose that these two targets cross, then the intensity function v_k at time step k is unimodal with the mean $(m_k^1 + m_k^2)/2$ when $|m_k^1 - m_k^2| < 2|P_k|^{1/2}$ [60]. This means that the GM-PHD tracker fails to distinguish between targets within this separation. Furthermore, these components could actually be merged into a Gaussian if their means fall within the merging threshold, U . Thus, if separate tracks of targets are to be maintained when targets are too close, alternative methods for data association are needed. Next, we show that the correct target identities can be maintained by using their past trajectories. Assuming, the targets have been detected and their state trajectories upto time step $k-1$ are available, we propose to apply an ‘estimate-to-track’ association scheme similar to the one proposed earlier in Chapter 4 for the SMC-PHD filter.

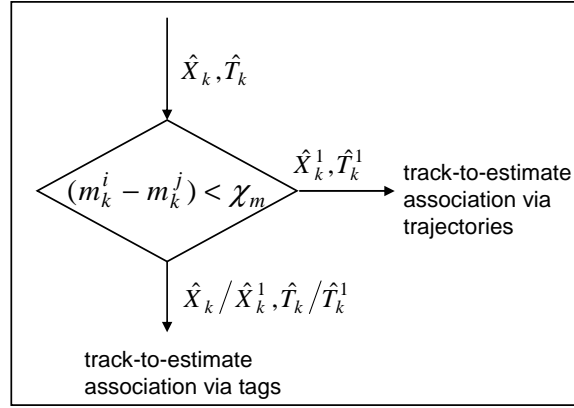


Figure 5.12: An schematic view of extending the GM-PHD filter to crossing targets. χ_m denotes a distance within which two Gaussian terms becomes unimodal and depends on the variances on the Gaussian terms.

5.6.1 Estimate-to-Track Association for the GM-PHD Tracker

Given the set of target state estimates \widehat{X}_k and their respective tags \widehat{T}_k , we first propose to construct \widehat{X}_k^1 and \widehat{T}_k^1 where for every $m_k^i \in \widehat{X}_k^1$ there exists at least another m_k^j ($i \neq j$) for which $|m_k^i - m_k^j| < 2|P_k|^{1/2}$ and \widehat{T}_k^1 denotes the set of tags of each $m_k^j \in \widehat{X}_k^1$. Given the track set \mathfrak{S}_{k-1} at time step $k-1$, the estimate-to-track association for the state estimates in $\widehat{X}_k \setminus \widehat{X}_k^1$ are performed according to the scheme presented in Section 5.3.1.

To resolve the track identities of target state estimates present in \widehat{X}_k^1 , the trajectories of these targets upto time step $k-1$ are obtained from the track set \mathfrak{S}_{k-1} and initialized as track hypotheses. The identity of a track hypothesis is given by the label of the initializing track. For each track hypothesis, we propagate its mean and covariance as $\tilde{m}_{k|k-1}^i = F_{k-1}\tilde{m}_{k-1}^i$, and $\tilde{P}_{k|k-1}^i = Q_{k-1} + F_{k-1}P_{k-1}^i(F_{k-1})^T$. The score of the track is represented by its *log-likelihood ratio* (LLR) that is initialized with $\log(w_{k-1}^i)$. For each track, an association track hypothesis is formed by associating it with every $m_k^j \in \widehat{X}_k^1$, and its *LLR* is incremented as

$$LLR_{k,i}^j = LLR_{k-1,i} + \log \left(\mathcal{N}(m_k^j; \tilde{m}_{k|k-1}^i, P_k^j + \tilde{P}_{k|k-1}^i) \right). \quad (5.36)$$

Figure 5.13 shows an example of two crossing target tracks. Trees are initialized with their respective past trajectories and labels at time step $k-1$, and association hypotheses are formed with both means m_k^i and m_k^j at time steps k and $k+1$. The

objective here is to resolve the labels of m_k^i and m_k^j at time step k and onwards.

At time step k , we have a number of hypothesis trees where a branch of a tree is an association track hypothesis. All branches of a tree represent the same target. At time step k , a branch of the highest LLR from each hypothesis tree denotes a possible track. The identity of the track and that of every Gaussian that belongs to it is given by the tree it belongs to. We propose to recursively extend each tree by forming association hypotheses for each branch with for every $\tilde{x}_{k,i} \in \widehat{X}_k^1$ that arrives next in time. Once $|m_k^i - m_k^j|$ is no longer smaller than $2|P_k|^{1/2}$ for any m_k^i and m_k^j in \widehat{X}_k^1 , an association track hypothesis of the the highest LLR is selected from each tree and are passed back to the GM-PHD tracker along their labels.

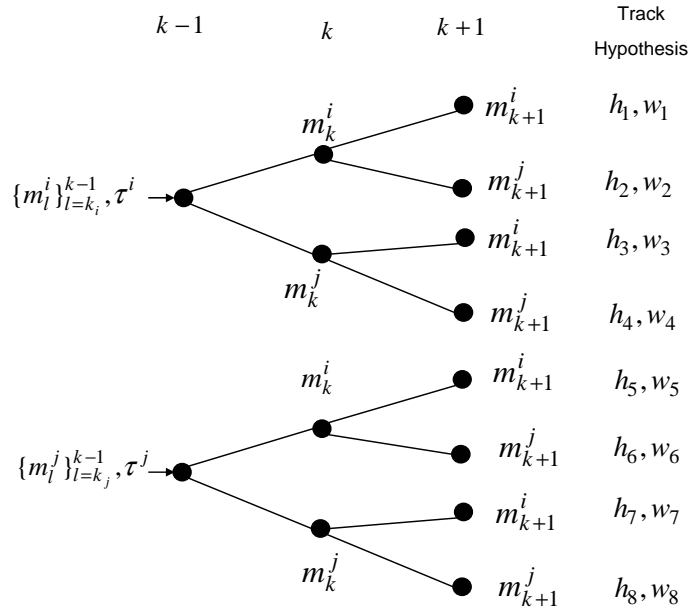


Figure 5.13: An example of estimate-to-track association for the crossing targets in the GM-PHD filter. w_i denotes the log-likelihood ratio (LLR) of a track hypothesis at the current time step, i.e. $k = 2$ in this case.

5.6.2 Example of Crossing Targets

For illustration purposes, Figure 5.11 shows two targets in the surveillance region who trajectories cross each other at time step $k = 53s$. While Figure 5.14 and 5.15 shows the results of two different simulation runs for the targets given in Figure 5.11. While the result of one simulation run presented in Figure 5.14 correctly keeps the identities of two crossing tracks, the GM-PHD tracker fails to correctly keep separate

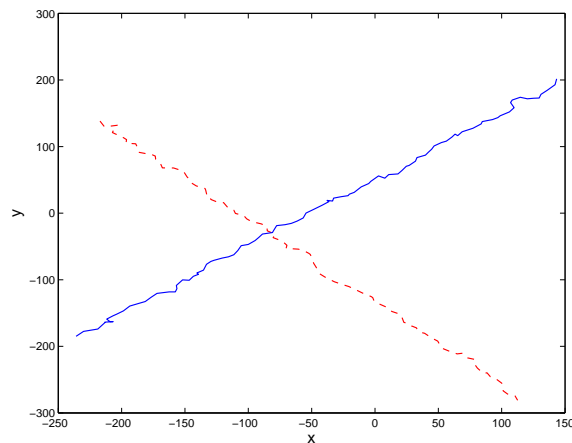


Figure 5.14: Trajectories (identified correctly) given by the GM-PHD tracker for crossing targets.

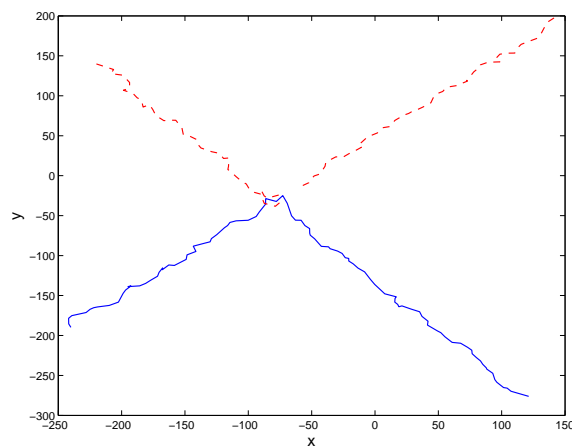


Figure 5.15: Trajectories (wrongly identified) given by the GM-PHD tracker for crossing targets.

target identities of the tracks in another simulation run as shown in Figure 5.15. Another possible outcome would be the assignment of the same identity to both of these tracks. Figure 5.16 shows the results of the improved GM-PHD tracker that consistently resolves the track identities of the crossing targets. However this will require computation of distances amongst all target estimates at every time steps and as a result adds to the computational load of the overall GM-PHD tracker.

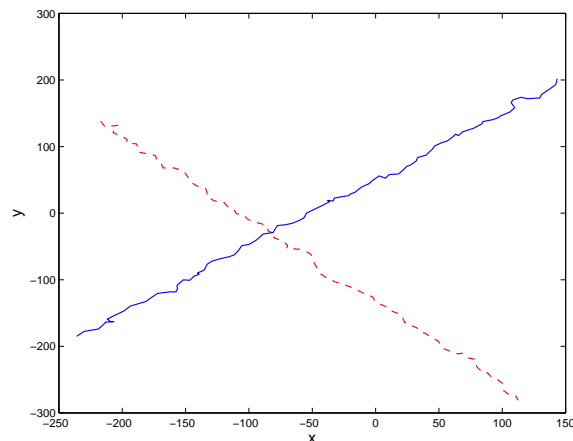


Figure 5.16: Trajectories given by the GM-PHD tracker that performs track-to-estimate association between time steps 52 and 55.

5.7 Summary

In this chapter, the class of the multi-target models for which the PHD recursion admits a closed-form solution has been presented. The closed-form solution of the PHD filter as the GM-PHD filter has been described. This chapter presented a new multi-target tracker, GM-PHD tracker capable of providing track continuity in addition to state estimates of unknown number of targets and their number. An efficient and systematic track management scheme has been proposed for the GM-PHD tracker. Simulation results are presented for the GM-PHD tracker and its performance was benchmarked against that of the MHT. It has been shown that the GM-PHD tracker has the ability to track an unknown and time-varying number of targets in the presence of association uncertainty, detection uncertainty and clutter with a fewer number of false tracks and smaller multi-target miss-distance. It should be noted that the MHT has only been used to benchmark the performance of the GM-PHD tracker. In practice, performance of the MHT depends on its particular implementation and can be improved upon at the expense of increased complexity and additional computation. Finally, the GM-PHD tracker has been extended to resolve individual identities of crossing target tracks.

Chapter 6

The Convolution PHD Filter

6.1 Introduction

A major limitation of the SMC-PHD filter is that it requires the analytical knowledge of the observation likelihood as it uses the observation likelihood to update the weights of posterior intensity particles. The filter is also limited in its ability to handle observations with small noise. Recently, Rossi *et. al.* have proposed to use the convolution kernel probability density estimation to overcome similar limitations in case of standard SMC implementations of the Bayes recursion and presented a new class of filters, called *convolution filters* [87]. This chapter extends the underlying idea behind the convolution filter to the SMC-PHD filter and accordingly presents a new kernel based SMC implementation of the PHD filter.

Section 6.2 introduces the convolution approach to the density estimation and the convolution filters. The convolution kernel based SMC implementation of the PHD filter is included in Section 6.3. Simulation results are presented in Section 6.4 to demonstrate the performance of the proposed filter when the observation noise is small and the SMC-PHD filter fails. Finally, Section 6.5 presents the summary of this chapter.

6.2 Convolution Kernels Approach to The Bayes Recursion

This section provides an introduction to the convolution kernel approach to the Bayes recursion. It gives a brief outline of the kernel density probability density estimation and its use in the approximation of the Bayes recursion. The new class of the convolution filters is also summarized.

6.2.1 Kernel Density Estimation

A kernel $\mathbb{K} : \mathbb{R}^d \mapsto \mathbb{R}$ is a bounded, positive and symmetric function for which

$$\int \mathbb{K}(x) dx = 1.$$

A Parzen-Rosenblatt kernel is a kernel such that $\|x\|^d \mathbb{K}(x) \rightarrow 0$ as $\|x\| \rightarrow \infty$, where $\|\cdot\|$ denotes the squared norm. Given that samples x^1, \dots, x^n be identically independent distributed (i.i.d.) random variables with the common density f , the kernel density estimator of f , \hat{f} is given by

$$\hat{f}(x) = \frac{1}{n \det(\mathbf{H})} \sum_{i=1}^n \mathbb{K} \left(\frac{x - x^i}{\mathbf{H}} \right), \quad (6.1)$$

where $\mathbf{H} \in \mathbb{R}^{d \times d}$ is positive definite and $\det(\cdot)$ represents the determinant of a matrix. Often, one chooses $\mathbf{H} = h\mathbf{I}_d$ [92, 113] so the same h is used for all variables. $h > 0$ is called the kernel bandwidth and \mathbf{I}_d denotes an identity matrix of dimension d . Now (6.1) reduces to

$$\hat{f}(x) = \frac{1}{nh^d} \sum_{i=1}^n \mathbb{K} \left(\frac{x - x^i}{h} \right). \quad (6.2)$$

Similarly, the kernel \mathbb{K} is often chosen as a product kernel,

$$\mathbb{K}(x_1, \dots, x_d) = \prod_{i=1}^d \mathbb{K}(x_i), \quad (6.3)$$

for some univariate kernel $\mathbb{K} : \mathbb{R} \mapsto \mathbb{R}$.

Given that an empirical measure associated with samples x^1, \dots, x^n , is μ_n i.e., $\mu_n = \frac{1}{n} \sum_{i=1}^n \delta_{x^i}$ ¹ exists, the kernel estimator \hat{f} can also be written as the convolution of appropriate kernels with the empirical measure [21, 92, 113],

$$\hat{f}(x) = (\mathbb{K}_h * \mu_n)(x). \quad (6.4)$$

where ‘*’ denotes the convolution operation and $\mathbb{K}_h(\cdot)$ is the scaled kernel density given by

$$\mathbb{K}_h(x) = \frac{1}{h^d} \mathbb{K}\left(\frac{x}{h}\right), \quad (6.5)$$

One such appropriate kernel is the Parzen-Rossenblatt kernel.

A survey of recent developments in the kernel density estimation can be found [38] which gives a good description of kernel density estimate and, a discussion on the choice of the kernels and kernel bandwidths. In practice, the choice of kernels has very little effect on the performance of a kernel density estimator whereas the choice of kernel bandwidths plays a crucial role. A small kernel bandwidth reduces the bias in the estimate but at the expense of higher variance. A detailed treatment of the kernel density estimation can be found in [21, 72, 92, 113].

6.2.2 The Convolution Filters

This section applies to single-object filtering. In single-object filtering, a target motion is modelled by

$$f_{k|k-1}(\cdot|x_{k-1})$$

and the observation likelihood is modelled by

$$g_k(\cdot|x_k).$$

Given that all observations upto time step k , $z_{1:k}$ is available, the posterior density $p_k(\cdot|z_{1:k})$ of a target can be recursively obtained from its initial density p_0 according

¹ δ_{x^i} is the dirac delta function centered at x^i .

to the optimal filter

$$p_k(x_k|z_{1:k}) = \frac{p_k(x_k, z_{1:k})}{p_k(z_{1:k})} \quad (6.6)$$

where $p_k(x_k, z_{1:k})$ is the joint density of $(x_k, z_{1:k})$, which is given as

$$p_k(x_k, z_{1:k}) = g_k(z_k|x_k) \int f_{k|k-1}(x_k|\xi) p_{k-1}(\xi|z_{1:k-1}) d\xi. \quad (6.7)$$

and $p_k(z_{1:k})$ is the marginal density of $z_{1:k}$.

Assuming we know how to draw samples from $f_{k|k-1}(\cdot|x_{k-1})$, $g_k(\cdot|x_k)$ and the initial density $p_0(\cdot)$, the *basic convolution* filter [87] approximates the filter given in (6.6) by

$$\hat{p}_k(x_k|z_{1:k}) = \frac{\sum_{i=1}^n K_{h_n}^{\bar{z}}(z_{1:k} - z_{1:k}^{(i)}) K_{h_n}^x(x_k - x_k^{(i)})}{\sum_{i=1}^n K_{h_n}^{\bar{z}}(z_{1:k} - z_{1:k}^{(i)})} \quad (6.8)$$

where $K_{h_n}^{\bar{z}}(z_{1:k} - z_{1:k}^{(i)}) = \prod_{l=1}^k K_{h_n}^z(z_l - z_l^{(i)})$, $x_{k-1}^{(i)} \sim \hat{p}_{k-1}(\cdot)$, $x_k^{(i)} \sim f_{k|k-1}(\cdot|x_{k-1}^{(i)})$ and the corresponding observation sample $z_k^{(i)} \sim g_k(\cdot|x_k^{(i)})$. $K_{h_n}^x$ and $K_{h_n}^z$ are the scaled Parzen-Rosenblatt kernels of appropriate dimensions. Kernel bandwidth h_n depends on n , dimensions of z_k and $z_k^{1:n}$ in $K_{h_n}^z$ (or n and dimensions of x_k and $x_k^{1:n}$ in $K_{h_n}^x$). Table 6.1 gives the recursive algorithm of the basic convolution filter. The basic convolution filter has also been extended to include the resampling step to account for the problem of particle degeneration over time. Table 6.2 summarizes the *resampled convolution filter* algorithm. Convergence properties of the basic convolution filter as well as the resampled convolution filter to the optimal filter are established in [87].

It has been noted in [12, 87], the convolution filter provides implicit regularization on both the state and observation space, thus improving the samples diversity. In contrast, kernel based regularization techniques such as those proposed in [23, 35, 70], either consider regularization in the state space or observation space separately and are computationally expensive.

Table 6.1: The Convolution Filter

For $k = 0$

- initial sampling: $x_0^{(i)} \sim p_0$ for $i = 1, \dots, n$
- weight initialization: $w_0^{(i)} = 1$ for $i = 1, \dots, n$

For $k \geq 1$

- state sampling: $x_k^{(i)} \sim f_{k|k-1}(\cdot|x_{k-1}^{(i)})$ for $i = 1, \dots, n$
- observation sampling: $z_k^{(i)} \sim g_k(\cdot|x_k^{(i)})$ for $i = 1, \dots, n$
- weight updating: $w_k^{(i)} = K_h^z(z_k - z_k^{(i)})w_{k-1}^{(i)}$ for $i = 1, \dots, n$
- filter updating:

$$\hat{p}_k(x_k|z_{1:k}) = \frac{\sum_{i=1}^n w_k^{(i)} K_{h_n}^x(x_k - x_k^{(i)})}{\sum_{i=1}^n w_k^{(i)}}$$

6.3 The Kernel based SMC-PHD Filter

This section presents the convolution kernel based SMC implementation of the PHD filter. We can use appropriate kernels to update the weights of posterior intensity particles instead of the observation likelihood as is the case with the SMC-PHD filter. The resulting SMC-PHD filter, termed the *convolution PHD filter* would neither require an analytical knowledge² for the observation likelihood nor the non-nullity of observation noise variances. It would require the ability to generate samples from the posterior intensity function, target birth intensity, target transition and likelihood function.

²Specifically one does not require the ability to evaluate the density $g_k(z|x_k^{(i)})$ when measurement z is available. We would only need the ability to generate $z_k^{(i)}$ for a given state sample $x_k^{(i)}$ using the observation process.

Table 6.2: The Resampled-Convolution Filter

For $k = 0$

- initialization: $\hat{p}_0 \leftarrow p_0$

For $k \geq 1$

- resampling: $x_{k-1}^{(i)} \sim \hat{p}_{k-1}$ for $i = 1, \dots, n$
- state sampling: $x_k^{(i)} \sim f_{k|k-1}(\cdot)$ for $i = 1, \dots, n$
- observation sampling: $z_k^{(i)} \sim g_k(\cdot | x_k^{(i)})$ for $i = 1, \dots, n$
- filter updating:

$$\hat{p}_k(x_k | z_{1:k}) = \frac{\sum_{i=1}^n K_{h_n}^z(z_k - z_k^{(i)}) K_{h_n}^x(x_k - x_k^{(i)})}{\sum_{i=1}^n K_{h_n}^z(z_k - z_k^{(i)})}$$

6.3.1 The Convolution PHD Filter

For simplicity, we have omitted spawning of targets in the formulation of the convolution PHD filter to be described next in this section.

Given the kernel estimate of the intensity function $\hat{v}_{k-1}(x)$ at time step $k - 1$, we first generate L_{k-1} samples as

$$x_{k-1}^{(i)} \sim \hat{v}_{k-1}(\cdot)$$

and initialize their respective weights as

$$w_{k-1}^{(i)} = \hat{N}_{k-1} / L_{k-1}$$

so that

$$\hat{v}_{k-1}(x) \approx \{x_{k-1}^{(i)}, w_{k-1}^{(i)}\}_{i=1}^{L_{k-1}}.$$

The choice of L_{k-1} depends on the target number estimate \hat{N}_{k-1} at time step $(k - 1)$ and the number of particles per target, ρ (i.e. $L_{k-1} \approx \rho \hat{N}_{k-1}$) as we try to maintain

the number of particles per target constant. In comparison the SMC-PHD filter, here samples are drawn from \hat{v}_{k-1} .

Next we obtain L_{k-1} state samples and their respective weights at the time step k as follows

$$x_k^{(i)} \sim f_{k|k-1}(\cdot|x_{k-1}^{(i)})$$

and

$$w_{k|k-1}^{(i)} = p_{S,k}(x_{k-1}^{(i)})w_{k-1}^{(i)}.$$

We also need to draw samples from the target birth intensity function to account for new targets appearing in the surveillance region. We generate J_k ($\approx \rho\lambda_b$, λ_b denotes the mean number of targets born at each time interval) samples from the target birth intensity γ_k as

$$x_k^{(i)} \sim \gamma_k(\cdot)$$

and compute their associated weights as

$$w_{k|k-1}^{(i)} = \lambda_b/J_k.$$

This step of generating $\{x_k^{(i)}, w_{k|k-1}^{(i)}\}_{i=1}^{L_{k-1}+J_k}$ is called state sampling. This replaces the prediction step of the SMC-PHD filter that uses the prior as the proposal density function. Drawing of samples from the target birth intensity function is similar to the one employed in the SMC-PHD filter (see 4.1).

Now, we have $\{x_k^{(i)}, w_{k|k-1}^{(i)}\}_{i=1}^{L_{k-1}+J_k}$ that approximates the predicted intensity $v_{k|k-1}$ at time step k . We next update of the sample weights as follows.

Generate an observation sample for each of the state samples according to

$$z_k^{(i)} \sim g_k(\cdot|x_k^{(i)}).$$

Here, we only need the ability to generate $z_k^{(i)}$ given $x_k^{(i)}$ according to the likelihood function (or observation process). We do not require the ability to evaluate $g_k(z|x_k^{(i)})$ for a given z as is the case with the existing implementation of the SMC-PHD filter (see 4.1).

Given the set of the state samples $\{x_k^{(i)}\}_{i=1}^{L_{k-1}+J_k}$, the associated weights $\{w_{k|k-1}^{(i)}\}_{i=1}^{L_{k-1}+J_k}$ and the observation samples $\{z_k^{(i)}\}_{i=1}^{L_{k-1}+J_k}$, the weights are updated as

$$w_k^{(i)} = \left[1 - p_{D,k}(x_k^{(i)}) + \sum_{z \in Z_k} \frac{p_{D,k}(x_k^{(i)}) K_h^z(z - z_k^{(i)})}{\kappa_k(z) + C_k(z)} \right] w_{k|k-1}^{(i)} \quad (6.9)$$

where $C_k(z) = \sum_{j=1}^{L_{k-1}+J_k} p_{D,k}(x_k^{(j)}) K_h^z(z - z_k^{(j)}) w_{k|k-1}^{(j)}$. This would produce the set of samples $\{x_k^{(i)}\}_{i=1}^{L_{k-1}+J_k}$ and its weights that are updated with measurement set, $\{w_k^{(i)}\}_{i=1}^{L_{k-1}+J_k}$, we can obtain the estimate of the posterior density function via kernel density estimation. An estimate of the posterior intensity function $\hat{v}_k(\cdot)$ at time step k given the measurement set $Z_{1:k}$ is given as

$$\hat{v}_k(x_k | Z_{1:k}) = \sum_{i=1}^{L_{k-1}+J_k} w_k^{(i)} K_h^x(x_k - x_k^{(i)}) \quad (6.10)$$

The estimate of the posterior intensity function given in (6.10) gives the kernel estimate of the posterior intensity function v_k at time step k . For the multi-target state estimation, we can apply standard clustering techniques on the weighted particle set $\{x_k^{(i)}, w_k^{(i)}\}_{i=1}^{L_{k-1}+J_k}$. The estimate of the target number at time step k is given as $\hat{N}_k = \int \hat{v}_k(x) dx$. Here, we need to be mindful that unlike a probability density, the integration of an intensity function over the state space gives the estimate of the number of targets.

The drawing of samples from \hat{v}_{k-1} effectively constitutes the step of resampling that uses the continuous approximation of the posterior intensity instead of the discrete one used in the SMC-PHD filter. The convolution PHD filter presented here also maintains the number of particles per target constant over time by drawing $\rho \hat{N}_{k-1}$ at the start of time step k . The convolution PHD filter is summarized in Table 6.3.

The convolution PHD filter does not require the observation likelihood to update the posterior intensity particle weights. The new SMC-PHD filter should be able to perform well in cases when the observation noise is too small as long as we can draw samples from the initial intensity and the likelihood function. Furthermore, we also need to be able to generate samples from the birth intensity function that governs the

spontaneously appearing new targets. It should be noted that the use of convolution kernels to approximate the PHD filter is purely from the Monte Carlo approximation point of view and has nothing to do with approximating the probability densities as is the case in the convolution filter.

6.3.2 Implementation Issues

The implementation of the convolution PHD filter proposed in the previous section requires careful consideration. While its performance depends on the choice of initial density, kernels and the number of particles per targets, the choice of the kernel bandwidth is crucial in practice. The kernel bandwidth affects the bias as well as the variance of the intensity estimate. Often, we want a kernel bandwidth that minimizes the *mean integrated squared error* (MISE) of the estimated function [92]. The optimal choice of the kernel for approximating a density function has been studied and a detailed discussion can be found in [38, 92] and the references therein. However, the optimal choice of the kernel bandwidth for approximating the intensity function requires further investigation. Here we use the recommended optimal choice of h_n^y for density of variable y is $h_n^y = C_y n^{-1/(4+n_y)}$ that is given for the convolution filter in [11] and it works well. The choice of C_y is important and in general $C_y = c_y P_y^{1/2}$ gives good results, where $c_y \simeq 1$ and P_y is the covariance matrix associated with y . The exact value of c_y that gives good results can be tuned in practice.

6.4 Simulation Results

For illustration purposes, we consider a two-dimensional scenario, in which a target moves in the region $[-150, 150] \times [-150, 150]$. Each target moves according to the following linear and Gaussian target dynamics,

$$x_k = \begin{bmatrix} 1 & T & 0 & 0 \\ 0 & 1 & 0 & 0 \\ 0 & 0 & 1 & T \\ 0 & 0 & 0 & 1 \end{bmatrix} x_{k-1} + \begin{bmatrix} T^2/2 & 0 \\ T & 0 \\ 0 & T^2/2 \\ 0 & T \end{bmatrix} \begin{bmatrix} v_{1,k} \\ v_{2,k} \end{bmatrix} \quad (6.11)$$

where $x_k = [p_k^x, \dot{p}_k^x, p_k^y, \dot{p}_k^y]^T$, and $[p_k^x, p_k^y]^T$ and $[\dot{p}_k^x, \dot{p}_k^y]^T$ represent position and velocity of the target at time step k . $T = 1$ unit in time is the sampling period. The process noise $v_{1,k}$ and $v_{2,k}$ are independent zero mean Gaussian noise with standard deviations of 1.0 and 0.1 respectively. An existing target has a survival probability of $p_{S,k} = 0.95$ and this probability is state independent.

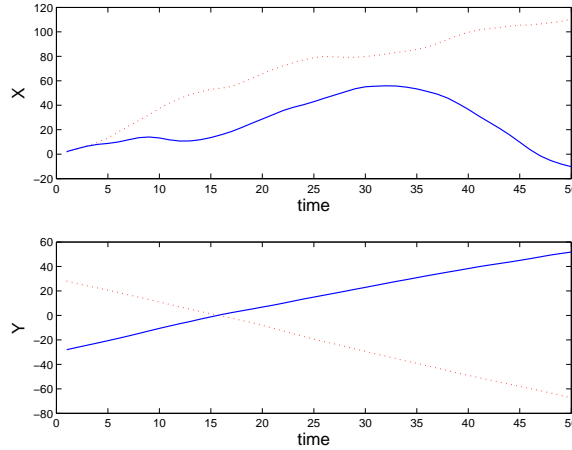


Figure 6.1: Target trajectories (target ‘1’ (solid line), target ‘2’ (dotted line)) in terms of x-coordinate positions and y-coordinate positions separately.

The bearing θ_k and range r_k observations of a target are generated by a sensor located at $[0, -100]^T$ and are given by

$$\theta_k = \arctan\left(\frac{p_k^x}{p_k^y + 100}\right) + w_{1,k} \quad (6.12)$$

$$r_k = \sqrt{((p_k^x)^2 + (p_k^y + 100)^2)} + w_{2,k} \quad (6.13)$$

The measurement noise $w_{1,k}$ and $w_{2,k}$ are independent zero mean Gaussian noise. Moreover, the measurement noise is independent of the process noise. Without loss of generality, the probability of detection is assumed unity. Clutter is uniformly distributed over the observation space with an average rate of 10 points per scan giving a return of $11.1 \times 10^{-5} m^{-2}$ per unit hyper volume. It should be noted that we use the abovementioned target and observation models for simplicity of comparing the performance of the convolution PHD filter with that of the SMC-PHD filter. In practice, the technique proposed here would be applied to problems that are more nonlinear and/or non-Gaussian.

Without the loss of generality, we consider two targets whose x-positions and y-positions over 50 time steps are given separately in Figure 6.1. Figure 6.2 shows the observations of these targets in clutter. At each time step, the target state estimates are extracted from the set of particles representing the updated intensity function by applying standard clustering techniques. Both the SMC-PHD filter and the convolution PHD filter use 500 particles per target. The kernel functions are used in the convolution PHD filter are Gaussian.

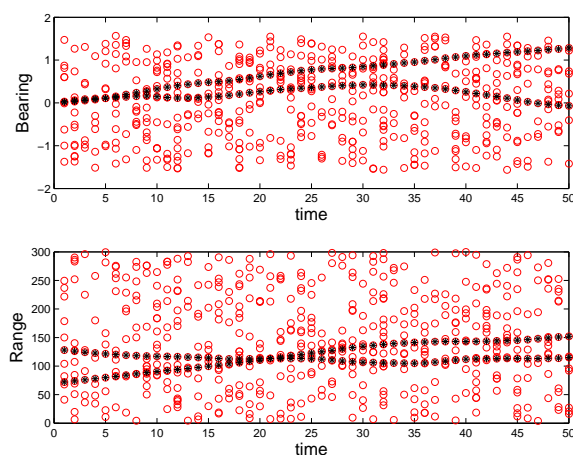


Figure 6.2: Observations generated by targets immersed in clutter.

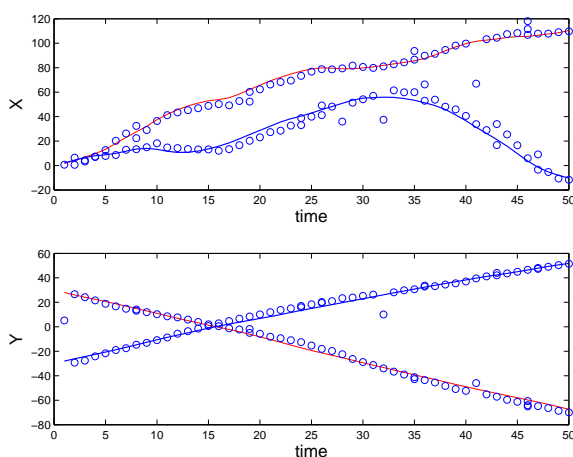


Figure 6.3: State estimates given by the convolution PHD filter for $\sigma_{w_{1,k}} = 0.05$ and $\sigma_{w_{2,k}} = 1.0$.

Figures 6.3 and 6.4 shows the state estimates given by the convolution PHD filter and SMC-PHD filter respectively when the observation noise variances $\sigma_{w_{1,k}} = 0.05$ and $\sigma_{w_{2,k}} = 1.0$. In this case, both the SMC-PHD filter and convolution PHD filter

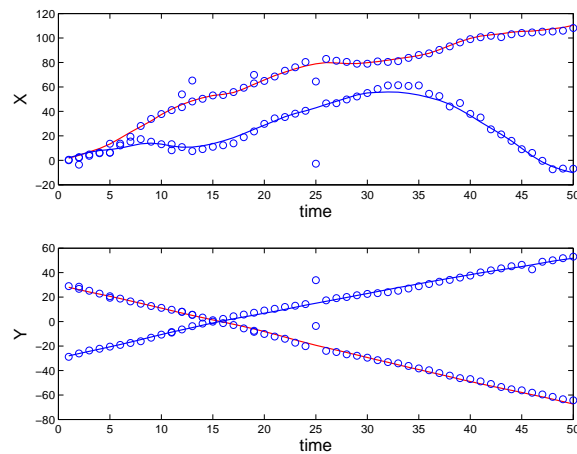


Figure 6.4: State estimates given by the SMC-PHD filter for $\sigma_{w_{1,k}} = 0.05$ and $\sigma_{w_{2,k}} = 1.0$.

pick up the targets very well. However as the observation noise is reduced, the performance of the SMC-PHD filter begins to degrade. When $w_{1,k} = 0.05/2$ and $w_{2,k} = 1.0/25$, the SMC-PHD filter is not reliable anymore. Its performance varies from one Monte Carlo run to another. Figure 6.5 shows the plot of state estimates given by the SMC-PHD filter. When the observation noise is further reduced, the SMC-PHD filter fails completely and does not pick up either of the targets at the next time step after initialization. Figure 6.6 shows the plots of the state estimates of targets generated by the convolution PHD filter when no observation noise is applied. This shows the ability of the convolution PHD filter to perform in zero or near-zero observation noise conditions.

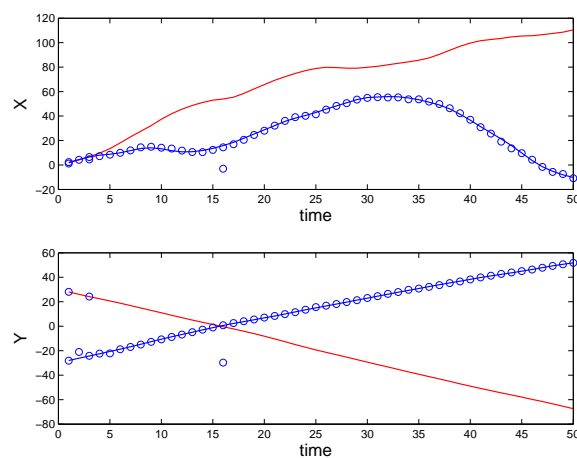


Figure 6.5: State estimates given by the SMC-PHD filter for $\sigma_{w_{1,k}} = 0.05/2$ and $\sigma_{w_{2,k}} = 1.0/25$.

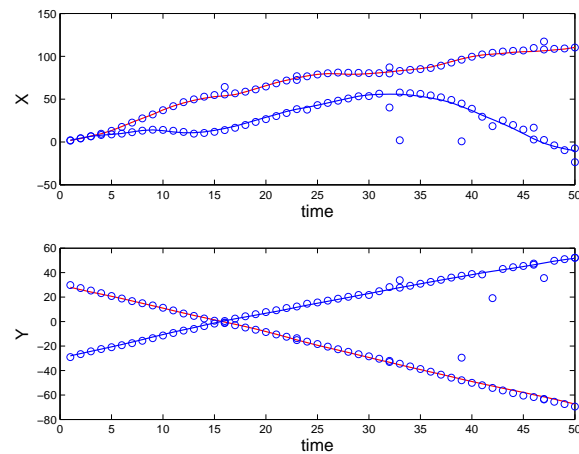


Figure 6.6: State estimates given by the convolution PHD filter with no observation noise.

6.5 Summary

This chapter has described a new SMC approximation of the PHD filter, namely the convolution PHD filter that overcomes the inability of the existing implementations of the SMC-PHD filter. The existing SMC-PHD filter implementations are limited in their applications to tracking scenarios that have small observation noise. Moreover, the new SMC-PHD filter does away with the need for the analytical knowledge of the likelihood function. Simulation results are also presented to demonstrate the performance of the proposed filter when the observation noise is small and the standard SMC-PHD filter fails. The proposed SMC-PHD filter here includes the resampling step to overcome the problem of particle degeneracy experienced by particle filters in general. A continuous approximation of the posterior intensity function is available during resampling instead of the discrete approximation that is used in the SMC-PHD filter.

Table 6.3: The Convolution PHD Filter

For $k = 0$

initialization: $\hat{v}_0 = \pi_0$

For $k \geq 1$

- *resampling*:

$$x_{k-1}^{(i)} \sim \hat{v}_{k-1}(\cdot) \text{ for } i = 1, \dots, L_{k-1},$$

$$w_{k-1}^{(i)} = \hat{N}_{k-1}/L_{k-1} \text{ for } i = 1, \dots, L_{k-1}$$

- *state sampling*:

$$x_k^{(i)} \sim f_{k|k-1}(\cdot | x_{k-1}^{(i)}) \text{ for } i = 1, \dots, L_{k-1},$$

$$w_{k|k-1}^{(i)} = p_{S,k}(x_{k-1}^{(i)}) w_{k-1}^{(i)} \text{ for } i = 1, \dots, L_{k-1},$$

&

$$x_k^{(i)} \sim \gamma_k(\cdot) \text{ for } i = L_{k-1} + 1, \dots, J_k,$$

$$w_{k|k-1}^{(i)} = \lambda_b/J_k \text{ for } i = L_{k-1} + 1, \dots, J_k$$

- *observation sampling*:

$$z_k^{(i)} \sim g_k(\cdot | x_k^{(i)}) \text{ for } i = 1, \dots, L_{k-1} + J_k$$

- *weight updating*:

$$w_k^{(i)} = \left[1 - p_{D,k}(x_k^{(i)}) + \sum_{z \in Z_k} \frac{p_{D,k}(x_k^{(i)}) K_h^z(z - z_k^{(i)})}{\kappa_k(z) + C_k(z)} \right] w_{k|k-1}^{(i)},$$

for $i = 1, \dots, L_{k-1} + J_k$ where $C_k(z) = \sum_{j=1}^{L_{k-1}+J_k} p_{D,k}(x_k^{(j)}) K_h^z(z - z_k^{(j)}) w_{k|k-1}^{(j)}$.

- *filtering estimation*:

$$\hat{v}_k(x_k | z_{1:k}) = \sum_{i=1}^{L_{k-1}+J_k} w_k^{(i)} K_h^x(x_k - x_k^{(i)})$$

Chapter 7

Conclusion

7.1 Concluding Remarks

In this thesis, the problem of multiple target tracking in the RFS framework has been studied. By approximating the multi-target Bayes recursion with the PHD recursion, the RFS framework provides an alternative approach to traditional approaches for multi-target tracking. In particular, this thesis considers the use of the PHD filter to track an unknown and time-varying number of targets in the presence of data association uncertainty. A number of extensions of the SMC-PHD and GM-PHD filter have been developed for the purpose of providing track association for the state estimates of individual targets. Furthermore, a kernel based SMC-PHD filter has also been proposed.

Three new extensions of the SMC-PHD filter have been proposed. The PHD-with-association filter proposes to apply data association on the state space instead of the measurement space. Given that the set-valued estimates of the multi-target state is recursively provided by the SMC-PHD filter, the ‘estimate-to-track’ association can be performed on the estimates by applying existing data association methods. For the purpose of data association, the state estimates of individual targets can be regarded as new observations that are actual target states plus additive noise. As a result, the PHD-with-association filter is readily applicable to general multi-target models. The PHD filter has also been proposed to improve the performance of existing trackers, in particular MHT. In the ‘MHT-with-PHD’ clutter filter, the PHD filter has been used as a clutter filter to eliminate clutter from the

observation set. The proposed scheme, called the global gating uses the good state estimates of individual targets obtained from the PHD filter to validate observations at each time step. The main use of the PHD filter in both of these schemes is to provide smaller observation sets to the data association functionality. The third scheme, the cluster-indexed SMC-PHD filter provides a computationally efficient way of performing ‘estimate-to-track’ association without the need for employing existing data association methods. It assigns extra indices, called cluster indices, to weighted particles representing the posterior intensity and uses these indices in conjunction with the peak extraction to create target identities of individual state estimates. Provided the targets are not close to each other and no more than one target appears in the surveillance region at each time interval, the cluster indices can be used to obtain the state estimates of targets. The performance of these new extensions of the SMC-PHD filter has been benchmarked against that of a track-oriented MHT for typical tracking scenarios. It has been shown that the SMC-PHD based tracking schemes provide better estimates of the target state trajectories and picks up a fewer number of false tracks.

A multi-target tracker based on the GM-PHD filter has also been proposed as a solution for the multi-target tracking problems. Using tags that are assigned to individual Gaussian terms of the mixture and their weights, the GM-PHD tracker has been shown to track an unknown and time-varying number of targets in the presence of data association uncertainty. A systematic and efficient track management scheme has also been developed for the proposed tracker as a part of this study. The performance of the GM-PHD tracker has been benchmarked against that of the MHT. It has been shown to outperform the MHT in terms of both, the error in the target number estimate and the multi-target miss-distance. We also proposed a technique for extending the GM-PHD tracker so that it can resolve the identities of crossing target tracks.

Finally, a new SMC-PHD filter based on the convolution approach to the kernel probability density estimation has been proposed. The proposed convolution PHD filter does not need the analytical knowledge of the observation likelihood and can operate on observations with small noise.

7.2 Future Research

The use of RFSs in the multi-target tracking is a relatively recent trend compared to the traditional approaches. The study carried out as a part of this thesis is amongst the early attempts at extending the use the PHD filter for the purpose of general multi-target tracking. There is a need as well as the scope for further studies of the use of the RFSs in multi-target tracking.

The performance of the SMC-PHD filter and its extensions mainly depends on the accuracy of the set-valued estimates of the multi-target state. As a result, further extensions to this work may consider the improvement in the performance of the SMC-PHD filter via better proposal densities and resampling schemes. There is also a need for peak extraction methods that are accurate and efficient. Further studies are also needed to study the performance of the MHT-with-PHD clutter filter and the merit of the tradeoff between the added computational cost of global gating using the PHD filter and the benefits of the global gating. Various issues associated with the complexities and computational requirements of the SMC-PHD filter based schemes could be the subjects of further research.

The data association and the track management scheme proposed for the GM-PHD filter provides a natural framework for clustering target trees so that the computational cost of the track association could be parallelized. There is also a scope for investigating the use of the GM-PHD tracker for sensor networks. The basic idea behind the formulation of the GM-PHD filter, i.e., tagging individual Gaussians, can also be employed with the non-linear extensions of the GM-PHD filter.

The final contribution of this thesis includes the convolution PHD filter. This thesis presents the preliminary results of the proposed filter. Further research is required to investigate for the optimal kernel bandwidth to be used in practice. Further study is also required to establish whether the standard convergence properties hold true for the convolution PHD filter.

Recently, the PHD filter has been extended to propagate the higher order statistics of the target number in what is called the *cardinalized PHD* (CPHD) filter to improve the performance of the PHD filter when the probability of detection is

low [63]. In particular, the performance of the CPHD filter have been promising [109, 110]. The issue of track continuity could be considered for the CPHD filter.

Finally, one pertinent question related to the RFS framework for multi-target tracking is whether it is possible to approximate the multi-target Bayes recursion by higher order moments of the multi-target RFS instead of just the first moment. This immediately leads to the question of whether tracking schemes based on the higher moments would be computationally tractable.

Bibliography

- [1] D. L. Alspach and H. W. Sorenson. Nonlinear Bayesian estimation using Gaussian sum approximations. *IEEE Transactions on Automatica*, AC-17(4):439–448, August 1972.
- [2] B. Anderson and J. Moore. *Optimal Filtering*. Prentice Hall, Englewood, NJ, 1979.
- [3] B. Balakumar, A. Sinha, T. Kirubarajan, and J. Reilly. PHD filtering for tracking an unknown number of sources using an array of sensors. In *Proc. IEEE Statistical Signal Processing Workshop*, Bordeaux, France, July 2005.
- [4] Y. Bar-Shalom and T. E. Fortmann. *Tracking and Data Association*. Academic Press, Boston/London, 1988.
- [5] Y. Bar-Shalom and X. R. Li. *Multitarget-Multisensor Tracking: Principles and Techniques*. YBS Publishing, Storrs, 1995.
- [6] Y. Bar-Shalom, X. R. Li, and T. Kirubarajan. *Estimation with Applications to Tracking and Navigation*. John Wiley & Sons, New York, 2001.
- [7] S. Blackman. *Multiple Target Tracking with Radar Applications*. Artech House, Norwood, 1986.
- [8] S. Blackman. Multiple hypothesis tracking for multiple target tracking. *IEEE Aerospace and Electronic Systems Magazine*, 19(1, Part-2):5–18, January 2004.
- [9] S. Blackman and R. Popoli. *Design and Analysis of Modern Tracking Systems*. Artech House, Norwood, 1999.
- [10] H. Blom and Y. Bar-Shalom. The interacting multiple models algorithms for systems with Markovian switching coefficients. *IEEE Transactions on Automatic Control*, 33:780–783, August 1988.

- [11] F. Campillo and V. Rossi. Convolution particle filtering for parameter estimation in general state-space models. In *The 45th IEEE Conference on Decision and Control*, San Diego, CA, December 2006.
- [12] F. Campillo and V. Rossi. Convolution particle filters for parameter estimation in general state-space models. Research Report 5939, INRIA, <https://hal.inria.fr/inria-00081956>, June 2006.
- [13] D. E. Clark. *Multiple Target Tracking with the Probability Hypothesis Density Filter*. Phd thesis, Department of Electrical Engineering, Heriot-Watt University, Edinburgh, U.K., October 2006.
- [14] D. E. Clark and J. Bell. Data association for the PHD filter. In *Proceeding of the Second International Conference on the Intelligent Sensor, Sensor Networks and Information Processing*, pages 217–222, Melbourne, Australia, 5-8 December 2005. IEEE Press.
- [15] D. E. Clark and J. Bell. Convergence results for the particle PHD filter. *IEEE Transactions on Signal Processing*, 54(7):2652–2661, July 2006.
- [16] D. E. Clark, Judith Bell, Yves de Saint-Pern, and Yvan Petillot. PHD filter for multi-target tracking in 3D sonar. In *Proceedings of Oceans European Conference*, volume 1, pages 265–270, Europe, 20-23 June 2005. IEEE Press.
- [17] D. E. Clark, K. Panta, and B. Vo. The GM-PHD filter multitarget tracker. In *Proc. of 9th International Conference on Information Fusion*, Florence, Italy, July 2006.
- [18] D. E. Clark, B. Vo, and J. Bell. The GM-PHD filter multitarget tracking in sonar images. In I. Kader, editor, *Proc. Signal Processing, Sensor Fusion and Target Recognition XV, SPIE Defense and Security Symposium*, Orlando, USA, April 2006.
- [19] I. J. Cox and S. L. Hingorani. An efficient implementation of Reid’s multiple hypotheses tracking algorithm and its evaluation for the purposes of visual

- tracking. *IEEE Transactions on Pattern Analysis and Machine Intelligence*, 18(2):138–150, February 1996.
- [20] D. Daley and D. Vere-Jones. *An Introduction to the Theory of Point Process*. Springer Verlag, Berlin, Germany, 1988.
- [21] L. Devroye and L. Gyöfri. *Nonparametric Density Estimation: The L_1 View*. Wiley Series in Probability and Mathematical Statistics. John Wiley & Sons, New York, first edition, 1985.
- [22] A. Doucet. On sequential simulation-based methods for Bayesian filtering. Technical Report CUED/F-INFENG/TR.310, Signal Processing Group, Department of Engineering, University of Cambridge, Cambridge, UK, 1998.
- [23] A Doucet, J.F.G. de Freitas, and N. J. Gordon. *Sequential Monte Carlo Methods in Practice*, chapter An Introduction to Sequential Monte Carlo Methods, pages 1–14. Statistics for Engineering and Information Science. Springer-Verlag, New York, 2001.
- [24] A. Doucet, S. J. Godsill, and C. Andrieu. On sequential Monte Carlo methods for Bayesian filtering. *Stat. Comp.*, 10:197–208, 2000.
- [25] O. Erdinc, P. Willett, and Y. Bar-Shalom. Probability hypothesis density filter for multitarget multisensor tracking. In *Proc. 2005 7th International Conference on Information Fusion*, volume 1, pages 146–153, Philadelphia, USA, 25–29 July 2005.
- [26] T. E. Fortmann, Y. Bar-Shalom, and M. Scheffe. Sonar tracking of multiple targets using joint probabilistic data association. *IEEE Journal of Oceanic Engineering*, OE-8:173–184, July 1983.
- [27] I. Goodman, R. Mahler, and H. Nguyen. *Mathematics of Data Fusion*. Kluwer Academic Publishers, Dordrecht/Boston/London, 1995.
- [28] N. Gordon. A hybrid bootstrap filter for target tracking in clutter. *IEEE Trans. on Aerospace and Electronic Systems*, 33(3):353–358, Jan. 1997.

- [29] N. Gordon, D. Salmond, and A. Smith. Novel approach to nonlinear/non-gaussian bayesian state estimation. In *IEE Proceedings-F*, volume 140, pages 107–113, 1993.
- [30] J. Goutsias, R. S. Mahler, and H. T. Nguyen, editors. *Random Sets: Theory and Applications*, volume 97 of *The IMA Volumes in Mathematics and its Applications*. Springer, Minneapolis, USA, 1997.
- [31] Y. C. Ho and R. C. K. Lee. A Bayesian approach to problems in stochastic estimation and control. *IEEE Trans. on Automatic Control*, AC-9:333–339, 1964.
- [32] J. Hoffman and R. Mahler. Multi-target miss distance via optimal assignments. *IEEE Trans. on Systems, Man, and Cybernetics - Part A*, 34(3):327–336, May 2004.
- [33] C. Hue, Jean-Pierre L. Cadre, and P. Perez. Sequential Monte Carlo methods for multiple target tracking and data fusion. *IEEE Trans. of Signal Processing*, 50(2):309–325, February 2002.
- [34] C. Hue, Jean-Pierre L. Cadre, and P. Perez. Tracking multiple objects with particle filtering. *IEEE Transaction on Aerospace and Electronic Systems*, 38(3):791–812, July 2002.
- [35] M. Hürzeler and H. Künsch. *Sequential Monte Carlo Methods in Practice*, chapter Approximating and Maximizing the Likelihood for a General State-Space Model, pages 159–175. Statistics for Engineering and Information Science. Springer-Verlag, New York, 2001.
- [36] N. Ikoma, T Uchino, and T Maeda. Tracking of feature points in image sequence by SMC implementation of PHD filter. In *Proc. ICE 2004 Annual Conference*, volume 2, pages 1696–1701, Sapporo, 2004.
- [37] N. Ikoma, T Uchino, and T Maeda. Image motion tracking by FRS state space model using SMC implementation of PHD filter. In *Proc. IEEE Vi-*

- sual Communications and Image Processing (VCIP)*, pages 129–140, Beijing, China, 12–15 July 2005.
- [38] A. J. Inzeman. Recent developmens in nonparametric density estimation. *Journal of the American Statistical Association*, 86(413):205–234, March 1991.
- [39] A. H. Jazwinski. *Stochastic Processes and Filtering Theory*. Academic Press, New York, 1970.
- [40] A. Johansen, S. Singh, A. Doucet, and B. Vo. Convergence of the sequential Monte Carlo implementation of the PHD filter. *Methodology & Computing in Applied Probability*, 8(2):265–291, June 2006.
- [41] S. Julier and J. Uhlmann. A new extension of the kalman filter to non-linear systems. In *Proc. of Aersosense: 11th International Symposium on Aerospace/Defence Sensing, Simulations and Controls*, Orlando, Florida, 1997.
- [42] R. Kalman. A new approach to linear filtering and prediction problems. *Trans. of ASME—Journal of Basic Engineering*, 82(Series D):35–45, 1960.
- [43] B. Kalyan, A. Balasuriya, and W. Wijesoma. Multiple target tracking in underwater sonar images using the particle-PHD filter. In *Proc. Oceans IEEE Asia Pacific*, Singapore, May 2006.
- [44] E. W. Kamen. Multiple target tracking based on symmetric measurement equations. *IEEE Transactions on Automatic Control*, AC(37):371–374, 1992.
- [45] E. W. Kamen and J. Su. *Introduction to Optimal Estimation*. Springer Verlag, London, first edition, October 1999.
- [46] R. Karlsson. *Simulaton Based Methods for Target Tracking*. Thesis, Division of Authomatic Control & Communication Systems, Department of Electrical Engineering, Linköping University, Linköping, Sweden, January 2002.
- [47] G. Kitagawa. Non-gaussian state-space modeling of nonstationary time series (with discussion). *Journal of American Statistical Association*, 82(400):1032–1063, 1987.

- [48] V. Krishnamurthy and R. Evans. The data association problem for hidden markov models. In *Proceedings of IEEE Conference of Decision and Control*, pages 2764–2765, New Orleans, 1995.
- [49] T. Kurien. *Multitarget-Multisensor Tracking: Advanced Applications*, chapter Issues in the design of practical multitarget tracking algorithms, pages 43–83. Artech House, Norwood, 1990.
- [50] T. Kurien. Framework for integrated tracking and identification of multiple targets. In *Proceedings of the 10th IEEE/AIAA Conference on Digital Avionics Systems*, pages 362–366, 14–17 October 1991.
- [51] T. Kurien and M. E. Liggins. Report-to-target assignment in multisensor multitarget tracking. In *Proceedings of the 27th IEEE Conference on Decision and Control*, pages 248–2488, Austin, Texas, 7-9 December 1988.
- [52] L. Lin, Y. Bar-Shalom, and T. Kirubarajan. Data association combined with the probability hypothesis density filter for multitarget tracking. In O. E. Drummond, editor, *Signal and Data Processing on Small Targets XIII, Proc. SPIE*, volume 5428, pages 464–475, Orlando, Florida, April 2004.
- [53] J. Liu and R. Chen. Sequential Monte Carlo methods for dynamical systems. *Journal of American Statistical Association*, 93:1032–1044, 1998.
- [54] N. Gordon M. Sanjeev Arulampalam, S. Maskell and T. Clapp. A tutorial on particle filters for online nonlinear/non-gaussian bayesian tracking. *IEEE Trans. on Signal Processing*, 50(2):174–188, February 2002.
- [55] W.-K. Ma, B. Vo, S. Singh, and A. Baddeley. Tracking an unknown time-varying number of speakers using TDOA measurements: A random finite set approach. *IEEE Trans. on Signal Processing*, 54(9):3291–3304, September 2006.
- [56] R. Mahler. An introduction to multisource-multitarget statistics and its applications. Lockheed Martin Technical Monograph, March 2000.

- [57] R. Mahler. Multitarget moments and their applications to multitarget tracking. In *Proc Workshop on Estimation, Tracking and Fusion*, pages 134–166, Monterey, CA, May 2001.
- [58] R. Mahler. Random set theory for target tracking and identification. In D. Hall and J Llinas, editors, *Data Fusion Handbook*, pages 14/1–14/33, Boca Raton, Florida, 2001. CRC Press.
- [59] R. Mahler. An extended first-order Bayes filter for force aggregation. In O. Drummond, editor, *Signal Processing of Small Targets 2002, Proc SPIE*, volume 4729, pages 196–207, Bellingham, WA, 2002.
- [60] R. Mahler. Multi-target Bayes filtering via first-order multi-target moments. *IEEE Trans. on AES*, 39(4):1152–1178, Oct. 2003.
- [61] R. Mahler. Objective functions for Bayesian control-theoretic sensor management, I: Multitarget first-moment approximation. In *Proc. 2003 IEEE Aerospace Conference*, volume 4, pages 1905–1923, March 8–15 2003.
- [62] R. Mahler. “Statistics 101” for multitarget, multisensor data fusion. *IEEE Magazine on Aerospace and Electronic Systems*, 19(1(2)):53–64, January 2004.
- [63] R. Mahler. A theory of PHD filters for higher order in target number. In I. Kader, editor, *Signal Processing, Sensor Fusion, and Target Recognition XV, SPIE Defence & Security Symposium*, Orlando, USA, April 2006.
- [64] R. Mahler and T. Zajic. Mult-object tracking using a generalized multi-object first order moment filter. In *Proc. 2003 Conference on Computer Vision and Pattern Recognition Workshop*, volume 9, page 99, 2003.
- [65] R. S. Mahler. *Random Sets: Theory and Applications*, chapter Random Sets in Information Theory: An Overview, pages 129–164. Springer, 1997.
- [66] A. D. Marrs. Asynchronous multi-sensor tracking in clutter with uncertain sensor locations using Bayesian sequential Monte Carlo methods. In *IEEE Proc. Aerospace Conference*, volume 5, pages 2171–2178, March 2001.

- [67] A. D. Marrs, S. Maskell, and Y. Bar-Shalom. Expected likelihood for target tracking in clutter with particle filters. In *Signal and Data Processing of Small Targets, Proc. SPIE*, volume 4728, Orlando, USA, April 2005.
- [68] Simon Maskell. *Sequentially Structured Bayesian Solutions*. Thesis, Engineering Department, Cambridge University, 2004.
- [69] D. Musicki, R. Evans, and S. Stankovic. Integrated probabilistic data association. *IEEE Transactions on Automatic Control*, 39(6):1237–1241, June 1994.
- [70] C. Musso, N. Oudjane, and F. LeGland. *Sequential Monte Carlo Methods in Practice*, chapter Improving Regularized Particle Filters, pages 247–271. Statistics for Engineering and Information Science. Springer-Verlag, New York, 2001.
- [71] W. Ng, J. Li, S. Godsill, and J. Vermaak. A review of recent results in multi-target tracking. In *Proc. International Symposium on Image and Signal Processing and Analysis*, 2005.
- [72] A. Pagan and A. Ullah. *Nonparametric Econometrics*. Themes in Modern Econometrics. Cambridge University Press, Cambridge/New York/Melbourne, 1995.
- [73] K. Panta, D. Clark, and B. Vo. Data association and track management for the Gaussian-mixture probability hypothesis density filter. *IEEE Transactions on Aerospace and Electronic Systems (submitted)*.
- [74] K. Panta and B. Vo. Convolution kernels based sequential Monte Carlo (SMC) implementation of the probability hypothesis density (PHD) filter. In *Proc. International Conference on Information, Decision and Control*, Adelaide, Australia, February 2007. IEEE Press.
- [75] K. Panta, B. Vo, and D. Clark. An efficient track management systems for the gaussian mixture probability hypothesis density (GM-PHD) tracker. In *Proc. 2006 Fourth International Conference on Intelligent Sensing and Information Processing*, Bangalore, India, December 2006. IEEE Press.

- [76] K. Panta, B. Vo, and S. Singh. Improved probability hypothesis density (PHD) filter for multi-target tracking. In *Proc. 2005 Third International Conference on Intelligent Sensing and Information Processing*, pages 213–218, Bangalore, India, December 2005. IEEE Press.
- [77] K. Panta, B. Vo, and S. Singh. Novel data association technique for the probability hypothesis density filter. *IEEE Transactions on Aerospace and Electronic Systems (In Press)*, 2006.
- [78] K. Panta, B. Vo, S. Singh, and A. Doucet. Probability hypothesis density filter versus multiple hypothesis tracking. In I. Kadar, editor, *Signal Processing, Sensor Fusion and Target Recognition XIII, Proc. SPIE*, volume 5429, pages 284–295, August 2004.
- [79] A. Papoulis. *Probability, Random Variables, and Stochastic Processes*. McGraw-Hill, third edition, 1991.
- [80] A. Pasha, B. Vo, H. D. Tuan, and W.-K. Ma. Performance of PHD based multi-target filters. In *Proc. ISIF 2006*, Florence, Italy, July 2006.
- [81] G. Pulford. Taxonomy of multiple target tracking methods. *IEE Proc. - Radar, Sonar and Navigation*, 152(5):291–304, October 2005.
- [82] K. Punithakumar and T. Kirubarajan. A sequential Monte Carlo probability hypothesis density algorithm for multitarget track-before-detect. In O. E. Drummond, editor, *Proc. SPIE Signal and Data Processing on Small Targets XIV*, volume 5913, pages 505–512, San Diego, CA, August 2005.
- [83] K. Punithakumar, T. Kirubarajan, and A. Sinha. A multiple model probability hypothesis density filter for tracking maneuvering targets. In O. E. Drummond, editor, *Proc. SPIE Signal and Data Processing on Small Targets XIII*, volume 5428, pages 113–121, Orlando, Florida, April 2004.
- [84] K. Punithakumar, T. Kirubarajan, and A. Sinha. A distributed implementation of a sequential Monte Carlo probability hypothesis density filter for sensor

- networks. In I. Kadar, editor, *Proc. SPIE Signal Processing, Sensor Fusion, Target Recognition*, volume 6235, Orlando, FL, 2006.
- [85] D. B. Reid. An algorithm for tracking multiple targets. *IEEE Trans. on Automatic Control*, AC-24:843–854, Dec. 1979.
- [86] B. Ristic, S. Arulampalam, and N. Gordon. *Beyond Kalman Filter: Particle Filters for Tracking Applications*. Artech House, Boston/London, 2004.
- [87] V. Rossi and J.-P. Vila. Nonlinear filter in discrete time: A particle convolution approach. Technical Report 04-03, Biostatic Group of Monetepellier, <http://vrossi.free.fr/recherche.html>, 2004.
- [88] D. Schultz, W. Burgard, D. Fox, and A. B. Cremers. Tracking multiple moving targets with a mobile robot using particle filters and statistical data association. In *Proceedings of the IEEE International Conference on Robotics Automation*, pages 1665–1670, Seoul, Korea, 21-26 May 2001.
- [89] P. Shoenfeld. A particle filter algorithm for the multi-target probability hypothesis density. In I. Kadar, editor, *Signal Processing, Sensor Fusion and Target Recognition XIII, Proc. SPIE*, volume 5429, pages 315–325, August 2004.
- [90] H. Sidenbladh. Multi-target particle filtering for the probability hypothesis density. In *Proc. of Fusion*, pages 1110–1117, Cairns, Australia, 2003.
- [91] H. Sidenbladh and S. Wirkander. Tracking random sets of vehicles in terrain. In *Proc. of IEEE Workshop on Multi-Object Tracking*, Madison, Wisconsin, 2003.
- [92] B. W. Silverman. *Density Estimation for Statistics and Data Analysis*. Monographs on Statistics and Applied Probability 26. Chapman & Hall, London/New York/Tokyo/Melbourne/Madras, first edition, 1986.
- [93] R. A. Singer. Estimating optimal tracking filter performance for manned maneuvering targets. *IEEE Transactions on Aerospace and Electronic Systems*, AES(6):473–483, July 1970.

- [94] L. D. Stone, C. A. Barlow, and T. L. Corwin. *Bayesian Multiple Target Tracking*. Artech House, Norwood, MA, 1999.
- [95] D. Stoyan, D. Kendall, and J. Mecke. *Stochastic Geometry and its Applications*. John Wiley & Sons, 1995.
- [96] M. Tobias. *Probability Hypothesis Densities for Multitarget, Multisensor Tracking with Application to Passive Radar*. Thesis, School of Electrical & Computer Engineering, Georgia Institute of Technology, May 2006.
- [97] M. Tobias and A. D. Lanterman. Multitarget tracking using multiple bistatic range measurements with probability hypothesis densities. In I. Kadar, editor, *Signal Processing, Sensor Fusion and Target Recognition XIII, Proc. SPIE*, volume 5429, pages 296–305, August 2004.
- [98] M. Tobias and A. D. Lanterman. Probability hypothesis density-based multitarget tracking with bistatic range and Doppler observations. *IEEE Proceedings on Radar, Sonar and Navigation*, 152(3):195–205, June 2005.
- [99] J. Vermaak, J. Godsill, and P. Perez. Monte Carlo filtering for multitarget tracking and data association. *IEEE Transactions on Aerospace and Electronic Systems*, 41(1):309–332, January 2005.
- [100] M. Vihola. *Random Sets for Multitarget Tracking and Data Fusion*. Licentiate Thesis, Department of Information Technology and Institute of Mathematics, Tampere University of Technology, August 2004.
- [101] M. Vihola. Random set particle filter for bearings-only multitarget tracking. In I. Kadar, editor, *Proc. SPIE Signal Processing, Sensor Fusion and Target Recognition XIV*, volume 5809, pages 301–312, Orlando, Florida, March 2005.
- [102] B. Vo and W.-K. Ma. Joint detection and tracking of multiple maneuvering targets in clutter using random sets. In *Proc. of 8th IEEE Conference on Control, Automatic, Robotics and Vision (ICARCV'04)*, volume 2, pages 1485–1490, Kuming, China, December 2004. IEEE Press.

- [103] B. Vo and W.-K. Ma. A closed-form solution for the probability hypothesis density filter. In *Proceedings of 2005 7th International Conference on Information Fusion*, volume 2, pages 856–863, Philadelphia, USA, 25–28 July 2005.
- [104] B. Vo and W.-K. Ma. The Gaussian mixture probability hypothesis density filter. *IEEE Transaction on Signal Processing*, 54(11):4091–4104, November 2006.
- [105] B. Vo and S. Singh. Technical aspects of the probability hypothesis density recursion. Technical Report TR-05-006, Dept. of E&E Engineering, The University of Melbourne, Melbourne, Australia, 2005.
- [106] B. Vo, S. Singh, and A. Doucet. Sequential Monte Carlo implementation of the PHD filter for multi-target tracking. In *Proc. of the Sixth International Conference on Information Fusion*, pages 792–799, Cairns, Australia, July 2003.
- [107] B. Vo, S. Singh, and A. Doucet. Sequential Monte Carlo methods for multi-target filtering with random finite sets. *IEEE Trans. on Aerospace and Electronic Systems*, 41(4):1224–1245, Oct. 2005.
- [108] Ba-Tuong Vo, B. Vo, and A. Cantoni. Analytic implementations of the cardinalized probability hypothesis density filter. *to appear in IEEE Transaction on Signal Processing*.
- [109] Ba-Tuong Vo, B. Vo, and A. Cantoni. The cardinalized probability hypothesis density filter for linear Gaussian multi-target models. In *Proc. 40th Conference on Information Sciences & Systems*, Princeton, USA, 2006.
- [110] Ba-Tuong Vo, B. Vo, and A. Cantoni. Performance of PHD based multi-target filters. In *Proc. ISIF 2006*, Florence, Italy, July 2006.
- [111] E. A. Wan and R. Van der Merwe. The unscented kalman filter for nonlinear estimation. In *Proc. Symposium of Adaptive Systems, Signal Processing, Communications and Control*, Lake Louise, AB, Canada, October 2000.

- [112] E. A. Wan and R. Van der Merwe. *Kalman Filtering and Neural Networks*, chapter The Unscented Kalman Filter, pages 129–164. Wiley, New York, 2001.
- [113] M. P. Wand and M. C. Jones. *Kernel Smoothing*. Monographs on Statistics and Applied Probability 60. Chapman & Hall, London/New York/Tokyo/Melbourne/Madras, first edition, 1995.
- [114] R. Washburn. A random point process approach to multi-object tracking. In *Proc. IEEE American Control Confence*, volume 3, pages 1846–1852, 1987.
- [115] X. Xie and R. Evans. Multiple target tracking and multiple frequency line tracking using hidden markov models. *IEEE Trans. on Signal Processing*, SP(39):2659–2676, 1991.
- [116] T. Zajic and R. Mahler. A particle-systems implementation of the PHD multi-target tracking filter. In I. Kadar, editor, *Signal Processing, Sensor Fusion and Target Recognition XII, Proc. SPIE*, volume 5096, pages 291–299, 2003.